UNIVERSITÀ DEGLI STUDI DI PAVIA
DOTTORATO DI RICERCA IN FISICA — XXX CICLO

NON-PERTURBATIVE INVESTIGATION OF $O(N)$ ϕ^4 THEORY IN TWO AND THREE DIMENSIONS

BARBARA DE PALMA

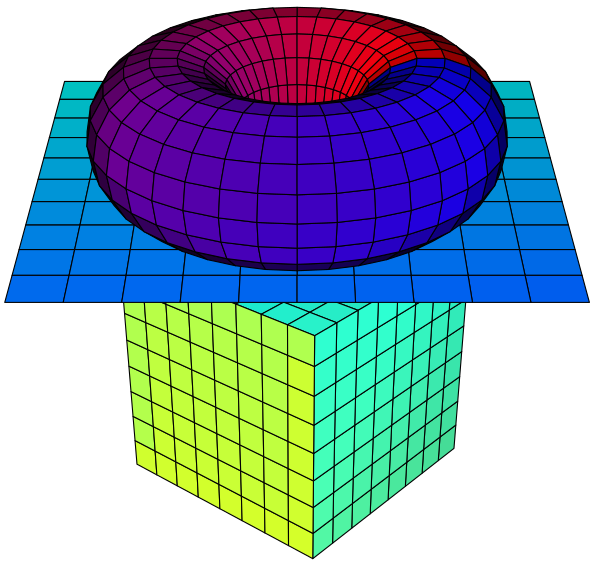

THESIS ADVISOR:
DOTT. MARCO GUAGNELLI

TABLE OF CONTENTS

LIST OF FIGURES

LIST OF TABLES

INTRODUCTION AND KEYWORDS

Quantum Field Theory [89, 121] is a theory which combines quantum mechanics, special relativity and classical fields. It allows us to study several fundamental interactions, ranging from subatomic particle physics to condensed matter. From a theoretical point of view we may characterize a particular physical phenomenon identifying *i)* the fundamental degrees of freedom, described in terms of *fields*, and *ii)* the relevant physical quantities and interactions, described by *bare parameters* and *operators*. Once this quantities have been identified, we write down the Lagrangian of the system, which is a function of fields, field derivatives and bare parameters. With it we try to predict some physical quantities at a particular energy scale, comparing the theoretical predictions to the experimental data. In this way we hope to confirm the theory and fix the parameters and the terms of Lagrangian.

Predictions of physical quantities from the bare parameters of a quantum field theory are often the result a *perturbative* calculation. It can happen that, in the computation of terms beyond the tree–level, infinite results are obtained. Whenever it is possible to take care of the infinite quantities by means of fixing only a *finite* number of parameters and exactly the number of the free parameters in the Lagrangian, we deal with a *renormalizable* theory.

The appearance of divergences in the perturbative treatment of interacting fields requires a procedure called *renormalization*: it includes all methods and procedures used to obtain finite quantities with a physical meaning. A deeper understanding of renormalization was reached with the advent of the *non–perturbative* approach to quantum field theory through the *regularized Euclidean functional integrals*. The path integral formulation [37] of Euclidean quantum field theory [90], regularized

adopting a *lattice regularization* [100] made evident, moreover, the deep connection between the *generating functional* of the Euclidean quantum field theory and the *partition function* of Statistical Mechanics.

Some classes of renormalizable local quantum field theories can be associated to equivalent statistical systems, characterized by a second order phase transition. Generally, a phase transition occurs when a system passes from an ordered phase at low temperature to a disordered phase at high temperature. In order to classify a phase transition, it is useful to identify a physical parameter, called *order parameter*, which is the other way around we can write down the following classification:

- *first order* phase transitions are those in which the order parameter changes discontinuously as the system cross the *critical value* of a control parameter. Moreover, at the critical point the two phases coexist;
- *second order* or *continuous* phase transition are characterized by a continuous change of the order parameter as a function of the control parameter, but the second derivative diverges at critical point.

Focusing on the continuous transitions, there is another quantity which diverges at T_c, the *correlation length* ξ. It is the distance over which the fluctuations of the microscopic degrees of freedom are significantly correlated with each other. The investigation of several systems near the critical point has revealed a power-law behaviour of ξ (and of other thermodynamic quantities) characterized by some *critical exponents*. These are identical for those systems which enter in the same *universality class*, *i. e.* which share *i)* the same number of degrees of freedom of the microscopic field, *ii)* the symmetry of the system and *iii)* the space time dimension. In other words, *universality* means that the long-range properties of a critical system do not depend on the details of the microscopic interaction. In particular, according to the *scaling hypothesis*, ξ is the only relevant length scale for the system near criticality. Scaling theory and universality can be studied and better understood through the Kadanoff–Wilson *renormalization group* [106, 107].

The *Euclidean quantum field theory* defined on a *lattice* is the natural framework for studying such critical phenomena [73, 121]. As we mentioned, in addition to give a precise definition of quantum field theory, it is useful for clarifying important topics as renormalization, scaling behaviour and universality. Moreover, the

connection to statistical physics due to the equivalence between the Euclidean generating functional and the canonical partition function, allows numerical simulations on a computer, giving truly non-perturbative results as well as new physical intuition into the behavior of the system. The first step for undertaking a numerical approach is to discretize the problem by introducing a lattice of volume L^d, where d is the space dimension, and with a lattice spacing that we denote with a. This expedient *regularizes* the theory, meaning that it provides a natural cut–off to the divergent UV quantity coming from the computation of Feynman diagrams. After the redefinition of the operators and the parameters in terms of a, one simulate the system at different lattice sizes. At the end of the simulations the infinite volume and continuum theory has to be recovered: the volume has to be sent to infinity and the lattice spacing to zero.

The ϕ^4 theory is one of the most simple field theory describing systems with local interactions, used as a basic model for various more complex theory, such as the Higgs sector of Standard Model. It also represents the breeding ground for renormalization group analysis. Indeed universal properties of vastly different physical systems at criticality are adequately described whit this model. Some examples are: ferromagnetism, liquid-vapour, binary mixtures, superfluid helium and, even more surprisingly, statistical properties of polymers. Moreover, successful results have been obtained from numerical, computational and theoretical point of view which, in many cases, have found experimental confirmations. In the last decades copious numerical and theoretical techniques have been developed with the aim to understand and to probe the non-perturbative physics of systems with $\lambda\phi^4$ interaction.

In this thesis we tried to use numerical and theoretical techniques in order to probe the critical region of systems with a quartic interaction. We refer to Monte Carlo simulation on the lattice, using, as numerical tools, cluster-like algorithms, as Wolff-single cluster and worm algorithm. To correctly asses the simulations results we employed a dedicated analysis: we perform an accurate study of the autocorrelation time of our simulations by means of an open-source analysis program developed in [31] and based on [111, 112]. These are the main topics of Part ii.

We applied these techniques in the study of ϕ^4. In [3, 40] the triviality of ϕ^4 theory in more than four dimensions has been proven, and there are numerous

analytical and numerical results for $d = 4$ [20, 66, 117], indicating that in this case the theory is trivial as well.

In $d = 2$ and $d = 3$ the theory is super–renormalisable: the coupling constant has positive mass dimensions. It can be described by the Euclidean Lagrangian

$$\mathcal{L}_E = \frac{1}{2}(\partial_\nu \phi)^2 + \frac{\mu_0^2}{2}\phi^2 + \frac{g}{4!}\phi^4,$$

where μ_0 and g are, respectively the bare mass and coupling.

In $d = 2$, dimensional analysis tells us that $[g] = [\mu_0^2]$ and, thus, the only physical relevant dimensionless parameter is the ratio $f \equiv g/\mu^2$, where now μ^2 is a renormalised squared mass in some given renormalisation scheme. Despite the simplicity of the model, there is still debate in the literature about the value of f, where the ratio is evaluated at the critical point. In particular we are interested in the value of f, computed in the limit in which both g and μ^2 go to zero; this corresponds to the critical value in the continuum. We decided to tackle this problem by using the same renormalisation scheme used in [64, 88], adopting the simulation technique of the *worm algorithm*, while using a completely different strategy to obtain f in the infinite volume limit. After a first result we introduce an improved preliminary estimation by means of the Wilson gradient flow. This technique exponentially suppresses ultraviolet modes of the correlation functions, which enters in the computation of the Feynman diagrams. This "smearing effect" guarantees a better approach to the continuum limit and more consistent extrapolations.

In $d = 3$ the ϕ^4 theory equipped with $O(2)$ symmetry can be seen as the effective theory for studying a dilute homogeneous Bose gas in the limit of weak interaction. Bose-Einstein condensation has a very long history [18, 36], and very different approaches have been used to study its critical properties at low temperature [5, 17, 108]. In particular, the determination of the shift of T_c in the Bose–Einstein condensation [12, 13, 43] is still a demanding problem since it involves non–perturbative physics. We tried to give a new estimation of this shift by means of worm–algorithm, extended to $O(N)$ symmetry [30].

The arguments of this thesis are organized as follows:

- In Part i we describe the theoretical background. In Chapter 1 we present the main aspect of Euclidean quantum field theory in the path integral formalism. We introduce the lattice regularization and the renormalization, as

methods for dealing with divergent integrals. In the end we give the basic idea of the renormalization group theory. In Chapter 2 we focus on the statistical system, used as effective theories. In particular we treat the second order phase transitions and derive the critical exponents by means of renormalization group scaling law.

- Part ii is devoted to the numerical tools and to the analysis method we use in our Monte Carlo simulation on the lattice. In Chapter 3 we review the main features of the Monte Carlo method, focusing in particular to the problem of the autocorrelation of data and presenting the Γ–method. The algorithm used our simulations are presented in 4: we start describing the *worm algorithm* in the case of ϕ^4 theory and σ–model and then we explain how we extend this algorithm to the $O(N)\phi^4$ model.

- Part iii we treat our first application, the determination of the critical coupling f in ϕ^4_2 theory. In Chapter 5, after summarizing the state of art of such computation, we describe the numerical strategy that lead us to our first result. In Chapter 6 we, then, explain how we try to improve this evaluation by means of the Wilson flow technique.

- Part iv focus on the determination of shift of the critical temperature of the Bose condensation. In Chapter 7 we introduce the effective theory $O(2)\,\phi^4_3$ and describe the numerical strategy. In the end we present our result and compare it to the last determinations.

Finally we draw the conclusions of this work and provide the future perspectives.

Part I

PRELIMINARY CONCEPTS

1

EUCLIDEAN QUANTUM FIELD THEORY

In the following we will briefly outline the non–perturbative approach to a local quantum field theory: we will start with the path integral formalism, considering a simple system with one degree of freedom in the Minkowski space-time and then we will define the functional integral measure, using the spacetime discretization in order to give to it a meaningful definition. After the introduction of the imaginary time we then focus on the properties of the correlation functions called *Schwinger functions*, and we see how to pass from Minkowski to Euclidean space-time. After the introduction of a lattice as a regulator in the Euclidean framework, we deal with the problem of renormalization and sketch the main idea of the renormalization group.

1.1 FUNCTIONAL FORMULATION OF EUCLIDEAN QUANTUM FIELD THEORY

Let us consider a system with one degree of freedom described by the Lagrangian $L = L(q, \dot{q})$ or the corresponding Hamiltonian function $H = H(q, p)$

$$L = \frac{m\dot{q}^2}{2} - V(q)$$
$$H = \frac{p^2}{2m} + V(q),$$

where the canonical coordinates p and q satisfy the relation $p = \partial L/\partial \dot{q}$ and $V(q)$ is a some kind of potential depending on q. The time evolution operator, given by

$$\hat{U}(t_1, t_2) = \exp\left\{-i\frac{t}{\hbar}\hat{H}(\hat{q}, \hat{p})\right\},$$

where $\hat{H}$ is obviously the Hamiltonian operator, can be described by the path integral formalism: we can write, in particular,

$$\langle q_1|\hat{U}(t_1, t_2)|q_2\rangle = \int \mathcal{D}[q]\, \exp\left\{\frac{iS[q]}{\hbar}\right\}, \tag{1}$$

where S is the action functional defined as

$$S[q] = \int_{t_1}^{t_2} dt\, L(q(t), \dot{q}(t)). \tag{2}$$

The symbol $\mathcal{D}[q]$ is the *functional integral measure* and it means that the integration is perform over all functions $q(t)$ such that $q(t_1) = q_1$ and $q(t_2) = q_2$. The path integral is, then, a summation over all paths or trajectories $q(t)$ which have given end points. The classical path, which satisfies the principle of least action $\delta S = 0$, is only one of the infinitely many possible paths and each of them is weighted by the factor $\exp\{iS/\hbar\}$.

The path integrals in its continuous time definition are sometimes not well defined. One way to complete the formal definition is by means of a limiting procedure based on a time discretized version (see [80] for further details). Considering a time interval $T = t_2 - t_1$, we break it up into small units ϵ, writing $t = n\epsilon$ and $q(t) = q_n$ where $n = 1, 2, \ldots, N$ identifies the n-temporal slice. For a smooth function $q(t)$ we can write the derivative $\dot{q}(t)$ as $\dot{q} = (q_{n+1} - q_n)/\epsilon$ and, in this way, the discretized lagrangian becomes

$$L = \frac{m}{2\epsilon^2}(q_{n+1} - q_n)^2 - \frac{1}{2}[V(q_{n+1}) + V(q_n)],$$

where $V(q)$ has been equally divided between q_n and q_{n+1}. The action consequently is

$$S = \sum_n \left[\frac{m(q_{n+1} - q_n)^2}{2\epsilon} - \frac{\epsilon}{2}[V(q_{n+1}) + V(q_n)] \right].$$

The path integral can be defined through the discretization of the time evolution operator which, for small ϵ, can be approximated with

$$\langle q_1 | U(t_1, t_2) | q_2 \rangle = \left(\frac{m}{2\pi i \epsilon} \right)^{1/2} \exp \left\{ i \frac{m}{2\pi i \epsilon} (q_1 - q_2)^2 - i \frac{\epsilon}{2} [V(q_1) + V(q_2)] \right\}. \quad (3)$$

Considering two points q' and q'' and the completeness property we can, thus, write:

$$\begin{aligned}
\langle q'' | U(t'', t') | q' \rangle &= \lim_{N \to \infty} \left(\frac{m}{2\pi i \hbar \epsilon} \right)^{N/2} \int \prod_{n=1}^{N-1} dq_n \, \langle q'' | T | q_1 \rangle \dots \langle q_{N-1} | T | q' \rangle \\
&= \lim_{N \to \infty} \left(\frac{m}{2\pi i \hbar \epsilon} \right)^{N/2} \int \prod_{n=1}^{N-1} dq_n \, \exp \left\{ \frac{im}{2\epsilon} \left[(q'' - q_1)^2 + \dots + (q_{N-1} - q')^2 \right] \right\} \\
&- i\epsilon \left[\frac{1}{2} V(q'') + \dots V(q_1) + \dots + V(q_{N-1}) + \frac{1}{2} V(q') \right] \\
&= \lim_{N \to \infty} \left(\frac{m}{2\pi i \hbar \epsilon} \right)^{N/2} \int \prod_{n=1}^{N-1} dq_n \, \exp \left\{ \frac{-iS(q, \epsilon)}{\hbar} \right\}.
\end{aligned}$$

The action $S(q, \epsilon)$ approximates the classical action of a particle moving from q' to q'' along the path $q(t)$ with $q_n = q(n\epsilon)$. The integral measure is defined with the formula

$$\mathcal{D}[q] = \lim_{N \to \infty} \left(\frac{m}{2\pi i \hbar \epsilon} \right)^{N/2} \prod_{k=1}^{N-1} dq_n, \quad (4)$$

and now the equation (1) acquire a meaningful definition. We used this unidimensional example in order to give only the basic idea of the path integral definition and for more complicated quantum system we refer the reader to [80, 121].

Thanks to (4) we have expressed the quantum mechanical amplitude (1) in term of an infinite-dimensional integral, the so-called path integral or functional integral. This powerful representation can be generalized and used in order to define quantum field theories in a compact and easy way. Since the integral is complex

and strongly oscillating, it is not immediate to give to it a satisfactory mathematical meaning as an integral over some space of functions. One way to solve this problem is to perform the following transformation to the time, named *Wick rotation* [34, 103],

$$t = -i\tau, \qquad \tau > 0,\, \tau \in \mathbb{R}, \tag{5}$$

which leads to the Feynman-Kac formula [75]. Considering from now on the natural units in which, in particular $\hbar = 1$, the time evolution operator becomes $U(\tau) = \exp(-H\tau)$: it is a well-defined positive bounded operator if the potential term V is bounded from below. The new time τ is called *Euclidean time* and with the transformation (5) the equation (1) can be rewritten as

$$\langle q_1|\hat{U}(t_1, t_2)|q_2\rangle = \int \mathcal{D}[q]\, e^{-S_E[q]}, \tag{6}$$

where now $\mathcal{D}[q]$ differs from the previous definition by the factor i and the relation between the old and the new Euclidean action is

$$S[q] = iS_E[q], \qquad \text{with} \qquad t \to \tau.$$

The path integral (6) is now manifestly real and the integrand is no more dangerously oscillating [41, 85].

The time analytic continuation (5) yield from the *Minkowskian metric* $g_{\mu\nu}$, for which the scalar product is

$$(x, y)_M \equiv g_{\mu\nu}x^\mu y^\nu = x^0y^0 - x^1y^1 - x^2y^2 - x^3y^3,$$

to the *Euclidean metric* $\delta_{\nu\mu}$, for which the scalar product is

$$(x, y)_E \equiv \delta_{\mu\nu}x^\mu y^\nu = x^0y^0 + x^1y^1 + x^2y^2 + x^3y^3.$$

Thus we passed from the Minkowski to the Euclidean space-time. In the next section we introduce the main properties of the *Euclidean quantum field theories*.

1.2 EUCLIDEAN GENERATING FUNCTIONAL

In the previous section we have shown the functional integral representation of the time evolution operator and built its Euclidean formulation up. In the following we define the main object of a path integral quantum field theory, the *generating functional* of correlation functions. In particular we see how to compute connected and disconnected correlation functions and how to deal with divergences appearing in loop integral calculations.

From now on we will work with scalar fields $\phi(x)$, which are operator-valued distribution [104] acting on a Hilbert space $\mathcal{H}$ of physical states containing the vacuum. We assume, in particular, that the fields transform covariantly under the action of Poincaré group and that locality principle holds (fields commute for space-like separations)[1].

Let us introduce the generating functional of disconnected correlation functions:

$$Z[J] = \mathcal{N} \int \mathcal{D}[\phi] \exp\left[-S[\phi] + \int \mathrm{d}^d x \; J(x)\phi(x)\right] \tag{7}$$

where $S[\phi]$ is the Euclidean action, J is an external source and the normalization factor is given by

$$\mathcal{N}^{-1} = \int \mathcal{D}[\phi]\, e^{-S[\phi]}.$$

The *Schwinger functions*, named even n-point correlation functions, can be obtained through the functional derivative of (7):

$$\begin{aligned} G^{(n)}(x_1, \ldots, x_n) = \langle \phi(x_1) \ldots \phi(x_n) \rangle &= \left[\frac{\delta}{\delta J(x_1)} \cdots \frac{\delta}{\delta J(x_n)} Z(J) \right]_{J=0} \\ &= \mathcal{N} \int \mathcal{D}[\phi] \phi(x_1) \ldots \phi(x_n) e^{-S[\phi]}. \end{aligned} \tag{8}$$

In A.1 we recall the main properties of functional derivative. We can also write the expansion series

$$Z[J] = \sum_{n=0}^{\infty} \frac{1}{n!} \int dx_1 \ldots dx_n G^{(n)}(x_1, \ldots, x_n) J(x_1) \ldots J(x_n). \tag{9}$$

1 All the mathematical properties that define a relativistic quantum field theory can be found, for example, in [121].

There is an analogous generating functional for *connected* correlation functions, defined as:

$$W[J] = \ln Z[J]. \tag{10}$$

Obviously, relations analogous to (8) and (9) hold:

$$G_c^{(n)}(x_1, \ldots, x_n) = \langle \phi(x_1) \ldots \phi(x_n) \rangle_c = \left[\frac{\delta}{\delta J(x_1)} \cdots \frac{\delta}{\delta J(x_n)} W(J) \right]_{J=0}, \tag{11}$$

and

$$W[J] = \sum_{n=0}^{\infty} \frac{1}{n!} \int dx_1 \ldots dx_n G_c^{(n)}(x_1, \ldots, x_n) J(x_1) \ldots J(x_n).$$

The generating functional (7) allows to define the integral measure $d\mu$ and thus to give a meaning to the computation of expectation values in the path integral formalism

$$\langle O[\phi] \rangle = \int d\mu \, O[\phi].$$

In particular $d\mu$ is fixed by the correlation functions (8) and formally it is expressed as

$$d\mu = \mathcal{N} e^{-S[\phi]} \prod_x d\phi(x) = \mathcal{N} e^{-S[\phi]} \mathcal{D}[\phi]. \tag{12}$$

The definition of the measure goes straightforwardly in the free case since the corresponding generating functional can be expressed in the form of a *Gaussian integral*. We have:

$$d\mu_0[\phi] = \mathcal{N}_0 \prod_x d\phi(x) \; e^{-S_0[\phi]} = \mathcal{N}_0 \; e^{-S_0[\phi]} \mathcal{D}[\phi] \tag{13}$$

where the normalization factor is given by

$$\mathcal{N}_0^{-1} = \int \mathcal{D}[\phi] \, e^{-S_0[\phi]}.$$

and the free lattice action is

$$S_0[\phi] = \frac{1}{2} \int \mathrm{d}^d x \, \left((\partial_\mu \phi)^2 + m^2 \phi^2(x) \right).$$

Therefore the free generating functional assumes a Gaussian integral form

$$Z_0[J] = \mathcal{N}_0 \int \mathcal{D}[\phi] \ \exp\left[-S_0[\phi] + \int \mathrm{d}^d x \ J(x)\phi(x)\right], \tag{14}$$

and it can be used as the definition of the integral measure

We obtained a well-defined infinite-dimensional integral and the Euclidean correlation functions computed with the correspondent generating functional are equal to the moments of the Gaussian distribution defined in (13):

$$\langle \phi(x_1) \dots \phi(x_n) \rangle = \mathcal{N}_0 \int \prod_x d\phi(x) \, e^{-S_0[\phi]} \phi(x_1) \dots \phi(x_n). \tag{15}$$

With this approach we are considering the fields not as operators but as random variables distributed as (4), whose expectation values yield the correlations functions, following the idea of Simanzik [99]. The representation of $Z[J]$ as a functional integral in the interactive case can be obtained formally in a way analogous to the free case.

1.3 LATTICE REGULARIZATION

The evaluation of the propagators (8) and (11) may yield to divergent results. This divergences indicate that the functional integral is formally not well defined. A way to deal with this problem is to adopt a non-perturbative regularization, such as *lattice regularization* in which a discretization of the space-time provides a cut-off to the loop integrals and allows us to avoid the occurrence of infinities. The advantages of this procedure are mainly the following: *i)* it give a meaningful definition to the functional integral even outside perturbation theory and, in fact, the regularized functional integral can be compute by numerical method, like stochastic methods or strong coupling expansion; *ii)* it preserves most global or local symmetries with the exception of the space $O(d)$ symmetry which is replaced by hypercubical symmetry.

Let us introduce an hyper-cubic lattice with lattice spacing a and linear lattice size $L = L_\mu$ over spatial and time directions:

$$\Lambda = a\mathbb{Z}^d = \{x_\nu/a \in \mathbb{Z} \mid 0 \leq x_\nu \leq a(L_\nu - 1)\}$$

The real scalar fields ϕ are defined at all lattice sites x and respect boundary condition $\phi(x + a\hat{\nu}L_\nu) = \phi(x)$. The introduction of the lattice provides a cut-off to the loop-integration since the allowed momenta are

$$p_\nu = \frac{2\pi n_\nu}{aL_\nu}, \qquad n_\nu = 1, 2, \ldots L_\nu - 1,$$

and they are restricted to the first *Brillouin zone*:

$$\mathcal{B} = \left\{p_\nu \mid -\frac{\pi}{a} < p_\nu \leq \frac{\pi}{a}\right\}$$

where π/a is the momentum cut-off. The scalar product is defined as

$$(\phi_1, \phi_2) = \sum_x a^d \phi_1(x)\phi_2(x)$$

and the derivative operator can be expressed as the difference between nearest neighbour sites

$$\partial_\nu \phi(x) \longrightarrow \nabla_\nu \phi = \frac{1}{a}(\phi(x + a\hat{\nu}) - \phi(x)) \tag{16}$$

where $\hat{\nu}$ is the unit vector in the ν direction. The Fourier transformation and the inverse operation of a function f are respectively

$$\tilde{f}(p) = \sum_x a^d e^{-p\cdot x} f(x)$$
$$f(x) = \frac{1}{a^d \Omega} \sum_p e^{ip\cdot x} \tilde{f}(p)$$

where Ω is the number of lattice points. The lattice summation is defined as

$$\int_p \equiv \frac{1}{a^d \Omega} \sum_{p\in\mathcal{B}}$$

and, in the limit of $L \to \infty$, becomes

$$\int_p = \frac{1}{(2\pi)^d} \int_{-\pi/a}^{\pi/a} d^d p.$$

The Euclidean propagator (23) in the spatial representation becomes

$$G(x, y; a) = \int_{-\pi/a}^{\pi/a} \frac{d^d p}{(2\pi)^d} e^{ip\cdot(x-y)} \tilde{G}(p; a). \tag{17}$$

where

$$\tilde{G}(p; a) = \left\{ \sum_{\nu=1}^{d} a^{-2} 4 \sin^2 \left(\frac{a p_\nu}{2} \right) + m^2 \right\}^{-1} \tag{18}$$

It easy to verify that in the continuum limit, where $a \to 0$, $\tilde{G}(p; a) \to \tilde{G}(p)$. The discretized Euclidean action for the interacting case can be written as

$$S[\phi, a] = a^d \sum_{x,\nu} \left\{ \frac{1}{2} |\nabla_\mu \phi(x)|^2 + \frac{1}{2} m^2 \phi(x)^2 + V(\phi(x)) \right\}, \tag{19}$$

where $V(\phi(x))$ is a local potential term. Finally the generating functional for the interacting theory on the lattice is

$$Z[J, a] = \mathcal{N} \int \prod_x d\phi(x) \exp \left\{ -S[\phi, a] + (J, \phi) \right\}, \tag{20}$$

where the integration over all scalar field configurations is defined through the discrete product:

$$\prod_x d\phi(x) = \mathcal{D}[\phi]. \tag{21}$$

The most important task is to find a continuum limit of $Z[J, a]$ which yields to a well-defined Euclidean Green's functions. We can see that the potential term $V(\phi)$ weights the functional integral according to the values of field at each point

independently, while the gradient squared term suppress the fields whih are too singular for $a \to 0$: in particular those for which the following quantity

$$|\phi(x + a\hat{v}) - \phi(x)|^2 a^{d-2}$$

diverges. This condition, however, becomes weaker when dimension increases. For $d < 2$ continuity is guaranteed, whereas for $d \geq 2$, in general, the continuum limit does not exist unless the correspondent statistical mechanics model has a continuum phase transition at a particular critical temperature and a specific parameter reach its critical value.

1.4 RENORMALIZATION OF ϕ^4 THEORY

A local field theory is characterized by the absence of a "small" fundamental length: the action depends only on products of fields and their derivatives at the same point. In perturbation theory the propagator has a simple power law behaviour at short distances. The physical quantities can be calculated as power series in the various interactions. As we now show, perturbative calculations are affected by divergences due to severe short distance singularities. After Fourier transformation, these divergences take the form of integrals diverging at large momenta: one speaks also of UV singularities.

The ϕ^4 model consists of a real scalar self–interacting field, with a quartic local interaction. The starting Lagrangian density is the following

$$\mathcal{L}_E = \frac{1}{2}\left[(\partial_\mu \phi_b(x))^2 + \mu_b^2 \phi_b^2(x)\right] + \frac{g_b}{4!}\phi_b^4(x), \tag{22}$$

where we the subscript b we indicate the *bare* parameters of th theory.

The evaluation of the n–point Green functions model may encounter *ultraviolet divergent* (or UV) integrals. In the momentum representation the Euclidean propagator is

$$G(p) = \int \frac{\mathrm{d}^d p}{(2\pi)^d} \frac{e^{i(p\cdot x)}}{p^2 + m^2} \tag{23}$$

and the correspondence between the analytic expressions and Feynman diagrams is given by

- for each propagator
$$\frac{1}{p^2 + m^2}$$
- for each vertex
$$-\frac{g}{4!}$$
- Integration over internal loops
$$\int \frac{\mathrm{d}^d}{(2\pi)^d}$$
- It is necessary to impose the momentum conservation at each vertex
$$\sum_{i=1}^{d} p_i = 0$$
- It is necessary to take in account the symmetric diagrams by dividing the integral by the symmetry factor.

Without going into details on how to computed Feynman diagrams, the awkward aspect is the appearance of divergences in the computation, beyond the tree-level approximation, of graphs containing closed loops, called loop integrals. The perturbative order corresponds to the number of vertices.

For example, the first order correction to the propagator in four dimensions is given by

$$\int \frac{\mathrm{d}^4\, q}{(2\pi)^4} \frac{1}{p^2 + m^2} \sim \Lambda^2 \tag{24}$$

where q is the arbitrary momentum that can circulate in the loop due to momentum conservation and the corresponding diagram, named self–energy diagram, is represented in Fig. 1. The Λ term in (24) is an a upper limit (or cut–off) on the momentum integration and it easy to see that the integral diverges like a power of Λ as we remove the cut–off.

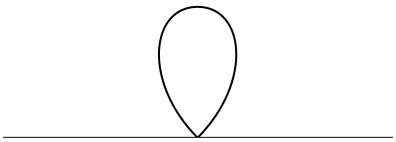

Figure 1: Self–energy diagram.

A formal criterion for understanding which diagram, or equivalently which Green functions, are UV divergent is the evaluation of the *superficial degree of divergences* ω: a diagram which diverges like Λ^ω has a degree of superficial divergence equal to ω. A logarithm divergence of the form $\log \Lambda$ counts as $\omega = 0$. The rule for computing ω is given by the *power counting theorem*: if we define with

- n the number of external legs;
- V the number of vertices;
- I the number of internal lines;
- L the number of loops;
- d the space dimension.

the superficial degree of divergences is given by

$$\omega = d + \left[i \left(\frac{d-2}{2} - d \right) \right] V - \left(\frac{d-2}{2} \right) n, \tag{25}$$

where i is the power of the interaction term ϕ^i. The quantity that multiplies V is minus the dimension of the coupling constant g

$$[g] = [m]^{d - i(d-2)/2} = [m]^{4-d},$$

where in the last step we consider $i = 4$. This relation holds also for other field theories and defines the following classification:

- *Super–renormalizable theory*: the coupling constant has a positive mass dimension. In this case only a finite number of Feynman diagrams superficially diverge.

- *Renormalizable theory*: the coupling is a dimensionless constant. This means that only a finite number of amplitudes superficially diverge.
- *Non–Renormalizable theory*: the coupling constant has a negative mass dimension. All diagrams are divergent at sufficiently high order in perturbation theory.

In this work we focus on the ϕ^4 model in $d = 2, 3$ dimensions. In these cases the theory is super–renormalizable: we have to take care of a finite number of divergent Feynman diagrams.

Using dimensional regularization, a feasible approach to renormalize the theory is to rewrite the Lagrangian density in terms of physical (or renormalized) quantity, by means of multiplicative constants

$$\phi_b(x) = Z_\phi^{1/2}\phi(x) \tag{26}$$

$$\mu_b = Z_\mu^{1/2}\mu \tag{27}$$

$$g_b = \bar{m}^{2\varepsilon}\frac{Z_\lambda}{Z_\phi^2}g, \tag{28}$$

where $\bar{m}$ is an arbitrary mass parameter, $\varepsilon = (4-d)/2$ and $Z_i = Z_i(\lambda, \frac{\mu}{m}, \varepsilon)$. Z_i is, by definition, a dimensionless constant and the dependence of Z_i on m and μ is only through their ratio. By means of relations (26), (27) and (28), the Lagrangian becomes

$$\begin{aligned}\mathcal{L} &= \frac{1}{2}(\partial_\mu\phi_b)^2 + \frac{\mu_b^2}{2}\phi_b^2 + \frac{g_b}{4!}\phi_b^4 \\ &= \frac{1}{2}Z_\phi(\partial_\mu\phi_b)^2 + \frac{\mu_b^2}{2}Z_m Z_\phi\phi_b^2 + \frac{g_b}{4!}Z_\lambda Z_\phi^2\phi_b^4\end{aligned} \tag{29}$$

The renormalized parameters Z_i are calculate perturbatively as series expansions in g. At tree–level $Z_i = 1$, otherwise $Z_i = 1 + \delta Z_i$.

If we now rewrite the Z_i factors in (29) as $Z_i = 1 + \delta Z_i$, the bare Lagrangian density $\mathcal{L}_E$ is split into a renormalized Lagrangian density and a counterterm Lagrangian density

$$\mathcal{L} = \mathcal{L}^{\text{ren}} + \mathcal{L}^{\text{c.t.}} \tag{30}$$

with

$$\mathcal{L}^{\text{ren}} = \frac{1}{2}(\partial_\mu \phi(x))^2 + \frac{\mu^2}{2}\phi^2(x) + \frac{g}{4!}\phi^4(x) \tag{31}$$

$$\mathcal{L}^{\text{c.t.}} = \frac{1}{2}\delta Z_\phi(\partial_\mu \phi(x))^2 + \frac{\mu^2}{2}(Z_\mu Z_\phi - 1)\phi^2(x) + \frac{g}{4!}(Z_g Z_\phi^2)\phi^4(x). \tag{32}$$

$\mathcal{L}^{\text{ren}}$ is expressed in terms of renormalized fields and parameters, which are physical in the sense that they can be measured. It gives rise formally to the same Feynman rules as the bare Lagrangian density. $\mathcal{L}^{\text{c.t.}}$ provides additional Feynman graphs which cancel the divergences from the Green functions. Since the bare Lagrangian density is not changed, the required counterterms, in terms of fields, have to be of the form of the terms already present in the bare Lagrangian density. The aim of renormalization is to find the Z_i functions of (26), (27) and (28) such that the renormalized Green functions are finite in the limit $\varepsilon \to 0$, order by order in perturbation theory. This requirement of finite Green functions fixes the counterterms δZ_i. While the divergent part of the counterterms is uniquely determined, the choice of the finite parts amounts to the choice of a renormalization schemes. To deepen this topics one may see [121].

The relation between the generating functional of the bare theory and the one of the renormalized theory is

$$Z[J] = Z^b[J^b] = Z[Z_\phi^{-1/2} J]. \tag{33}$$

Using this equation we can derive the relation between the n–point Green function and the renormalized one by means of (8):

$$G_b^{(n)}(x_1, \ldots, x_n) = Z_\phi^{n/2} G^{(n)}(x_1, \ldots, x_n), \tag{34}$$

and a completely analogous relations hold for the connected Green functions, generated by the $W[J]$ functional, and for the 1PI Green functions, generated by the effective action Γ. The n-point vertex function $\Gamma^{(n)}$ is equal to the amputate, one-particle-irreducible part of the connected n-point correlation function $G_c(p_1, \ldots, p_n)$.

We do not want to go further into details about the renormalization of the divergent diagrams, since they will be treated in the Parts related to the applications. Here we only want to translate the main relations present so far in the lattice framework.

The discretized action, derivable from (22), is

$$S[\phi] = \sum_{x,\mu} \phi_b(x)\phi_b(x+\hat{\mu}) - \sum_x \left[\frac{1}{2}(2d+\mu_b^2)\phi_b^2(x) + \frac{1}{4!}g_b(\phi^2(x))^2\right]. \tag{35}$$

Using the following parametrization

$$\begin{aligned} a^{(d-2)/2}\phi_b &= \sqrt{\beta}\varphi, \\ a^2\mu_b^2 &= \frac{2(1-2\lambda)}{\beta} - 2d, \\ a^{4-d}g_b &= \frac{24\lambda}{\beta^2}, \end{aligned} \tag{36}$$

we rewrite the action (35) as

$$S[\varphi] = \beta \sum_{x,\mu} \varphi(x)\varphi(x+\hat{\mu}) - \sum_x \left[\varphi^2(x) + \lambda(\varphi(x)^2-1)^2\right], \tag{37}$$

which contains only dimensionless quantities. The first term of (37) is the interaction term of strength β, while the other one is the single site contribution.

Then we have

$$\phi(x) = Z_\phi^{-1/2}\phi_b(x) = \left(\frac{\beta}{a^{(d-2)}Z_\phi}\right)^{1/2}\varphi(x) \tag{38}$$

The *renormalized mass* μ it is introduced through the small momentum behaviour of the propagator

$$\tilde{G}(p;a)^{-1} = \left(\frac{\beta}{a^2 Z_\phi}\right)\left[m_R^2 + p^2 + \mathcal{O}(p^4)\right].$$

The *bare coupling* g_b is renormalized by means of the four-point vertex function at zero momentum. The relation between the renormalized and the bare effective action is

$$\Gamma^{(n)} = \left(\frac{\beta}{a^2 Z_R}\right)^{-n/2} \Gamma_b^{(n)}.$$

1.5 THE RENORMALIZATION GROUP IDEA

Now we give a very brief idea on the general theory of renormalization group. Consider the original action S of the system with a cut-off Λ embedded in an infinite-dimensional space of actions

$$S = \sum_i K_i S_i \tag{39}$$

where the coefficients K_i are called couplings and where

$$S_i = \sum_x \mathcal{L}_i(\phi(x), \dots).$$

The terms $\mathcal{L}_i$ are called *local operators* and they are functions depending the fields ϕ at point x, and a finite number of points near x. A renormalization group transformation is a mapping R_λ that transforms

$$S \to S^{(\lambda)}$$

such that both S and $S^{(\lambda)}$ describe the same physics at large distances, but the cut-off Λ gets lowered like

$$\Lambda \to \frac{\Lambda}{\lambda}, \qquad \lambda > 0.$$

In this way we are, in practice, integrating out degrees of freedom with high momenta near the cut-off. The most important points in the actions space are the *fixed points* S^*, defined through the equation

$$R_\lambda S^* = S^* \tag{40}$$

and, in particular, those at which the correlation length is infinite. The action of R_λ can be described in terms of the changes of coefficients $K \to K_i^{(\lambda)}$ and, near a fixed point it can be linearized and diagonalized in a suitable basis

$$K_\alpha = K_\alpha^* + \delta K_\alpha \quad \to \quad K_\alpha^{(\lambda)} = K_\alpha^* + \lambda^{d_\alpha} \delta K_\alpha. \tag{41}$$

The exponent d_α is called *scaling dimension* and its value determines the relevance of the corresponding coefficients K_α with respect to the long-distance physics: the terms with $d_\alpha < 0$ are called *irrelevant* since they vanish after repeated application of the renormalization transformation, the terms with $d_\alpha = 0$ are called *marginal* and the terms with $d_\alpha > 0$ are called *relevant* since the values of the corresponding K_α are decisive for the long-distance physics. The property of universality is expressed by the fact that if we consider S' and S'' belonging to the same fixed point domain, the renormalization group maps them into the neighborhood of the same low-dimensional manifold

$$S = S^* + \sum_{\text{relevant}} K_\alpha S_\alpha$$

where no marginal operator are present for simplicity. The criticality is then determined by the few relevant operator in the vicinity of the fixed point, which determines the universality class of the action.

1.5.1 *Fixed points*

Now we want to study the behaviour of the bare and renormalized coupling near the continuum limit. The function that describe the variation of the renormalized g with the cut-off is the β function and reads

$$\mu a \left.\frac{\partial g}{\partial a\mu}\right|_{g_b} = \left.\frac{\partial g}{\partial \ln(a\mu)}\right|_{g_b} = \beta(g) \tag{42}$$

The solution of this equation is given by

$$a\mu = C \exp \int_g \frac{dg_r}{\beta(g_r)} \tag{43}$$

and it gives the dependencies of g on μa. These equations describe the situation in which we move in the space of bare parameter $(a\mu_b, g_b)$ along a line of g_b constant towards the continuum limit $\mu a \to 0$.

- If we start out in a region where $\beta(g) > 0$, then g decreases until a zero of (42). The zero would be reached asimptotically in the limit of $\mu a \to 0$.
- If we are in a region where $\beta(g) < 0$, then g increases and approaches the next zero from below.
- if are in region where $\beta(g) = 0$, then it wold not change under the variations of the cut-off. In this case we may distinguish two kind of fixed points: *i)* the infrared fixed point (or IR fixed point) at which the slope of $\beta(g)$ at $g = 0$ is positive, meaning that g is driven towards the fixed point; *ii)* ultraviolet fixed point (or UV fixed point) at which the slope of $\beta(g)$ at $g = 0$ is negative and therefore the coupling g is driven await from th fixed point,

There is an analogous equation of (42) in the bare coupling case:

$$\left.\frac{\partial g_b}{\partial \ln(a\mu)}\right|_g = -\beta(g) \tag{44}$$

This equation applies to the movement in the space parameter along lines of constant g. The minus sign causes the opposite situation to that considered before.

The picture that emerges from the behaviour of g_b and g is that the critical line, as well as curves of constant g, are drawn in the space parameters. The movement of a point in the parameter space in the vicinity of the fixed point reflects the concept of universality.

In the next Chapter we will apply the concepts to the study of phase transitions.

2

PHASE TRANSITIONS AND CRITICALITY

The advantage of working in the Euclidean framework is that the generating functional has the same form of the partition function of Statistical Mechanics: this make possible to treat local renormalizable quantum field theories as ferromagnetic systems characterized by a second order phase transition, using interpretations and sharing tools coming from the both research branches. This "cooperation" allowed to better understand the meaning of the *renormalization* procedure and of the *renormalization group*. Nevertheless we should keep in mind that the real physics lives in the Minkowskian space-time and thus all the results obtained in the Euclidean approach need to be led back to Minkowski framework.

2.1 EQUIVALENCE BETWEEN EQFT AND SM

In the previous chapter we presented the main aspects of the Euclidean quantum field theory with lattice regularization. Let's focus again on the ϕ^4 theory in d dimensions, introduced in 1.4, described by the discretized lattice action (37). Notice that, in this parametrization, the first term of the action represents the interaction between neighbouring sites with a coupling of strength β and the second one is the action of a single site. Using (37), the generating functional

$$Z = \int \mathcal{D}[\varphi] e^{-S[\varphi]}. \tag{45}$$

has the form of a partition function of a model of statistical mechanics, where the exponential factor is the analogous of the Boltzmann weight. As we stressed previously, we need to specify the measure in order to give a formal meaning to the functional integral:

$$\begin{aligned} &\mathcal{D}[\varphi] = \prod_x d\mu(\varphi(x)) \\ &d\mu(\varphi(x)) = \exp\left\{-\varphi(x)^2 - \lambda(\varphi(x)^2 - \lambda(\varphi(x)^2 - 1)^2)\right\} d\phi, \text{ with } \lambda > 0. \end{aligned} \tag{46}$$

Thanks to the equivalence between partition function and generating functional we can consider a quantum field theory as an effective theory of a system of statistical mechanics. For example, the action (37) can be considered as the effective action of a magnetic system where the fields $\varphi(x)$ represent the spin variables lying on lattice sites and the where the discretized action can be considered as the configuration energy of the lattice model. In this correspondence the vacuum expectation value of the field is the mean magnetization M per site of a ferromagnet:

$$M = \langle \varphi(x) \rangle.$$

The propagator $G_c(x, y) = \langle \varphi(x)\varphi(y) \rangle$ is equal to the spin–spin correlation function and the magnetic susceptibility

$$\chi = \sum_x \langle \varphi(x)\varphi(0) \rangle_c$$

equals the propagator at zero momentum. The correlation length ξ, which governs the exponential decay of the correlation function, is related to the mass gap

$$\xi = \frac{1}{am} \tag{47}$$

where m corresponds to the energy of the lowest state above the vacuum and therefore is the mass of the lightest particle in the theory and a is the lattice spacing. In Table 1 we report the most significants correspondences between the two fields.

Euclidean field theory	**Classical magnetic system**
Field variables φ	Spin variables
External source J	External magnetic field
e^{-S}	Boltzmann factor
Euclidean actions S_E	Energy configuration
Functional integral	Sum over spin configurations
Physical mass m	Inverse correlation length ξ
Field vacuum expectation value	Magnetization
Two-point correlation function	Susceptibility χ
Massless theory	Critical theory
Locality	Short-range forces
$Z[J]$	Partition functions
$W[J]$	Free energy in a magnetic field
$\Gamma[J]$	Thermodynamic potential

Table 1: Correspondences between euclidean quantum field theories and classical magnetic system.

We can, also, derive the thermodynamic properties of a system. In fact, the free energy can be determined from the partition function as

$$F = -k_B T \ln Z \tag{48}$$

and all other thermodynamic quantities can be calculated by appropriate differentiation of (48).

2.1.1 *Phase transitions, renormalization and continuum limit*

As we have already mentioned in the Introduction, some classes of renormalizable local quantum field theories can be associated to equivalent statistical systems, characterized by a second order phase transition. A *second-order or continuum phase transition* is a point in the space parameters (β, λ), called even *critical point*, at which the order parameter changes continuously and the intrinsic length scale, called *correlation length* ξ, diverges. Looking at (47) we can say that finding the continuum limit of a theory means that, with a suitable choice of the bare param-

eters, we approach a limit where $a \to 0$ while the physical parameters remain finite. In this limit we automatically concentrate our attention on the quantities that are dominated by the critical fluctuations, and we neglect all short-distance phenomena.

The only dimensionless parameter in the action is the ratio $g/\mu^{(4-d)}$, related to the dimensionless parameters (β, λ) through (36). Therefore, in order to reach the critical point, or equivalently the renormalized parameters, is suitable to send $a \to 0$ in way that the ratio remain finite. If we send $a \to 0$ naively we obtain, in fewer than four dimensions, the critical Gaussian model, whose correlation functions are well defined in more than two dimensions.

2.1.2 *RG group and universality*

For most systems the behaviour of many thermodynamical quantities near a critical point is governed by simple powers laws [39, 92], of the form

$$f(p) \sim p^s, \qquad \text{with} \qquad \lim_{p\to 0} \frac{\ln f(p)}{\ln p} = s, \tag{49}$$

where p is the parameter approaching its critical value and s is the so–called *critical exponent*. For example, the susceptibility and the correlation length behaves, as $\beta \to \beta_c$, like

$$\xi \sim |\beta - \beta_c|^{-\nu} \qquad \chi \sim |\beta - \beta_c|^{-\gamma}.$$

The intriguing aspect is that the critical exponents are universal values for those system belonging to the same universality class.

Now we see how we can obtain these exponents by means of the renormalization group equations. In the 1.5 we introduced the idea of a renormalization group transformation. It is useful to define the *scaling variables* u_i which are linear combinations of the deviations δK_α from the fixed point . These variables transform multiplicatively near the fixed point:

$$u_i' = b^{y_i} u_i$$

where b is a scaling factor, called *block parameter*, Equivalence between eqft and ms to λ (see 1.5) , and y_i are the *renormalization group eigenvalues*.

Consider now the free energy density $f = -N^{-1} \ln Z$ and write it as a function of the coupling K_i, introduced in 1.5, $f(K_i)$. Under the renormalization group equations the partition function of the system is preserved, while f transforms as

$$f(K_i) = g_r(K_i) + b^{-d} f_s(K_i') \tag{50}$$

where g_r is the *regular part* of f while f_s is the *singular part*. The critical exponents are obtained only from the singular part of the free energy and, therefore, we may drop the inhomogeneous g_r term. In this way we obtain an homogeneous transformation law for the singular part:

$$f_s(K_i) = b^{-d} f_s(K_i'). \tag{51}$$

Near the fixed point we can write f_s in terms of scaling variables

$$f_s(u_t, u_h) = b^{-d} f_s(b^{y_t} u_t, b^{y_h u_h}) = b^{-nd} f_s(b^{n y_t} u_t, b^{n y_h u_h}) \tag{52}$$

where u_t, u_h are the two parameters with whom we are approaching the fixed point in the space of parameter, trough the renormalization group transformations (for further details see [33, 121] and references therein). In the last expression of (52) we have iterated the renormalization group n times. In order to keep the linear approximation (41) valid, we need to stay in the vicinity of the fixed point. Therefore we stop the iteration at the point where $|b^{n y_t} u_t| = u_{t0}$, where u_{t0} is arbitrary but fixed and sufficiently small so that the linear approximation is still valid. With a little algebra one arrives to

$$f_s(u_t, u_h) = |u_t / u_{t0}| f_s(\pm u_{t0},\ u_h |u_t / u_{t0}|^{-y_h / y_t}) \tag{53}$$

This equation can be rewrite as function of some reduced physical variables t (a temperature–like parameter) and h (a magnetics–like parameter), and u_{t0} may be incorporated into a redefintion of the scale factor t_0:

$$f_s(t, h) = |t / t_0|^{d / y_t} \Phi \left(\frac{h / h_0}{|t / t_0|^{y_h / y_t}} \right) \tag{54}$$

were Φ is a scaling function and it is *universal*: it depends on the particular system only through the scale factors t_0 and h_0.

2.1.3 *Critical exponents*

The critical exponents can be determined by an opportune derivation of the free energy expressed as the scaling law (54):

- For the specific heat
$$\frac{\partial^2 f}{\partial t^2}|_{h=0} \propto |t|^{d/y_t - 2},$$
the critical exponent is $\alpha = 2 - d/y_t$;
- For the spontaneous magnetization
$$\frac{\partial h}{\partial f}|_{h=0} \propto (-t)^{(d-y_h)/y_t},$$
the critical exponent is $\beta = \dfrac{d - y_h}{y_t}$;
- For the susceptibility
$$\frac{\partial^2 f}{\partial h^2}|_{h=0} \propto |t^{(d-2y_h)/y_t}|$$
the critical exponent is $\gamma = \dfrac{2y_h - d}{y_t}$
- For the magnetization
$$M = \frac{\partial h}{\partial f}$$
the computation is a little more cumbersome and we do not report here the explicit calculation. The critical exponent is $\delta = \dfrac{y_h}{d - y_h}$

Critical exponents	α	β	γ	δ	η	ν
Ising 2d	0	1/8	7/4	15	1/4	1
XY 3d [23]	0.0146(8)	0.3485(2)	1.3177(5)	4.780(2)	0.0380(4)	0.67155(27)

Table 2: Critical exponents of the Ising universality class and of XY universality class .

Between these exponents exist general *scaling relations*:

$$\begin{aligned} \alpha + 2\beta + \gamma &= 2 \\ \alpha + \beta(1+\delta) &= 2 \\ 2 - \alpha &= 3\nu \\ (2-\eta)\nu &= \gamma \end{aligned}$$

The theories belonging to the same universality class have the same critical exponents. In this thesis we deal with the ϕ^4 theory in two dimensions and with the $O(2)\,\phi^4$ in three dimensions, which belong, respectively, to the Ising and the XY universality classes. In Table 2 we report the critical exponents for such universality classes, where, for the XY case we refer to the latest determination provide in [23], while for the Ising case the analytical evaluations.

Part II

MC SIMULATIONS AND ERROR ANALYSIS

3

MONTE CARLO SIMULATIONS ON THE LATTICE

Monte Carlo simulations constitute an essential tool to perform non–perturbative numerical calculations in quantum and statistical field theories. A thorough dissertation about the general ideas, the error estimation and the practical algorithms can be found in numerous textbooks (see for example [16, 60, 74, 78, 86] and references therein).

In the following we will give a very brief review of the basics concepts of the method. After that we will describe the algorithms used in our simulations.

3.1 BASIC CONCEPTS

The typical quantity we compute in a numerical simulation is the expectation value of a generic observable $\mathcal{O}$:

$$\langle \mathcal{O} \rangle = \frac{\int \mathcal{D}[\phi]\, \mathcal{O}\, e^{-S[\phi]}}{\int \mathcal{D}[\phi]\, e^{-S[\phi]}} \tag{55}$$

through the evaluation of the lattice path integral over the field configurations $\sigma^{(j)}$.The Monte Carlo method uses pseudo–random numbers to extract a representative sample of field configurations with the probability distribution

$$P_{eq} = \frac{\exp\{-\beta \mathcal{S}[\phi]\}}{\int \mathcal{D}[\phi]\, e^{-\mathcal{S}[\phi]}}. \tag{56}$$

In this way the following relation holds

$$\langle \mathcal{O} \rangle = \lim_{M\to\infty} \frac{1}{M} \sum_{j=1}^{M} \mathcal{O}[\sigma^{(j)}] \tag{57}$$

where M is the number of extracted configurations. Basically, we are uniformly weighting configurations that has been extracted accordingly with (56): this procedure is called *importance sampling*.

A way to extract the set of configurations with the desired probability distribution is a *Markov process*. Starting from a trial configuration σ, the consecutive one σ' is obtained with a certain transition probability $W(\sigma \to \sigma')$. The set of configurations obtained is called a *Markov chain*.

In order to be a proper transition probability $W(\sigma \to \sigma')$ has to respect the following properties:

- *non–negativity*,
$$W(\sigma \to \sigma') \geq 0;$$
- *normalization*,
$$\sum_{\sigma'} W(\sigma \to \sigma') = 1.$$

Moreover, in order to fulfill the relation (57), $W(\sigma \to \sigma')$ must satisfy:

- *Ergodicity*:
$$W^M(\sigma \to \sigma') > 0, \qquad \forall\, \sigma, \sigma'; \tag{58}$$
- *Stability*:
$$\sum_{[\sigma]} e^{-S[\sigma]} W(\sigma \to \sigma') = e^{-S[\sigma]}. \tag{59}$$

The property (58) means that, starting from any configuration σ, repeated M application of W bring the system arbitrarily close to any other configuration σ'. In other words, all the elements of the phase space have a non-zero probability to be visited.

Instead of the stability property it is possible to use the *detailed balance* condition

$$\frac{W(\sigma \to \sigma')}{W(\sigma' \to \sigma)} = e^{-(\mathcal{S}[\sigma'] - \mathcal{S}[\sigma])} \tag{60}$$

which implies (59). In our work we consider algorithms which respect ergodicity and detailed balance condition.

3.2 AUTOCORRELATION AND ERROR ESTIMATION

The most common choice for W is the Metropolis algorithm. This is a stochastic dynamical algorithm which generates a Markov chain of configurations by local moves: starting from an initial field configuration σ of fields φ, the update configuration σ' is generated by randomly choosing a site x and by changing the value of the correspondent field $\varphi(x)$. This is an example of a *local algorithm* and a problem associated to this type of algorithms is that they produce correlated configurations.

The correlation enlarges the statistical error in the Monte Carlo estimations: in fact if we generate N configurations, the number of those effectively independent is N/τ, where τ is the *autocorrelation time* [69]. It represents the number of update sweeps required to make the configuration of the system statistically independent from the initial one. We can, actually, define two kind of autocorrelation time. The *exponential autocorrelation time*, τ_{exp}, represents the relaxation time of the slowest mode in the system. The *integrated autocorrelation time*, τ_{int}, which controls the statistical error in Monte Carlo measurements once the equilibrium has been attained.

τ_{exp} is defined through the *normalized autocorrelation function*

$$\rho_{AA}(t) \equiv C_{AA}(t)/C_{AA}(0) \tag{61}$$

where $C_{AA}(t) = \langle A_s A_{s+t} - \mu_A^2 \rangle$ is the unnormalized autocorrelation function. Then τ_{exp} is

$$\tau_{exp,A} = \limsup_{t \to \infty} \frac{t}{-\log |\rho_{AA}(t)|} \tag{62}$$

and

$$\tau_{exp} = \sup_A \tau_{exp,A}. \tag{63}$$

For a given observable A the integrated autocorrelation time is given by

$$\tau_{int,A} = \frac{1}{2} \sum_{t=-\infty}^{\infty} \rho_{AA}(t) = \frac{1}{2} + \sum_{t=1}^{\infty} \rho_{AA}(t) \tag{64}$$

The factor $1/2$ is inserted so that $\tau_{int,A} \sim \tau_{exp,A}$ if $\rho_{AA}(t) \sim e^{-|t|/\tau}$ with $\tau >> 1$. Thus the number of effectively independent samples in a run of length N is roughly $N/2\tau_{int,A}$ and the real variance of $\bar{A}$ is a factor $2\tau_{int,A}$ larger that it would be if the set of observables were statistically independent. In our simulations we used the method presented in [112] for the determination of the autocorrelation time and for the error estimation.

The determination of the autocorrelation time is an important aspect of simulations of critical phenomena, like continuous phase transitions. In fact at the critical point the correlation length ξ diverges following a power law. The relation between τ and ξ, at the criticality, is

$$\tau \sim \xi^z \sim \left(\frac{\beta_c - \beta}{\beta_c} \right)^{-z\nu}, \tag{65}$$

where ν is the critical exponent of the correlation length and z is the *dynamic critical exponent* which depends only on the update algorithm and on the observable to be computed. Usually, for local algorithms like Metropolis, $z \approx 2$. In real simulations we deal with finite lattice of size L and thus ξ could be at most $\xi \sim L$. Generally the CPU–time cost of one sweep is $\propto L^d$, where d is the system dimensionality. Near the transition, however, the effective cost is L^{d+z}, due to (65). Now if we want to simulate a system with a size two times greater then before ($2L$), keeping the number of the effectively independent N_{conf} constant, the simulation cost using a local algorithm would be $\sim 2^{d+z} = 2^{d+2}$. The fast increasing of τ as the system

approach the critical point is called *critical slowing down* [115]. A way to avoid this phenomenon, and equivalently to reduce CPU-time cost, is to adopt non–local update algorithm, characterized by z as small as possible.

In the following we see an effective method for the autocorrelation estimation of data generated through Monte Carlo simulations.

3.3 THE Γ–METHOD

In this section we describe the analysis tool we used to estimate the autocorrelation time of data generated with Markov Chain Monte Carlo (MCMC) algorithms.

Considering an ensembles of configurations $\{\sigma\}$, we suppose that, for each configuration σ_i we evaluate a set of physical observables $\{O_\alpha\}_{\alpha=1}^{N_\alpha}$, called *primary observables*. The MC evaluations of the α observables are denoted as $\mathcal{O}(\sigma_i) = o_\alpha^i$ where $i = 1, \ldots, N$, where N is the sample dimension.

The statistical correlation is captured by the *correlation matrix*, defined as

$$\begin{aligned}\Gamma_{\alpha\beta}(n) &= \left\langle \left(o_\alpha^i - O_\alpha\right)\left(o_\beta^{i+n} - O_\beta\right)\right\rangle \\ &= \sum_{q,q'\in\mathcal{S}} P(q)W^n(q\to q')(\mathcal{O}_\alpha(q) - O_\alpha)(\mathcal{O}_\beta(q') - O_\beta).\end{aligned}$$

The diagonal elements $\Gamma_\alpha \equiv \Gamma_{\alpha\alpha}$ are called *autocorrelation functions*. The averages indicated by the bracket notation $\langle\cdot\rangle$ are taken on ensembles of identical numerical experiments with independent random numbers and initial states. Typically, the autocorrelation functions exhibit an exponential decay for large times

$$\Gamma_\alpha(n) \sim \exp\left(-\frac{n}{\tau}\right), \quad n \to \infty. \tag{66}$$

In a broad variety of cases, the decay constant τ has the same order of magnitude of the equilibration time: accordingly, as a rule of thumb, an estimate of τ can be used to verify, *a posteriori*, that the thermalization time of the system was much bigger than τ

In order to compute the statistical error we define, for each observable O_α and through (64), the so called *integrated autocorrelation time*:

$$\tau_{\text{int},\alpha} = \frac{1}{2}\sum_{t=-\infty}^{\infty}\rho_\alpha(t) = \frac{1}{2}\frac{C_\alpha}{\Gamma_\alpha(0)}, \tag{67}$$

where C_α is the autocorrelation sum given by

$$C_\alpha = \sum_{t=-\infty}^{\infty}\Gamma_\alpha(t). \tag{68}$$

The quantity $\tau_{\text{int},\alpha}$ gives an estimate of the error of O_α due to the autocorrelation, once the Markov chain has been equilibrated. If we consider the sample mean

$$\bar{o}_\alpha = \frac{1}{N}\sum_{i=1}^{N} o_\alpha^i, \tag{69}$$

as an estimator of the exact value O_α, it can be shown that the resulting error σ_α of $\bar{o}_\alpha$ is given by

$$\sigma_\alpha^2 \approx \frac{2\tau_{\text{int},\alpha}}{N}\Gamma_\alpha(0) \quad \text{for} \quad N \gg \tau. \tag{70}$$

Therefore the variance given by $\Gamma_\alpha(0)$ is modified by a factor of $\frac{2\tau_{\text{int},\alpha}}{N}$ in presence of autocorrelations.

A significant issue, that may also affect the interpretation of the analysis results, concerns the practical estimate of the integrated autocorrelation time. We first need to introduce the estimator of the autocorrelation function associated to the observable O_α:

$$\bar{\Gamma}_\alpha(t) = \frac{1}{N-|t|}\sum_{i=1}^{N-|t|}\left(o_\alpha^i - \bar{o}_\alpha\right)\left(o_\alpha^{i+t} - \bar{o}_\alpha\right). \tag{71}$$

As a natural estimator for $\tau_{\text{int},\alpha}$ we could take

$$\bar{\tau}_{\text{int},\alpha} = \frac{1}{2}\frac{\bar{C}_\alpha(N-1)}{\bar{\Gamma}_\alpha(0)}, \tag{72}$$

where

$$\bar{C}_\alpha(N) = \bar{\Gamma}_\alpha(0) + 2\sum_{t=1}^{N}\bar{\Gamma}_\alpha(t) \tag{73}$$

is the estimator for the autocorrelation sum (68). However, it turns out that the variance of the estimator (72) does not vanish as N goes to infinity [69, 81], due to the presence of noise in the tail of $\rho(t)$. For this reason, we need to introduce a summation window $W < N$ into (72). As a side effect, such a truncation leads to a bias in the autocorrelation sum,

$$\frac{\left\langle \bar{C}_\alpha(W)\right\rangle - C_\alpha}{C_\alpha} \sim -e^{-\frac{W}{\tau}}, \tag{74}$$

which eventually translates into a systematic error associated to the observable O_α. Therefore, the choice of the summation window W should be made with care: it has to be large enough compared to the decay time τ so as to reduce the systematic error, but at the same time not too large in order to avoid the inclusion of excessive noise. We take as optimal the summation window W that minimizes the total relative error (sum of the statistical and systematic errors) on the considered observable [111, 112]

$$\frac{\delta_{\text{tot}}(\bar{\sigma}_\alpha)}{\bar{\sigma}_\alpha} \approx \frac{1}{2}\min_W\left(e^{-\frac{W}{\tau}} + 2\sqrt{W/N}\right), \tag{75}$$

where $\bar{\sigma}_\alpha^2 = \bar{C}_\alpha(W)/N$. In practice, such a value of W can be determined by using the automatic procedure proposed in Ref. [111, 112]. Under the assumption of an exponential decay of the autocorrelation function, we can write

$$2\bar{\tau}_{\text{int},\alpha}(W) = \sum_{t=-\infty}^{\infty}\exp\left(-\frac{S|t|}{\bar{\tau}(W)}\right) \tag{76}$$

where S is a positive factor and $\bar{\tau}(W)$ is an estimator for the decay rate τ. The S factor can be adjusted to account for possible discrepancies between τ and $\bar{\tau}(W)$. By inverting 76 one finds, at the first order, $\bar{\tau}(W) \sim S\bar{\tau}_{\mathrm{int},\alpha}$: we use this value of $\bar{\tau}(W)$ to evaluate the minimum of 75, which yields the optimal value for W (see As a consistency check of the resulting summation window, one can verify, by adjusting the value of S, that the plot of the integrated autocorrelation time as a function of W exhibits a plateau around the optimal value.

Generally one is interested in compute a *derived quantity*, namely a function f of the primary observables which we denote as

$$F = f(O_1, O_2, \ldots, O_{N_\alpha}) = f(O_\alpha).$$

In particular, this is necessary for those observables which can not be defined configuration by configuration, such as the magnetic susceptibility. Here we do not describe how the Γ–method is modified in the case of derived quantities, since it is quite similar to this case. For further details we refer the reader to [111, 112]. We only want to introduce a slight generalization to the case in which an ensemble of N data can be split into R statistically independent replica of experiments, each of them containing N_r estimates: we denote with $a_\alpha^{i,r}$ the i-th MC estimate of the r-th replicum. The autocorrelation function satisfies

$$\left\langle \left(o_\alpha^{i,r} - O_\alpha\right) \left(o_\beta^{i+n,s} - O_\beta\right) \right\rangle = \delta_{rs}\Gamma_{\alpha\beta}(n).$$

Notice that N_r must be chosen carefully, in order to effectively end up with statistically independent replica; in particular, if $N_r \gg \tau$ does not hold, the error estimation fails. The definition of the estimators for the general case with $R > 1$ is given in [112]

In the following we describe the analysis program we use to estimate the mean values, the statistical errors and the autocorrelation function we compute in our applications.

3.3.1 *Unew program*

We now present the main feature of the analysis program, called UNEW, we develop for doing the statistical analysis of our MC results. It implements the Γ–method, based on the work [112] and on the code [113]. The motivation of UNEW is to provide a user-friendly interface in an open-source environment. To this end, we consider Python to be the optimal language, since it features a rich set of modules—from statistical and numerical scopes to simple yet powerful graphics capabilities—and it is also widely used in academia. The program is devised so that the analysis process applies to both primary and derived observables. In the next we show some examples of autocorrelation analysis of data generated with the algorithm that will be presented in Chapter 4.1. For further details about the UNEW program we refer the reader to [31].

3.3.2 *Autocorrelation analysis*

Here we present an analysis of the following observables:

- The internal energy, defined as the average nearest neighbour correlation:

$$E = \frac{1}{d}\sum_{\nu} G(\nu, 0) = \frac{1}{2d}\frac{\langle\langle \rho(u-v)\delta_{|u-v|,1}\rangle\rangle}{\langle\langle \delta_{u,v}\rangle\rangle}$$

- The susceptibility

$$\chi^{-1} = \frac{1}{\sum_z G(z,0)} = \frac{\langle\langle \delta_{u,v}\rangle\rangle}{\langle\langle \rho(v-u)\rangle\rangle}.$$

- We define the following observable which, at the criticality, follows a scaling as a power of its critical exponent (see (2.1.3)):

$$f_\chi = L^{7/4}/\chi$$

The meaning of the double brackets and of $\delta_{u,v}$ and $\rho(u-v)$ will be clear after Chapter 4.1.

In Table 3 we report the results of the analysis. For each algorithm we consider different lattice sizes L and evaluate E and f_χ along with the respective autocorrelation times. In Fig. 3, 2 we show the UNEW plots of the autocorrelation time and of the normalized autocorrelation for the derived quantity f_χ in the case L = 32.

L	f_χ	τ_{f_χ}	E	τ_E
16	0.9162(28)	0.810(8)	0.7246(10)	0.558(6)
32	0.9162(33)	0.823(11)	0.7178(9)	0.568(15)
64	0.9182(38)	0.866(13)	0.7131(9)	0.557(22)
128	0.9149(44)	0.942(17)	0.7092(7)	0.499(1)
256	0.9203(50)	0.963(19)	0.7079(7)	0.503(1)

Table 3: Results obtained with the worm algorithm, performing 10^5 thermalization steps and 10^6 sweeps.

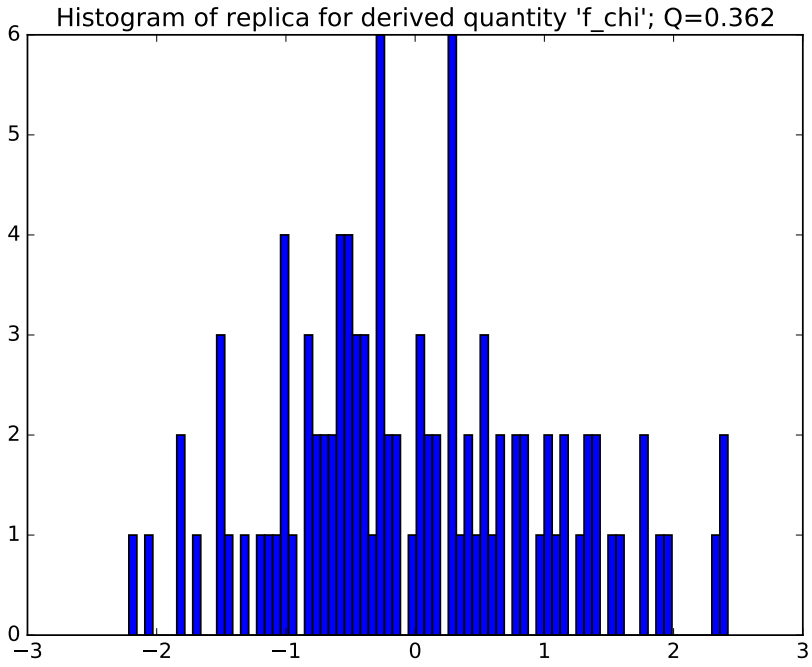

Figure 2: Histogram of 100 replica for the derived quantity f_χ.

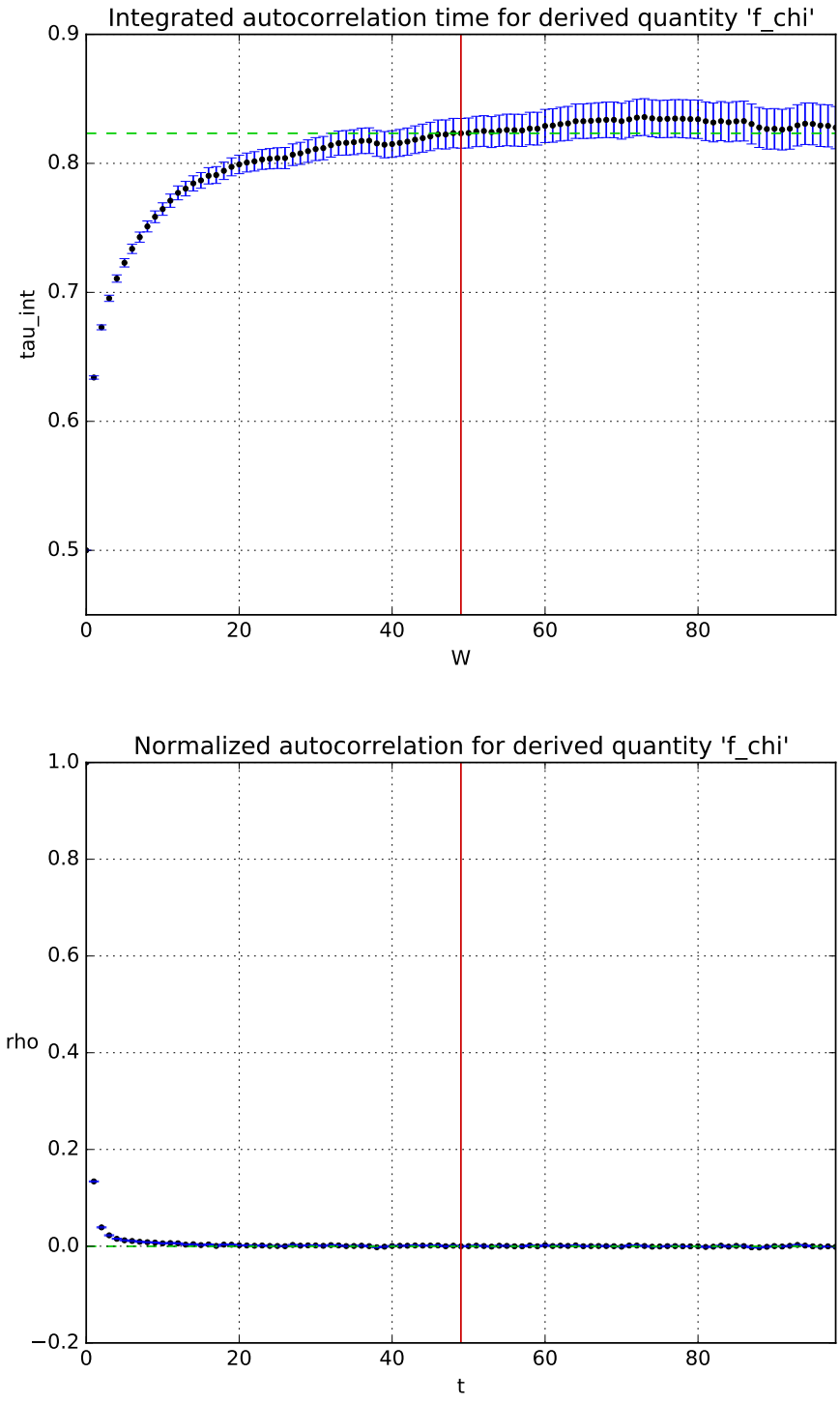
Integrated autocorrelation time for derived quantity 'f_chi'
tau_int
W
0.9
0.8
0.7
0.6
0.5
0
20
40
60
80
Normalized autocorrelation for derived quantity 'f_chi'
rho
t
1.0
0.8
0.6
0.4
0.2
0.0
−0.2
0
20
40
60
80

Figure 3

4

WORM ALGORITHM FOR SIMULATING $O(N)$ ϕ^4 THEORY

Now we present the non-local update algorithms we used in our simulations: the worm or PS algorithm, a method introduced by Prokof'ev and Svistunov in [84] and based on the *high temperature* or *strong coupling expansion* [14]. This procedure allow to translate the single site configurations in strong coupling representation by means of an exact reformulation: we pass from configurations of continuous fields located at the site of a d–dimensional lattice to configurations of discrete fields lying on links between neighbours sites, organized in closed path, called, for this reason, *closed path* or *CP configurations*. The different update steps for generating the CP configurations are constituted by local moves in the new representation and they can be pictorially described by the motion and the growth of a *worm* through the bonds of the lattice. The name *worm algorithm* came from this interpretation. The local moves in the new representation do not correspond to local moves in the original one and this is the main reason why the critical slowing down is drastically reduced [32, 83, 117].

In the following we review the procedure for translating the single site representation into CP representation for *i)* φ^4 theory, for *2)* $O(N)$ σ model and for the general *iii)* $O(N)$ φ^4 theory. Finally we describe the update steps of the algorithm in the three cases. For this scope we consider, from now on, a d–dimensional system defined on an hypercubical lattice of linear size L and lattice spacing $a = 1$, with periodic boundary conditions. The number of sites is $N_x = L^d = V$ and the

number of links is $N_l = dN_x$. The referring works of this chapter are [30, 102, 114, 118].

4.1 LOOP REPRESENTATION FOR φ^4 THEORY

Let us consider a system of one–component scalar fields φ located at the sites x of the hypercubical lattice, described by the Euclidean lattice action (37):

$$S[\varphi] = -\beta \sum_{x,\mu} \varphi(x)\varphi(x+\hat{\mu}) + \sum_{x} \left[\varphi^2(x) + \lambda(\varphi(x)^2 - 1)^2\right] = \mathcal{S}_{int} + \mathcal{S}_{site},$$

where we highlight the interaction term $\mathcal{S}_{int}$ and the single site contribution $\mathcal{S}_{site}$. The starting point of the strong coupling expansion is to consider the n–point correlation function:

$$G(x_1, ..., x_n) = \langle \varphi(x_1) \cdots \varphi(x_n) \rangle = \frac{\prod_x \int d\varphi(x) \mathrm{e}^{-\mathcal{S}[\varphi]} \varphi(x_1) \cdots \varphi(x_n)}{\prod_x \int d\varphi(x) \mathrm{e}^{-\mathcal{S}[\varphi]}} = \frac{Z(x_1, \cdots, x_n)}{Z(0)}. \tag{77}$$

Focusing on the numerator, we perform the power series expansion for small β of the exponential of the interaction term $e^{\mathcal{S}_{int}}$:

$$Z(x_1, \cdots, x_n) = \prod_x \int d\varphi(x) \mathrm{e}^{-\mathcal{S}_{site}(\varphi)} \left[\prod_{l=\langle y_1 y_2 \rangle} \mathrm{e}^{\beta \varphi(y_1)\varphi(y_2)} \right] \varphi(x_1) \cdots \varphi(x_n) \tag{78}$$

$$= \prod_x \int d\varphi(x) \mathrm{e}^{-\mathcal{S}_{site}(\varphi)} \left[\prod_{l=\langle y_1 y_2 \rangle} \sum_{k(l)=0}^{+\infty} \frac{[\beta \varphi(y_1)\varphi(y_2)]^{k(l)}}{k(l)!} \right] \varphi(x_1) \cdots \varphi(x_n), \tag{79}$$

The link index l labels each pair of neighbours; to each link we associate an integer number $k(l)$, used as summation variable over l. The product of infinite sums in the square brackets of (79) is then expanded into an infinite sum of products with l factors, where every term represents one distinct possibility to choose a value $k(l)$

for each l. Therefore, the sum $\sum_{k=0}^{\infty}$ is substitute with the sum over all possible configuration $\{k\}$ of k, and we can invert the summation with the product

$$\prod_{l} \sum_{k(l)} \longrightarrow \sum_{\{k\}} \prod_{l} .$$

In this way the product over fields at different sites can be reordered,

$$\left(\prod_{l=\langle y_1 y_2 \rangle} [\varphi(y_1)\varphi(y_2)]^{k(l)} \right) \varphi(x_1) \cdots \varphi(x_n) =$$
$$\left(\prod_{x} \varphi(x)^{\sum_{(l,dl)\ni x} k(l)} \right) \varphi(x_1) \cdots \varphi(x_n) = \prod_{x} \varphi(x)^{d(x)},$$

where, in the last member we have incorporated the n field insertions. We introduce the *integer site field* $d(x)$, defined as

$$d(x) = \sum_{(l,dl)\ni x} k(l) + \sum_{m=1}^{n} \delta_{x_m,x}. \tag{80}$$

where $\sum_{(l,dl)\ni x} k(l)$ indicates the sum over neighbours of the site x. The first term of (80) represents the sum of all links with value $k(l)$ connected to the x site and the second one is the number of time x appears in the sequence $x_1, ..., x_n$. If we joining together all the previous relations, the (79) can be expressed as :

$$Z(x_1, \cdots, x_n) = \sum_{\{k\}} w(k) \prod_{x} c(\lambda, d(x)), \tag{81}$$

where

$$\begin{aligned} c(\lambda, d(x)) &= \int_{-\infty}^{+\infty} d\varphi(x) \mathrm{e}^{-\varphi(x)^2 - \lambda[\varphi(x)^2-1]^2} \varphi(x)^{d(x)}, \\ w(k) &= \prod_{l} \frac{\beta^{k(l)}}{k(l)!}. \end{aligned} \tag{82}$$

In this way we reach the goal: the exact reformulation of the original partition function, in which the scalar fields $\varphi(x)$, lying on the lattice sites, have been translated

into integer link fields $k(l)$, lying on the bonds of the lattice. For what concerns the explicit computation of (82) we refer the reader to [102].

Observing the first equation in (82), we notice that, if $d(x)$ is odd, the integrand is clearly antisymmetric and, therefore, the integral is equal to zero. This defines a constraint and, at the same time, a rule for selecting valid configurations: at each site the sum of the all incident links must be even,

$$d(x) = 2n \qquad\qquad n \in \mathbb{N}. \tag{83}$$

In the case of the proper partition function $Z(0)$, $d(x)$ becomes:

$$d(x) = d_0(x) = \sum_{(l,dl)\ni x} k(l). \tag{84}$$

and the constraint implies that at each site there are not loose ends and thus the configurations are considered as *closed paths*.

Coming back to the initial point, the n-point correlation function (77), we need to take in account the fields insertion $\varphi(x_1)\cdots\varphi(x_n)$ at sites $x_1,\ldots,x_n$. In order to identify all valid configurations it is useful to define the following two sets of points [2].

- $Q(k)$ is the set containing all the sites surrounded by an odd number of links, namely

$$Q(k) = \left\{ x \quad t.c. \quad \sum_{(l,dl)\ni x} k(l) = 2n+1 \quad n \in \mathbb{N} \right\}, \tag{85}$$

- X is the one containing all the sites which appear an odd number of times

$$X = \left\{ x \quad t.c. \quad \sum_{m=1}^{n} \delta_{x_m,x} = 2n+1 \quad n \in \mathbb{N} \right\}.$$

The condition (83) is then translated in the following equivalence

$$Q(k) \equiv X. \tag{86}$$

In other words, if a site x is inserted an odd number of times, the number of links attached to this site must be odd.

Let us now consider the 2–point function in the new ensemble:

$$G(x_1, x_2) = \langle \varphi(x_1)\varphi(x_2) \rangle = \frac{Z(x_1, x_2)}{Z(0)}.$$

The condition (86) implies that, if $x_1 \neq x_2$, then the only allowed configurations are those with x_1 and x_2 as end points. On the other hand if $x_1 = x_2$ the sets X and $Q(k)$ are equal to zero. This implies that the only allowed paths for $Z(x_1, x_2)$ turn out to be closed paths (CP), which are already contained in $Z(0)$.

Relating the expression of $Z(x_1, x_2)$ and $Z(0)$ allows to define a new partition function which enlarges the link ensemble. Using the equation (81) and (84) we can write

$$Z(x, x_1) = \sum_{\{k\}} w(k) \left(\prod_{x \neq x_1} c(d_0(x)) \right) c(d_0(x_1) + 2), \tag{87}$$

$$Z(0) = \sum_{\{k\}} w(k) \left(\prod_{x \neq x_1} c(d_0(x)) \right) c(d_0(x_1) + 2) \frac{c(d_0(x_1))}{c(d_0(x_1) + 2)}. \tag{88}$$

As a matter of convenience we define $\tilde{c}(d(x))$ as

$$\tilde{c}(d(x)) = \frac{c(d(x-2))}{c(d(x))}.$$

Then $Z(x_1, x_2)$ and $Z(0)$ can be computed in one simulation, if we define the new partition function

$$\mathcal{Z} = \sum_{u,v} Z(u, v), \tag{89}$$

enlarging the ensemble. Consequently, the expectation value of an observable $A(k,u,v)$ now reads:

$$\begin{aligned}\langle\langle A(k,u,v)\rangle\rangle =& \frac{1}{\mathcal{Z}}\sum_{u,v} Z(u,v)A(k,u,v) \\ =& \frac{1}{\mathcal{Z}}\sum_{\{k\},u,v} w(k)\prod_x c(d(x))A(k,u,v).\end{aligned} \tag{90}$$

Therefore, $Z(x_1,x_2)$ is, in the new ensemble, the expectation value of delta functions

$$Z(x_1,x_2) = \mathcal{Z}\langle\langle \delta_{x_1,u}\delta_{x_2,v}\rangle\rangle,$$

and, accordingly, $Z(0)$ is expressed as

$$Z(0) = \frac{\mathcal{Z}}{V}\langle\langle \tilde{c}(d(u))\delta_{u,v}\rangle\rangle.$$

In conclusion the two point function is given by the following equation:

$$\begin{aligned}G(x_1,x_2) =& \langle\varphi(x_1)\varphi(x_2)\rangle = \frac{Z(x_1,x_2)}{Z(0)} \\ =& V\frac{\langle\langle \delta_{x_1,u}\delta_{x_2,v}\rangle\rangle}{\langle\langle \tilde{c}(d(u))\delta_{u,v}\rangle\rangle},\end{aligned} \tag{91}$$

where $V = L^d$ is the lattice volume.

4.1.1 *Worm update steps for φ^4 theory*

So far we have seen how to obtain the CP–configurations by means of the strong coupling expansion of (79). we have already mentioned that this procedure lead to a graphical representation of the ensemble configurations as collection of path, that we called *loop*. The worm algorithm sample them by local moves [49, 114, 117] and the different update steps of can be pictorially described by the motion and the growth of a *worm* through the links of the lattice. We indicate with u the head and with v the tail of the worm. They will indicate the extremities of the only path wit two loose ends, which is called *active loop*.

Let's now see the several update steps. The initial configuration can be any one that satisfies the constraint (83) or (86): the trivial choice corresponds to $k(l) = 0$ and $u = v$ located at a site x randomly selected, which we call *seed*. In this case it is necessary to await the achievement of the equilibrium before accumulating measurements. This happens after the thermalization process.

The Metropolis update is composed of two main steps :

1. *Moving the head.* We extract with equal probability one of the neighbouring site of u and we call it u'. The trial configuration is

$$\begin{aligned} u &\longrightarrow u', \\ k(\hat{l}) &\longrightarrow k(\hat{l}) \pm 1, \end{aligned} \tag{92}$$

   where $\hat{l}$ is the link between u and u'. At this stage we choose with equal probability to increment or decrement $k(\hat{l})$. The corresponding Metropolis acceptance probabilities are given by

$$P_{1,+} = \min\left(1, \frac{\beta}{(k(l)+1)\tilde{c}(d(u')+2)}\right) \tag{93}$$

   if the trial configuration is $k(\hat{l}) + 1$ and, in analogous way,

$$P_{1,-} = \min\left(1, \frac{k(l)}{\beta}\tilde{c}(d(u))\right) \tag{94}$$

   otherwise. Notice that the values of $k(l)$ must be positive or zero, since the probability of decreasing a bond with $k(l) = 0$ is equal to zero.

2. *Kick the seed.* The second step is not performed until the result of step 1 is $u = v$. In this case we choose randomly a site u' from the volume V with equal probability. The trial configuration is

$$\begin{aligned} u &\longrightarrow u' \\ v &\longrightarrow u'. \end{aligned} \tag{95}$$

This new configuration is accepted with probability

$$P_2 = \min\left(1, \frac{\tilde{c}(d(u))}{\tilde{c}(d(u'+2))}\right). \tag{96}$$

Performing this step does not change the value of $k(l)$. It is a "kick" to the worm seed to an other site and we will refer to it as the *kick* move.

One update is an execution of this two steps. For symmetry, we perform a number of $V/2$ updates once for the head and once for the tail: this constitute a *sweep* of the algorithm. Each of these two steps satisfy by construction the detailed balance condition. Furthermore an algorithm that performs this updates respects the condition of ergodicity, since there is a nonzero probability of generating all possible configurations in a finite number of steps starting from the trivial configuration.

4.2 LOOP REPRESENTATION FOR $O(N)$ σ−MODEL

Now we consider N components $\varphi(x) = (\varphi_1(x), \dots \varphi_N(x))$ fields of unit length with standard lattice action

$$\mathcal{S}_E = -\beta \sum_{x,\mu} \varphi(x)\varphi(x+\hat{\mu}).$$

In order to pass to the loop representation we start considering the partition function with two field insertion (in u and v) :

$$Z(u,v) = \int \left[\prod_z d\mu[\varphi[z]]\right] e^{\beta \sum_{\langle xy\rangle} \varphi(x)\cdot\varphi(y)} \varphi(u)\varphi(v) \tag{97}$$

The dot between pairs of spins mean $O(N)$ invariant scalar products, $\varphi(x)\cdot\varphi(y) = \sum_{i=1}^{N} \varphi(x)_i\varphi(y)_i$. The integration employ the normalized $O(N)$ invariant measure on the sphere

$$\int d\mu(\varphi) f(\varphi) = C_N \int_\Omega d^N x f(\mathbf{x}), \qquad \Omega = \{\mathbf{x} \in \mathbb{R}^N | \sum_i x_i^2 = 1\}$$

where C_N is the normalization constant, that is

$$C_N \int_\Omega d^N x = 1.$$

The n-dimensional surface area of the N-sphere with radius R is

$$S_N(R) = \frac{2\pi^{N/2}}{\Gamma(\frac{N}{2})} R^{N-1}.$$

In this particular case $R = 1$ and the normalization constant reduces to

$$C_N \int_\Omega d^N x = C_N \frac{2\pi^{N/2}}{\Gamma(\frac{N}{2})} = 1 \quad \Longrightarrow \quad C_N = \frac{\Gamma(\frac{N}{2})}{2\pi^{N/2}} \tag{98}$$

In order to discretise the problem we need to express the integral measure by means of the generating function for a general source j_α

$$\int d\mu(\varphi) e^{\mathbf{j}\cdot\mathbf{s}} = G_N(\mathbf{j}) = \sum_{n=0}^{\infty} c[n;N](\mathbf{j}\cdot\mathbf{j})^n \tag{99}$$

We write the left side of (99) in term of the volume element of the $(N-1)$–sphere, which generalizes the area element of the 2–sphere:

$$\int d\mu(\varphi) e^{j\cdot\varphi} = C_N \int \frac{d\,\Omega_{N-1}}{2} \int_0^{2\pi} d\theta\, (\sin\theta)^{N-2} e^{js\cos\theta} \tag{100}$$

We then use the modified Bessel function [1],

$$I_\nu(j) = \left(\frac{j}{2}\right)^\nu \frac{1}{\pi^{1/2}\Gamma(\nu+\frac{1}{2})} \int_0^\pi d\theta\, e^{\pm j\cos\theta} (\sin\theta)^{2\nu}. \tag{101}$$

and rewrite the second integral in the right hand side of (100) as follow:

$$\begin{aligned}
&\int_0^{2\pi} d\theta\, (\sin\theta)^{N-2} e^{js\cos\theta} \\
&= \int_0^{\pi} d\theta\, (\sin\theta)^{N-2} e^{js\cos\theta} + \int_\pi^{2\pi} d\theta\, (\sin\theta)^{N-2} e^{js\cos\theta} \\
&= \int_0^{\pi} d\theta\, (\sin\theta)^{N-2} e^{js\cos\theta} + \int_0^{\pi} d\theta\, (\sin\theta)^{N-2} e^{-js\cos\theta} \\
&= \int_0^{\pi} d\theta\, (\sin\theta)^{2(N/2-1)} (e^{js\cos\theta} + e^{-js\cos\theta}) \\
&= \int_0^{\pi} d\theta\, (\sin\theta)^{2\nu} (e^{js\cos\theta} + e^{-js\cos\theta}) = 2\left[\left(\frac{2}{j}\right)^\nu \pi^{1/2}\Gamma(\nu+\frac{1}{2}) I_\nu(j)\right].
\end{aligned} \tag{102}$$

The integral over the solid angle in (100) provides the result

$$\int \frac{d\,\Omega_{N-1}}{2} = \frac{2\pi^{(N-1)/2}}{2\Gamma((N-1)/2)} = \frac{2\pi^{(\nu+1/2)}}{2\Gamma(\nu+\frac{1}{2})} \tag{103}$$

Collecting (98), (102), (103) and using this other expression of the modified Bessel function with $\nu = N/2 - 1$

$$I_\nu(x) = \left(\frac{x}{2}\right)^\nu \sum_{k=0}^{\infty} \frac{1}{\Gamma(k+1)\Gamma(\nu+1+k)} \left(\frac{x}{2}\right)^{2k} \tag{104}$$

the generating function becomes:

$$\begin{aligned} G_N(j) =& \frac{2\,\pi^{\nu+1}\Gamma(\nu+1)\Gamma(\nu+1/2)}{2\,\pi^{\nu+1}\Gamma(\nu+1/2)} \left(\frac{2}{j}\right)^\nu \left(\frac{j}{2}\right)^\nu \sum_{k=0}^{\infty} \frac{1}{k!\Gamma(\nu+k+1)} \left(\frac{j}{2}\right)^{2k} \\ =& \sum_{k=0}^{\infty} \frac{\Gamma(\nu+1)}{2^{2k}k!\Gamma(\nu+k+1)} (j\cdot j)^k = \sum_{k=0}^{\infty} \frac{\Gamma(N/2)}{2^{2k}k!\Gamma(N/2+k)} (j\cdot j)^k. \end{aligned} \tag{105}$$

Again, the high temperature expansion is obtained by writing the exponential in (97) as a Taylor series, where the sum is over the integer link field $k(l) = 0, 1, 2, \ldots$

$$Z(u,v) = \sum_k \int \left[\prod_z d\mu(\varphi(z))\right] \prod_{l=\langle xy\rangle} \frac{\beta^{k(l)}}{k(l)!} [\varphi(x)\cdot\varphi(y)]^{k(l)} \varphi(u)\cdot\varphi(v). \tag{106}$$

Notice that the expression is similar to (79). For a give configuration z, we write the field integral as

$$X = \frac{\partial}{\partial j_\alpha(u)} \frac{\partial}{\partial j_\alpha(v)} \prod_l \left[\frac{\partial}{\partial j_\gamma(x)} \frac{\partial}{\partial j_\gamma(y)}\right]^{k(l)} \prod_z G_N(j(z))|_{j\equiv 0}.$$

As in the case of φ^4 we introduce the integer site field (80), which counts the number of fields or, equivalently, the number of j derivatives at x. In the case of two field insertion in u and v it reads:

$$d(x) = \sum_{(l,dl)\ni x} k(l) + \delta_{u,x} + \delta_{v,x}.$$

The admissible configuration are those for which $d(x)$ is even on all sites. The contribution of the filed integral becomes

$$X' = \frac{\partial}{\partial j_\alpha(u)} \frac{\partial}{\partial j_\alpha(v)} \prod_l \left[\frac{\partial}{\partial j_\gamma(x)} \frac{\partial}{\partial j_\gamma(y)} \right]^{k(l)} \prod_z [j(z) \cdot j(z)]^{d(z)/2}, \tag{107}$$

where there are as many j factor as derivatives. As in the φ^4 case, each term in (107) has a graphical representation through a graph, that with denote with Λ, drawn on the lattice: there are $k(l)$ lines between each nearest neighbour sites and all lines are arranged in closed loops. The difference with the previous case derive from the $O(N)$ structure. At each site all the incident lines close geometrically, made exception for u and v, where two lines are left locally unpaired and are, instead, closed with respect to $O(N)$ contractions. The number of graphs, or equivalently, the number of terms in (107) from taking all the derivatives is

$$\mathcal{M}_0[u, v; k] = \prod_z d(z)!.$$

Due to the $O(N)$ lattice symmetry, i.e. due to the structure of the index contraction at each site, each graph, for given u, v, k, appears many times among the $\mathcal{M}_0$ terms. Its multiplicity is given by

$$\mathcal{M}[u, v; k] = \frac{1}{\mathcal{S}[\Lambda]} \left(\prod_l k(l)! \right) \prod_x \left[\frac{d(x)}{2} \right]! 2^{d(x)/2}$$

where $\mathcal{S}[\Lambda]$ is a symmetry factor which take into account the overcounting of graphs due to the permutation of lines on the same link. Therefore, the total number of different graph for given u, v, k is equal to the ratio $\mathcal{M}_0/\mathcal{M}$.

Now we can write the analogous of (89): it is now expressed in term of a sum over graphs $\Lambda \in \mathcal{L}_2$, which include all possible location of u and v and all possible $k(l)$ assignments to links producing non–vanishing contributions.

$$\mathcal{Z} = \sum_{u,v} \rho^{-1}(u - v) Z(u, v) = \sum_{\Lambda \in \mathcal{L}} \rho^{-1}(u - v) W[\Lambda] \tag{108}$$

where

$$W[\Lambda] = \frac{N^{|\Lambda|}}{\mathcal{S}[\Lambda]}\beta^{\sum_l k(l)}\left[\prod_x 2^{-d(x)/2}\frac{\Gamma(N/2)}{\Gamma(N/2+d(x)/2)}\right] = \frac{N^{|\Lambda|}}{\mathcal{S}[\Lambda]}\beta^{\sum_l k(l)} f(x;N). \quad (109)$$

ρ is a positive weight to be chosen to roughly anticipate the decay of the two point function. With the new ensemble the expectation values reads

$$\langle\langle A\rangle\rangle = \frac{1}{\mathcal{Z}}\sum_{\Lambda\in\mathcal{L}^2}\rho^{-1}(u-v)W[\Lambda]A(\Lambda). \quad (110)$$

From this equation the two point function is given by

$$\langle\varphi_\alpha(0)\varphi_\beta(x)\rangle = \frac{\delta_{\alpha\beta}}{N}\rho(x)\frac{\langle\langle\delta_{u-v,x}\rangle\rangle}{\langle\langle\delta_{u,v}\rangle\rangle}, \qquad \text{with} \quad \rho(0)=1. \quad (111)$$

The expectation values referring to the vacuum configurations $\Lambda \in \mathcal{L}_2$ having $u = v$ are obtained as

$$\langle\langle A(\Lambda)\rangle\rangle_0 = \frac{\langle\langle A\delta_{u,v}\rangle\rangle}{\langle\langle\delta_{u,v}\rangle\rangle} \quad (112)$$

which is independent on the choice of ρ.

4.2.1 *Worm update steps for $O(N)$ σ model*

Now we describe the several probabilities ratio q for each possible move of the algorithm [118]. For this purpose we need to introduce some definitions: the active loop is the loop participant to the update process, u indicates the head and v the tail of the active loop, and an active loop is called trivial if it does not contain 2–vertex and $u = v$. The acceptance probability P is, as usual, given by $P = \min(1, q)$.

- *Extension*: in this move we try to extend the head u of the active loop to one of the nearest neighbours, u'. Thus the loop and worm parameters become

$$|\Lambda| \to |\Lambda|, \quad \mathcal{S}[\Lambda] \to \mathcal{S}[\Lambda],$$
$$d(u') \to d(u') + 2, \quad \kappa(u,u') \to \kappa(u,u') + 1$$

where (u, u') is the link joining u and u'. The amplitude ratio of this move is

$$q_1 = \frac{W[\Lambda']}{W[\Lambda]} = \frac{\beta}{N + d(u')} \tag{113}$$

Note that if $q_1 < 1$ then $P(\Lambda \to \Lambda') = q_1$, $P(\Lambda' \to \Lambda) = 1$ and detailed balance holds. The same is true if $q_1 > 1$.

$$\begin{aligned} &|\Lambda| \to |\Lambda|, \quad \mathcal{S}[\Lambda] \to \mathcal{S}[\Lambda], \\ &d(u') \to d(u') - 2, \quad \kappa(u, u') \to \kappa(u, u') - 1. \end{aligned}$$

- *Retraction*: now the head u is retracted by one link along the active loop and u' becomes the new head. In this case we have

$$\begin{aligned} &|\Lambda| \to |\Lambda|, \quad \mathcal{S}[\Lambda] \to \mathcal{S}[\Lambda], \\ &d(u') \to d(u') - 2, \quad \kappa(u, u') \to \kappa(u, u') - 1 \end{aligned}$$

and the amplitude ratio is

$$q_2 = \frac{W[\Lambda']}{W[\Lambda]} = \frac{N + d(u') - 2}{\beta}. \tag{114}$$

- *Re–routing of type* 1: this move starts with a trivial active loop and with $d(u) > 2$. Then we pick a 2–vertex at u and replace it by two 1–vertex (head and tail). In other words, we are opening a closed (passive) loop. We have

$$\begin{aligned} &|\Lambda| \to |\Lambda| - 1, \quad \mathcal{S}[\Lambda] \to \mathcal{S}[\Lambda'], \\ &d(u') \to d(u'), \quad \kappa(u, u') \to \kappa(u, u') \end{aligned}$$

and we easily obtain

$$\frac{W[\Lambda']}{W[\Lambda]} = \frac{1}{N} \frac{\mathcal{S}[\Lambda']}{\mathcal{S}[\Lambda]} \tag{115}$$

To quantify the amplitude ratio we have to understand how to compute the symmetry factor $\mathcal{S}[\Lambda]$ for a given local loop configuration. The simple loop has obviously $\mathcal{S} = 1$ (point F in Fig. 4). The symmetric factor of higher-loop

can be computed counting the number of permutations that leave the loop connectivity unchanged.

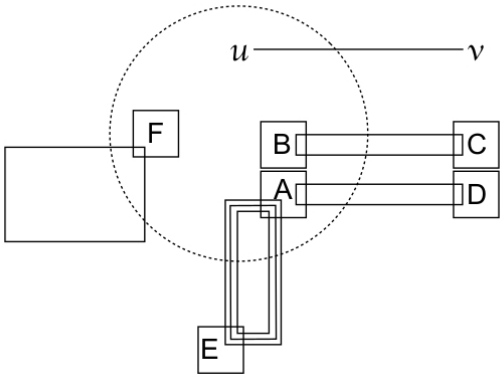

Figure 4: Exemplification of the loop connectivity at a particular site u.

Consider for example the triple loop in figure 4. Draw a point A with three exiting lines inside the site u (a circle) and a point E with three entering lines out of the sites. The first line in A can be attached to E in 3 ways (one of the three entering lines). The second line in A has only two choices left, the third just one. We end up with $\mathcal{S} = 3!$.

Consider now the double simple loop. Draw two point A and B inside the site, with two exiting lines each, and two points (C and D) outside the site (two entering line each). Now we have to connect the two points inside with the two point outside in all possible way leading to two loops. It is clear that we can join the first A line to C or D in four possible ways, bu at this point the second line A must be joined to the same outside point, so just one possibility. Now there are two choices left for the first B line, one choice for the second. All in all we have a factor $\mathcal{S} = 2^2 2! = 8$

Now consider the picture with a trivial active loop instead of the non–trivial one. Applying *re–rounting of type* 1, $\mathcal{S}[\Lambda]$ decreases of a factor 1, if we pick the simplest loop, of a factor 3, if we pick the triple loop or of a factor 4, if we pick the double–simple loop. In any case, the factor

$$f = \frac{\mathcal{S}[\Lambda]/\mathcal{S}[\Lambda']}{d(u) - 2} \tag{116}$$

is less then 1. This is a general property which holds in each case we are considering. Note that $d(u)-2$ is just the number of choices we can do in this type of move.

Now we pick randomly, with a flat distribution, a 2–vertex amongst the $d(u)-2$ possibilities at our disposal: it means that the probability to pick a particular 2–vertex is $1/(d(u)-2)$ and moreover have effectively $\mathcal{S}[\Lambda]/\mathcal{S}[\Lambda']$ choices. The amplitude ratio is now

$$q_3 = \frac{\mathcal{S}[\Lambda]/\mathcal{S}[\Lambda']}{d(u)-2}. \tag{117}$$

If $q_3 < 1$ we have that the effective probability to open the loop is

$$P(\Lambda \to \Lambda') = \frac{\mathcal{S}[\Lambda]/\mathcal{S}[\Lambda']}{d(u)-2}\frac{d(u)-2}{N} = \frac{1}{N}\frac{\mathcal{S}[\Lambda]}{\mathcal{S}[\Lambda']}$$

and the probability for the inverse move is 1. If $q_3 > 1$ then $P(\Lambda \to \Lambda') = 1$ and the probability of the inverse move is such that detailed balance holds in both cases.

- *Re–routing of type* 2: in this configuration the active loop is not trivial but $u = v$ holds. In this case we perform the inverse move of Re–routing of type 1 and thus

$$q_4 = \frac{N}{d(u)-2} \tag{118}$$

and

$$\begin{aligned} &|\Lambda| \to |\Lambda|+1, \quad \mathcal{S}[\Lambda] \to \mathcal{S}[\Lambda'], \\ &d(u') \to d(u'), \quad \kappa(u,u') \to \kappa(u,u') \end{aligned}$$

- *Re–routing of type* 3: the starting configuration correspond to $u \neq v$ and $d(u) > 2$. With equal probability we pick one of the lines connected to any of the 2–vertices at u and propose to redirect it to the 1–vertex. The line previously connected to the latter is joined to the open 2–vertex. We need to distinguish several sub-cases.

a) If the chosen 2–vertex belongs to a passive loop, the latter gets inserted into the active loop and thus $|\Lambda| \to |\Lambda - 1|$ and

$$q_5 = \frac{1}{N} \tag{119}$$

b) If the chosen 2–vertex belongs to the active loop, which self intersects at u, the chosen line leads towards the 1–vertex at v. A new passive loop is created, $|\Lambda| \to |\Lambda + 1|$ and

$$q_6 = N \tag{120}$$

c) The chosen 2–vertex belongs to the active loop as the previous move, but now only a reorganisation of the active loop connections is performed. We have $|\Lambda| \to |\Lambda|$ and

$$q_7 = 1 \tag{121}$$

- Kick: if the the active loop is trivial, we choose randomly a site x and promote it to trivial active loop following the amplitude ratio

$$q_8 = \frac{N + d(u) - 2}{d(x) + N}. \tag{122}$$

The loop and worm parameters remain unchanged.

4.3 LOOP REPRESENTATION FOR $O(N)$ φ^4 THEORY

Now we show the extension of the worm algorithm to the case of ϕ^4 theory with $O(N)$ symmetry, already presented in [30]. In this case we consider N components scalar fields $\varphi(x) = (\varphi_1(x), \dots \varphi_N(x))$, described by the lattice action

$$S[\varphi] = -\beta \sum_{x,\mu} \varphi(x)\varphi(x+\hat{\mu}) + \sum_x \left[\varphi^2(x) + \lambda(\varphi(x)^2 - 1)^2\right] = \mathcal{S}_{int} + \mathcal{S}_{site},$$

where the scalar product is implied. As usually, we start writing the partition function with two field insertions

$$Z(u,v) = \int \left[\prod_z d\varphi(z) e^{-\mathcal{S}_{site}}\right] e^{\beta \sum_{\langle xy\rangle} \varphi(x)\cdot\varphi(y)} \varphi(u)\varphi(v). \tag{123}$$

The discretisation procedure is quite similar to the previous case. In order to obtain an expression similar to (99), we absorb the $e^{-S_{site}}$ factor in the integral measure:

$$\int \prod_x d\varphi(x) e^{-\varphi\cdot\varphi - \lambda(\varphi\cdot\varphi - 1)^2} = \int \prod_x d\mu[\varphi(x)] \tag{124}$$

providing the following integration over a N-sphere of radius R,

$$\int d\mu(\varphi) f(\varphi) = C_N \int d\,r\, d\theta \frac{d\,\Omega}{2} r^{N-1} (\sin\theta)^{N-2} f(r,\theta,\Omega),$$

where C_N is the normalization coefficient, r is the radial integration variable and θ, Ω constitute the total solid angle for the N-sphere. Now the radial integral is switched on since the N component fields $\varphi(x)$ have a length varying from zero to infinity. The calculation of the generating function (99) goes more or less as in the σ– model case (see Subsec. 4.2) and we need to work out the integration over spherical coordinates in N dimension:

$$\int d\mu[\varphi(x)] e^{j\cdot\varphi} = \int r^{N-1} (sin\theta)^{N-2} e^{j\varphi\cos\theta} e^{-|\varphi|^2 - \lambda(|\varphi|^2-1)^2} d\,r\, d\theta \frac{d\,\Omega}{2} \tag{125}$$

The only different with the $O(N)$ case is the presence of the radial integral that can be computed only numerically. In order to simplify the notation we indicate with $\varrho(N,k)$ the result of the radial integration:

$$\int d\mu[\varphi(x)]e^{j\cdot\varphi} = \sum_{k=0}^{\infty} c[k;N](\tilde{j}\cdot\tilde{j})^k = \sum_{k=0}^{\infty} \frac{\varrho(N+k-1)\Gamma(N/2)}{\varrho(N-1)2^{2k}k!\Gamma(N/2+k)}(j\cdot j)^k \quad (126)$$

Again, these expression are obtained using the modified Bessel function $I_{N/2-1}$. The (126) is the key quantity for computing the observables in a $O(N)\phi^4$ model.

4.3.1 *Worm update steps for $O(2)$ φ^4 theory*

The several worm moves are formally the same as in the σ–model case, but now some of them have a different acceptance probability. Here we only mention those which differ with respect to 4.2, implying that the other ones remain the same.

- *Extension*: we try to move the head u to one of the nearest neighbor u'.

$$q_1 = \frac{\varrho(N+d(u')/2)}{\varrho(N+d(u')/2-1)}\frac{\beta}{N+d(u')} \quad (127)$$

- *Retraction*: we try to retract the head u by on link along the active loop and u' is the new head.

$$q_2 = \frac{\varrho(N+d(u)/2-2)}{\varrho(N+d(u')/2-1)}\frac{N+d(u')-1}{\beta} \quad (128)$$

- *Kick*: if the loop is trivial, we randomly pick a site x and try to move the trivial loop in that site.

$$q_3 = \frac{\varrho(N+d(x)/2)\varrho(N+d(u)/2-2)}{\varrho(N+d(x)/2-1)\varrho(N+d(u)/2-1)}\frac{N+d(u)-2}{N+d(x)} \quad (129)$$

Part III

LATTICE SIMULATIONS ON ϕ^4 THEORY IN TWO DIMENSION

5

DETERMINATION OF THE CRITICAL COUPLING: PART I

In this Part we focus on the ϕ^4 theory in a two–dimensional Euclidean space time. The model is described by the Lagrangian density

$$\mathcal{L}_E(\phi, \partial\phi, \ldots, x) = \frac{1}{2}(\partial_\nu \phi)^2 + \frac{1}{2}\mu_0^2\phi^2 + \frac{g}{4}\phi^4, \tag{130}$$

where μ_0 and g are, respectively the bare mass and the bare coupling. The Euclidean action is given by

$$\mathcal{S}_E[\phi] = \int d^2x\, \mathcal{L}_E(\phi, \partial\phi, \ldots, x).$$

As we have already seen, in $d < 4$ ϕ^4 theory is super–renormalizable, meaning that the coupling constant g has a positive mass dimension. Since the action is, by its definition, a dimensionless quantity, we find, in particular that $[g] = [\mu_0^2]$. Therefore, the only physically relevant parameter is the dimensionless ratio $f \equiv g/\mu^2$, where μ^2 is a renormalised squared mass in some given renormalisation scheme.

The evaluation of f at the critical point, i. e. in the limit in which both μ^2 and g go to zero, is still a challenging goal, as one can see from Table 4. The several results are obtained with different techniques: the works [44, 62, 71, 87, 97] are based

on Hamiltonian truncation (variational) methods, while in [119] lattice theory is simulated by using non–local SLAC derivative. In [19] we obtained our first determination of f by means of lattice simulations, using the worm algorithm, already presented in 4.1. In this chapter we are going to describe the numerical strategy we adopt in order to obtain our first results.

Table 4: Sample of the results for the continuum critical parameter f_0 from the literature. DLCQ stands for *Discretized Light Cone Quantization*, QSE diagonalization for *Quasi–Sparse Eigenvector* diagonalization, DMRG for *Density Matrix Renormalization Group* and for DLCH-FS *Diagonalized light-front Hamiltonian in Fock-Space representation*.

Method	f_0	year, Ref.
DLCQ	5.52	1988, [44]
QSE diagonalization	10	2000, [62]
DMRG	9.9816(16)	2004, [97]
Monte Carlo cluster	$10.8^{0.1}_{0.05}$	2009, [88]
Monte Carlo SLAC derivative	10.92(13)	2012, [119]
Uniform Matrix product states	11.064(20)	2013, [71]
Renormalised Hamiltonian	11.88(56)	2015, [87]
Monte Carlo worm	11.15(6)(3)	**2015**, [19]
Borel summability	11.00(4)	2015, [79]
DLCH-FS	4.40(12)	2016, [22]

5.1 ON THE CONTINUUM LIMIT OF f

We start by putting system on a 2–dimensional lattice with spacing a and introduce the following parametrization

$$\hat{\mu}_0^2 = a^2\mu_0^2, \qquad \hat{g} = a^2 g. \tag{131}$$

In this way we obtain a dimensionless discretized action

$$\mathcal{S}_E = \sum_x \left\{ -\sum_\nu \phi_x \phi_{x+\hat{\nu}} + \frac{1}{2}\left(\hat{\mu}_0^2 + 4\right)\phi_x^2 + \frac{\hat{g}}{4}\phi_x^4 \right\}, \tag{132}$$

where $\phi_{x\pm\hat{\nu}}$ are fields at neighbor sites in the $\pm\nu$ directions.

The continuum limit of the theory is reached when the correlation length ξ is finite and the lattice spacing a is zero. We can change the point of view and consider a as fixed and sending ξ to infinity in lattice spacing units. As showed in [58, 91, 108], quantities that are not dimensionless will behave very differently if measured in units of ξ or of a respectively. In the first approach, if we simply take the limit $a \to 0$, at fixed physical quantities, we obtain, in $d < 4$, the critical Gaussian model [76].

Consider now the ratio ξ/a: it is a function only of $\hat{\mu}_0^2$ and $\hat{g}$ and it diverges on the critical line $\hat{\mu}_0^2 = \hat{\mu}_c^2(\hat{g})$. If g measured in units of ξ remains finite in the limit of $a \to 0$, also $\hat{g}$ goes to zero. In this case we can find the critical value $\hat{\mu}_c^2$ using perturbation theory, getting $\hat{\mu}_c^2(\hat{g}) = A\hat{g} + \text{corrections}$. This means that all the quantities that receive contributions mainly from the large–scale fluctuations are finite in units of ξ, while the quantities that receive contributions mainly from the short–scale fluctuations are finite in their natural unit a, but diverges if measured in unit of ξ. Therefore we want to study the limit $a \to 0$ because it corresponds to focus on the quantities dominated by the critical fluctuations, neglecting all short–distance phenomena. In this limit the only dimensionless parameter in the action (132) is the ratio $f = g/\mu_0^2$. We want to determine its finite value when $a \to 0$ by fixing a value of g and search for a value of μ_0^2 such that we reach, in the infinite volume limit, a second order phase transition point in the plane (g, μ_0^2) (i.e. we reach the critical line $\hat{\mu}_0^2 = \hat{\mu}_c^2(\hat{g})$). In the continuum limit the bare mass parameter diverges like $\log(a)$ and thus we have to work out an additive renormalisation, while we do not care about self–coupling and strength renormalisation, since they amount to finite factors.

5.1.1 *Renormalization of ϕ_2^4*

The renormalisation procedure we adopt is the same as used in [64, 88]. The mass renormalization is performed by adding a proper divergent mass–squared counterterm in the Lagrangian (130). To this scope we introduce the following parametrization

$$\mu^2 = \mu_0^2 + \delta\mu^2. \tag{133}$$

Then (130) becomes

$$\mathcal{L}_E = \frac{1}{2}\left(\partial_\mu \phi\right)^2 + \frac{1}{2}(\mu^2 - \delta\mu^2)\phi^2 + \frac{g}{4}\phi^4. \tag{134}$$

where the ultraviolet dependence of μ_0^2 is completely moved into $\delta\mu^2$. The partition of the finite part of μ_0^2 into μ^2 and $\delta\mu^2$ is defined only once the renormalization condition is specified. The effective coupling f manifestly depends on the choice of renormalization condition which fixes the finite part of $\delta\mu^2$.

We choose the mass renormalization to be equivalent to normal ordering the interaction in the interaction picture in the symmetric phase: in this way the critical value of the effective dimensionless coupling distinguishes between the symmetric phase and the broken symmetry phase.

In order to eliminate the ultraviolet divergence we write the inverse propagator $G^2(p^2)$ as

$$G^{-1}(p^2) = p^2 + \mu_0^2 + \Sigma_0(p^2) = p^2 + \mu^2 + \Sigma(p^2) \tag{135}$$

and put the divergent contribution into $\Sigma(p^2)$

$$\Sigma(p^2) = 3\lambda A(\mu_0^2) - \delta\mu^2 + \text{two–loop} \tag{136}$$

The factor $A(\mu^2)$ in the continuum limit is the ultraviolet divergent Feynman integral

$$A(\mu^2) = \int \frac{d^2p}{(2\pi)^2}\frac{1}{p^2 + \mu_0^2}.$$

and corresponds to the 1–Particle–Irreducible divergent diagram shown in Fig. 1. Its expression on a lattice with $N \times N$ points is

$$A(\mu_0^2) = \frac{1}{N^2}\sum_{k_1=0}^{N-1}\sum_{k_2=0}^{N-1}\frac{1}{4\left(\sin^2\frac{\pi k_1}{N} + \sin^2\frac{\pi k_2}{N}\right) + \mu_0^2}, \tag{137}$$

and a suitable renormalisation condition consists in putting μ^2 equal to the solution, in the infinite volume limit, of the equation

$$\mu^2 = \mu_0^2 + 3gA(\mu^2). \tag{138}$$

Applying this renormalization condition to (134) and using the definition of the effective coupling $f = g/\mu^2$, we obtain

$$\begin{aligned} \mathcal{L} &= \frac{1}{2}\left(\partial_\mu \phi\right)^2 + \frac{1}{2}\mu^2\phi^2 - \frac{3}{2}gA(\mu_0^2)\phi^2 + \frac{g}{4}\phi^4 \\ &= \frac{1}{2}\left(\partial_\mu \phi\right)^2 + \frac{1}{2}\mu^2(1 - 3fA(\mu^2))\phi^2 + \frac{f\mu^2}{4}\phi^4. \end{aligned} \tag{139}$$

As f varies from zero to infinity, we can observe the two different phase: on the lattice $A(\mu^2)$ is finite and for small values of f, the exact effective potential has single minimum at $\langle\phi\rangle = 0$, representing the symmetric phase region. For large values of f, instead, the coefficient of ϕ^2 is negative and this suggests a transition to the broken symmetry phase. Due to the strong coupling, the effective potential cannot be approximated by its tree level form, this argument is not enough to demonstrate the existence of the transition. In [25, 26] a duality transformation from the strong coupling regime to a weakly coupled theory normal ordered with respect to the vacuum of the broken symmetry phase is constructed.

5.1.2 *Numerical strategy*

In order to simulate the system in the vicinity of criticality, it is useful to resort to relations (36) that, in $d = 2$, are given by:

$$\phi_x = \sqrt{\beta}\varphi, \qquad \mu_0^2 = 2\frac{1-2\lambda}{\beta} - 4, \qquad g = \frac{4\lambda}{\beta^2}. \tag{140}$$

With this parametrization the (132) becomes:

$$\begin{aligned} \mathcal{S}_E &= -\beta \sum_x \sum_\nu \varphi_x \varphi_{x+\hat{\nu}} + \sum_x \left[\varphi_x^2 + \lambda(\varphi_x^2 - 1)^2\right] \\ &= \mathcal{S}_I + \mathcal{S}_{Site}, \end{aligned} \tag{141}$$

where we recognize an interaction term between neighbour sites, $\mathcal{S}_I$, with a coupling constant of strength β and a term related to a single site, $\mathcal{S}_{Site}$. Thanks to this parametrization the *Ising limit* can be easily recovered for $\lambda \to \infty$: in fact, in this limit, configurations with $\varphi^2 \neq 1$ are completely suppressed and the fields assume only values $\varphi(x) = \pm 1$. As a result, the second term of (141) can be disregarded and the action becomes the well–known Ising action $\mathcal{S}_E = -\beta \sum_x \sum_\nu \varphi_x \varphi_{x+\hat{\nu}}$.

Using this parametrization, the critical point is obtained by fixing a value of λ and searching the corresponding critical value β such that the following relation is satisfied:

$$mL = \frac{L}{\xi} = \text{const} = z, \tag{142}$$

where m is determined by the second moment mass:

$$\frac{G(p^*)}{G(0)} = \frac{m^2}{\hat{p}^{*2} + m^2}, \quad \text{with} \quad \hat{p}^* = (2\pi/L, 0). \tag{143}$$

$G(p)$ is the two-point function in momentum space, and $\hat{p}^*$ is the smallest momentum on a lattice of linear size L. The condition (142) and the mass definition (143) imply that the correlation length ξ grows linearly with L and when $L/a \to \infty$ at fixed a we get the infinite volume limit (we are adopting the point of view in which a is finite and $\xi \to \infty$, as discussed in 5.1).

Practically we simulate several lattices with different values of $N \equiv L/a$; for each couple (λ, N) we obtain a value of $\beta(\lambda, N)$ such that $mL = z$. We chose in particular

$$z = mL = \frac{L}{\xi} = 4. \tag{144}$$

This means that the lattice is four times larger then the correlation length and this ensures that the finite size effect are small (we will discuss the role of the value chosen for z). After this step we extrapolate our results to $a/L \to 0$ in order to compute $\beta_\infty(\lambda)$ in the infinite volume limit. Using the relations (140) we derive $g(\lambda, \beta)$ and $\mu_0^2(\lambda, \beta)$ and then we compute $\mu^2(g)$ by means of the renormalisation condition (138). Finally we pin down the ratio g/μ^2. This procedure is repeated for several values of λ (and hence of g) and, in the end, we extrapolate our results

to $g \to 0$, in order to get f in the continuum limit.

In the following sections we describe more in depth the several steps of simulations.

5.1.3 *Finding β at finite lattice*

At a fixed value of λ we simulate the system for five values of L/a, namely: $L/a =$ 192, 256, 384, 512 and 768. For each value of L/a few preliminary simulations are needed to roughly find the value of β such that $z \simeq 4$. In few cases (see for example Fig. 5) we have explicitly checked that using five values of β such that $z \in [3.8, 4.2]$, no sign of non–linearity of z as a function of β are observed. The difference in $\beta(z = 4)$ between the case in which we use 5 points to interpolate and the case in which we use only 3 points is one order of magnitude less than the statistical error itself. We then decided to use just 3 values of β for the real simulations to linearly interpolate the results and to obtain in this way $\beta(\lambda, N)$. In Tables 6, 7, 8, 9 we show some examples of our linear regression.

The number of thermalization sweeps for all our simulations is several hundreds times τ_z, the autocorrelation time of $z = mL$. We computed τ with the method presented in [111, 112], using a Python program described in [31]. After the thermalization time, we start to accumulate measurements. We vary the number of worm–sweeps N_{sweep} between two consecutive measurements according to L and λ, increasing N_{sweep} for large L or small λ, in order to minimize the simulation time. A typical full simulation ($\lambda = 0.25$) is synthesized in Table 5.

Table 5: Summary of simulations performed at $\lambda = 0.25$

L/a	N_{meas}	N_{sweep}	$\beta_c(z = 4)$
192	1×10^5	15	0.655357(12)
256	5×10^4	15	0.656177(11)
384	5×10^4	15	0.656984(8)
512	3×10^4	20	0.657399(7)
768	2×10^4	25	0.657818(10)
∞			0.658628(10)

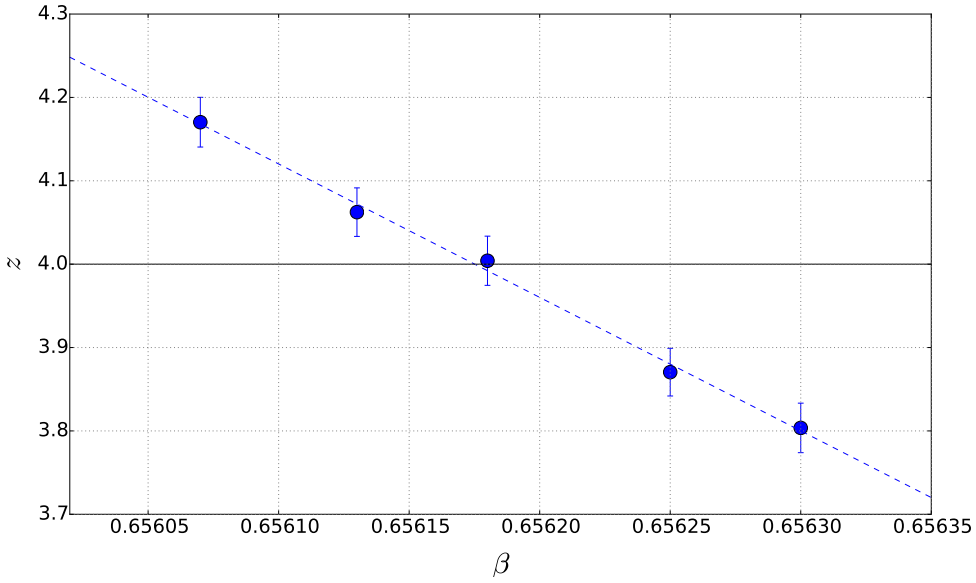

Figure 5: Linear interpolation ($\lambda = 0.25$, $L = 256$) to obtain $\beta(z = 4)$.

5.1.4 *Finding β_c in the infinite volume limit*

The extrapolation of β at $L \to \infty$ involves, again, a linear regression. This time the extrapolation is performed following finite size scaling arguments.

ϕ^4 theory is in the same universality class of the Ising model [70], and we know that in $d = 2$ the critical exponent of the correlation length is $\nu = 1$. At the critical point the behaviour of the mass, or equivalently of the correlation length, is given by the universal relation

$$\xi = \frac{1}{m} = \kappa \left(\beta - \beta_c\right)^{-\nu} = \kappa \left(\beta - \beta_c\right) \implies m = \kappa \left(\beta - \beta_c\right), \tag{145}$$

where κ is a constant. Using the condition (144) we have

$$\beta = \beta_c + \frac{4}{\kappa L}. \tag{146}$$

The behaviour expressed in (146) is numerically confirmed for all value of λ we explored. In Figure 6 we report the linear regression of β_c at $\lambda = 0.75, 0.2, 0.5, 0.75$

and in Tables 10, 11, 12, 13 we presented the related data points. For every value of λ considered, we obtain a very reasonable value of $\chi^2 \leq 1$.

Table 6: Results of β at $\lambda = 0.25$ and size $L = 256$

L	β	mL	Nmeas/10^4	Nbins	Nsweep	τ_{int}
256	0.65607	4.170(31)	5	10^3	12	0.49
256	0.65619	3.978(30)	5	10^3	12	0.57
256	0.65630	3.803(30)	5	10^3	12	0.71
Linear Regression						
256		$mL = 4$		$\beta = 0.65617(1)$		

Table 7: Results of β at $\lambda = 1$ and size $L = 384$

L	β	mL	Nmeas/10^4	Nbins	Nsweep	τ_{int}
384	0.6780	4.154(26)	8	10^3	10	0.59
384	0.6781	3.990(26)	8	10^3	10	0.57
384	0.6782	3.841(25)	8	10^3	10	0.51
Linear Regression						
384		$mL = 4$		$\beta = 0.67809(1)$		

Table 8: Results of β at $\lambda = 0.0625$ and size $L = 512$

L	β	mL	Nmeas/10^4	Nbins	Nsweep	τ_{int}
512	0.58133	4.274(42)	2	10^3	70	0.59
512	0.58137	4.031(45)	2	10^3	70	0.54
512	0.58141	3.779(38)	2	10^3	70	0.49
Linear Regression						
512		$mL = 4$		$\beta = 0.581374(4)$		

Table 9: Results of β at $\lambda = 0.38$ and size $L = 768$

L	β	mL	Nmeas/10^4	Nbins	Nsweep	τ_{int}
768	0.67741	4.200(51)	1	10^3	40	0.46
768	0.67749	3.911(54)	1	10^3	40	0.51
768	0.67757	3.513(56)	1	10^3	40	0.48
Linear Regression						
768	$mL = 4$		$\beta = 0.677460(8)$			

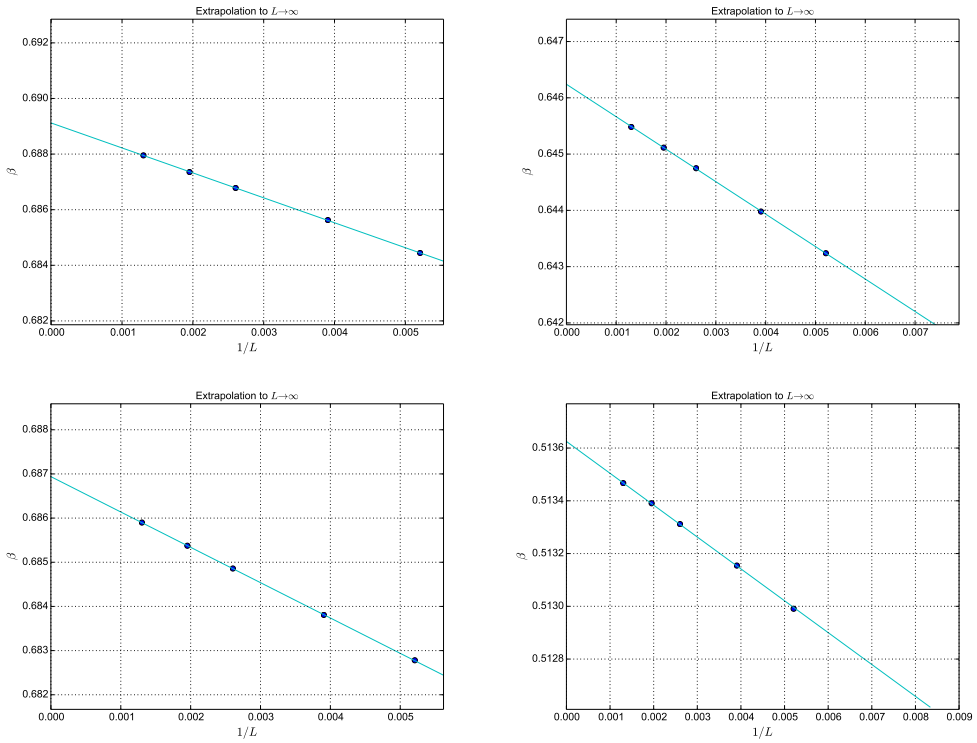

Figure 6: Linear regression of β at infinite lattice size

5.1.5 β_c *in the continuum limit*

In order to reach the continuum limit we need to send $\lambda \to 0$. The relations between the physical parameter (140) fix the limit value $\beta(\lambda = 0) = 1/2$, as shown in Figure 8, where we display the values of β_c as function of λ.

Table 10: Linear regression of β_{crit} at $\lambda = 0.75$

λ	L	β
0.75	192	0.684442(15)
0.75	256	0.685627(19)
0.75	384	0.686780(12)
0.75	512	0.687354(15)
0.75	768	0.687953(10)
	Linear Regression	
β_{crit}	0.689117(13)	
χ^2/d.o.f.	0.41	

Table 11: Linear regression of β_{crit} at $\lambda = 0.5$

λ	L	β
0.5	192	0.682780(19)
0.5	256	0.683808(10)
0.5	384	0.684858(10)
0.5	512	0.685374(5)
0.5	768	0.685899(9)
	Linear Regression	
β_{crit}	0.686938(10)	
χ^2/d.o.f.	0.27	

We now focus on the choice of the value of z. The condition (144) is not crucial: it is known that we could choose another value of z without affecting the results in the finite volume. From a numerical point of view a different choice of z could affect the statistical error of the extrapolation. In Figure 9 we show, as an example, a double extrapolation to $a/L = 0$ in the case $\lambda = 1$. For $z = 4$ the extrapolation to $a/L = 0$ is steeper than for $z = 1$, since in the latter case, at finite volume, we are nearer to criticality, so that $\beta(\lambda, N)$ is not so far from the infinite volume value. Nevertheless at $z = 4$ we obtain a much more clear signal; we can extrapolate to the $a/L = 0$ value with a much smaller statistical error even if the number of

Table 12: Linear regression of β_{crit} at $\lambda = 0.2$

λ	L	β
0.2	192	0.643238(10)
0.2	256	0.643979(8)
0.2	384	0.644749(7)
0.2	512	0.645114(9)
0.2	768	0.645482(9)
Linear Regression		
β_{crit}	0.646247(8)	
χ^2/d.o.f.	1.30	

Table 13: Linear regression of β_{crit} at $\lambda = 0.005$

λ	L	β
0.005	192	0.512990(4)
0.005	256	0.513154(3)
0.005	384	0.513311(2)
0.005	512	0.513390(2)
0.005	768	0.513467(1)
Linear Regression		
β_{crit}	0.513625(2)	
χ^2/d.o.f.	1.15	

measures is $(5-10)$–times smaller than the case $z = 1$. The results in the infinite volume limit coincide within the statistical errors; $\beta(z = 1) = 0.68060(4)$, to be compared with the equivalent value in Table 16, $\beta(z = 4) = 0.680601(11)$.

5.1.6 *Combined Metropolis and single cluster Wolff simulations*

In order to individuate the most suitable fit function for the extrapolation of f as $g \to 0$, we decide to adopt the same strategy as used in [88], but for computing higher values of g, namely $g = 4$ and $g = 6$. In particular the field configura-

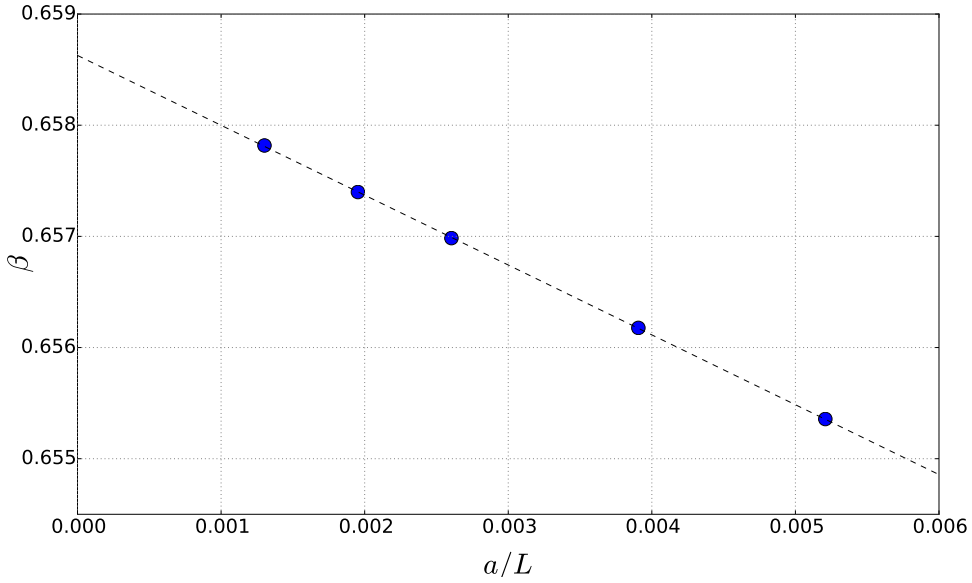

Figure 7: Linear extrapolation of β to $a/L = 0$ at $\lambda = 0.25$.

tions are generated using a mixture of Metropolis steps and single cluster Wolff steps [109, 110, 116].

The numerical strategy, as showed in [88], consists in finding the peak of the magnetic susceptibility χ in order to reach the pseudo–transition point at finite volume. In particular for each L/a we search for the value of μ_0^2 that maximize $\chi = \langle \bar{\phi}^2 \rangle - \langle |\bar{\phi}| \rangle^2$. $\bar{\phi}$ is the average of the field over the whole lattice. μ_0^2 is then extrapolated to $a/L \to 0$ and the corresponding μ^2 is obtained by means of condition (138).

The simulations are performed on a square lattice of sizes $L = 128, 192, 256, 384, 512$. After the thermalization we accumulate 10^5 measurements for each input parameter μ_0^2. We checking the autocorrelation times in each simulations, finding $\tau \sim 10 \div 100$ measurements, and then we group data into bins with different magnitude according to the size of the lattice. In Table 14 and 15 we show results of f respectively at finite volume (for $g = 4$) and at infinite volume limit.

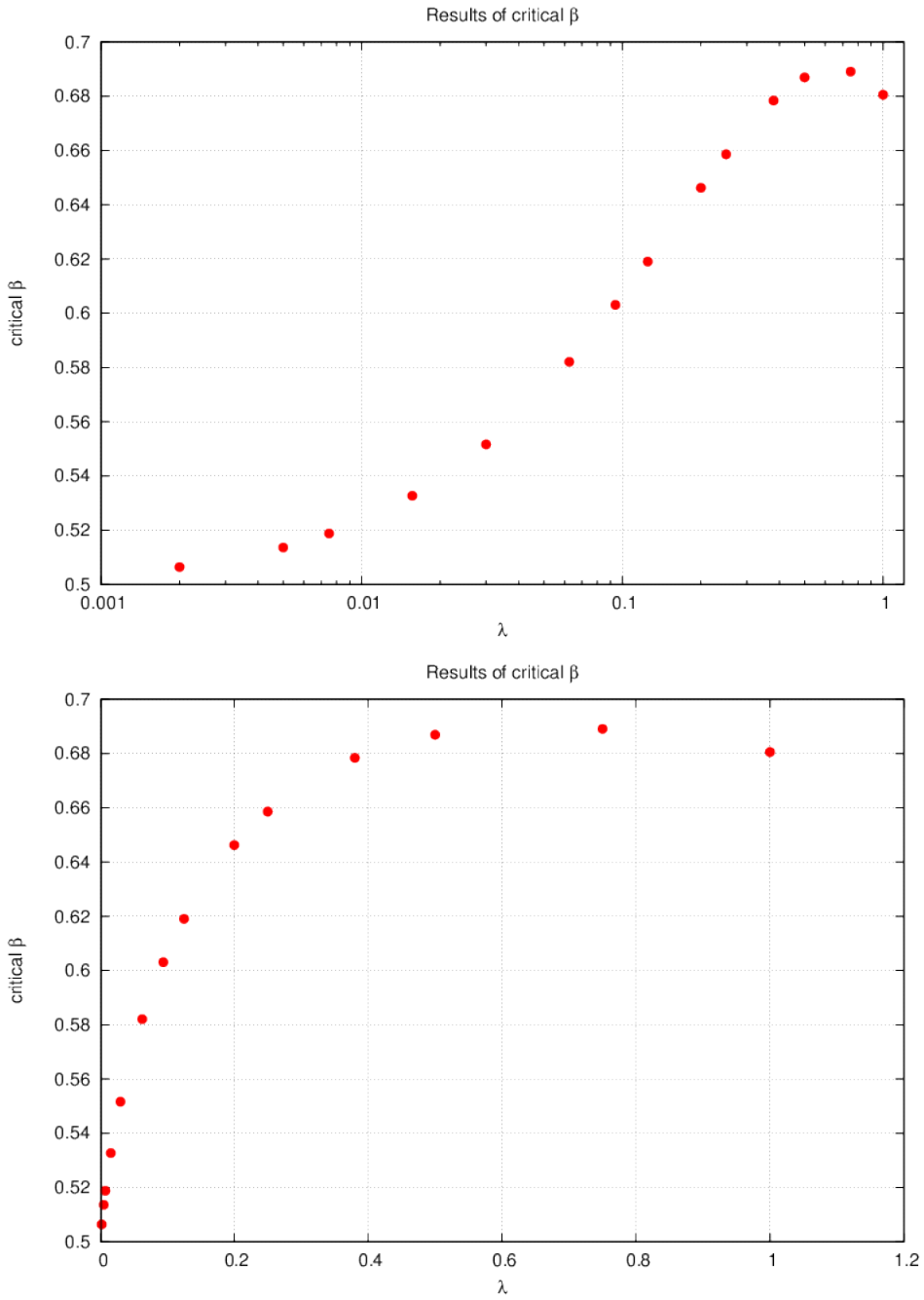

Figure 8: Plots of β_c against λ: in the upper plot we use logarithm scale for λ. As expected for $\lambda \to 0$ the value of $\beta_c \to 0.5$.

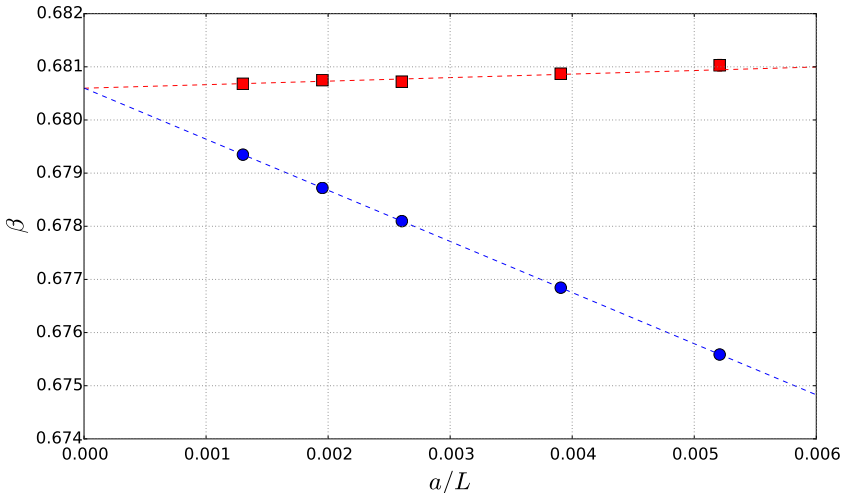

Figure 9: Extrapolation of β_c to $a/L = 0$ with $z = 4$ (blue steep curve) and $z = 1$ (red curve) ($\lambda = 1$).

g	L	g/μ^2	Nmeas	Nbins	Niter
4	128	11.2631(13)	10^5	200	500
4	192	11.3227(9)	10^5	200	500
4	256	11.3533(7)	10^5	200	500
4	384	11.3826(3)	10^5	125	800
4	512	11.3969(3)	10^5	100	1000

Table 14: Results of f at $g = 4$ at finite lattice volume.

5.2 FIRST RESULT OF f

So far we described how we computed the values of β_c at different couplings λ. The critical effective coupling is, then, obtained in the following way: using the relations (140) we evaluate μ_0^2 and g by means of a bootstrap method [35]; then the values of μ^2 are obtained through the relation (138). In Table 16 we collect our final results and we can visualize them in Fig. 10. The x–log scale emphasizes the fact that we covered over two order of magnitude in g. Blue round points are the results taken from Table 16, red triangular points are those coming from Table [88] and green square points are taken from 15.

g	g/μ^2	χ/d.o.f.
4	11.4417(5)	0.76
6	12.2649(11)	1.78

Table 15: Results of f at $g = 4, 6$ in the limit of $L \to \infty$.

Table 16: Final extrapolations to infinite volume limit: g and μ^2 are computed at β_c using equations (138) and (140)

λ	β_c	g	μ^2	g/μ^2
1.000000	0.680601(11)	8.63523(29)	0.649451(67)	13.2962(18)
0.750000	0.689117(13)	6.31733(24)	0.509730(59)	12.3935(19)
0.500000	0.686938(10)	4.23833(12)	0.367173(31)	11.5431(13)
0.380000	0.678405(11)	3.30267(10)	0.296195(32)	11.1503(15)
0.250000	0.6586276(98)	2.305261(69)	0.214762(27)	10.7340(17)
0.200000	0.6462478(78)	1.915543(46)	0.181077(21)	10.5786(15)
0.125000	0.6190716(52)	1.304633(25)	0.125924(15)	10.3605(15)
0.094000	0.6030936(89)	1.033757(30)	0.100518(23)	10.2843(26)
0.062500	0.5820989(60)	0.737813(15)	0.072073(15)	10.2370(23)
0.030000	0.5516594(71)	0.394311(10)	0.038407(17)	10.2666(48)
0.015625	0.5326936(27)	0.2202547(22)	0.0211916(63)	10.3935(32)
0.007500	0.5187729(29)	0.1114722(12)	0.0105457(67)	10.5704(68)
0.005000	0.5136251(17)	0.07581192(49)	0.0071014(38)	10.6757(57)
0.002000	0.5064230(16)	0.03119343(19)	0.0028637(35)	10.8925(132)

Now we explain our theoretical issues that lead us to the form of the fit function showed in Fig. 10.

We said that ϕ^4 theory reduces to the Ising model in the limit $\lambda \to \infty$. In particular in two dimensions we have

$$\beta = \beta_c^{Ising} = \frac{\log(1+\sqrt{2})}{2} = 0.44068679\ldots \tag{147}$$

At the critical point $\beta(\lambda)$ is a highly non–linear function of λ itself. In fact at $\lambda = 0$, $\beta = 0.5$; then, for intermediate values of λ, we note a maximum with a value around 0.69; in the end $\beta(\lambda)$ has to go asymptotically to the Ising limit value (147).

In [52] it is shown that to $\lambda = 10$ corresponds a value of β at criticality that is already near the asymptotic value. Therefore, for very large values of λ we can then safely approximate β with β_c^{Ising}: in this limit, looking at the relations (140) we note that g is going to infinite linearly with λ, and μ_0^2 diverges proportionally to g. This is not true for μ^2 due to the renormalisation condition (138). Then, using the approximation $\beta = \beta_c^{Ising}$ for $g \geq 10^4$, we numerically checked that μ^2 can be linearly extrapolated in $1/g$ to $g \to \infty$ (see Fig. 11). The value obtained is $\mu^2_{Ising} = 3.40669(1)$, where the error is subjectively estimated from the fit.

The previous considerations lead us to use a rational function for the final fit:

$$f = \frac{g}{\mu^2} = \frac{a_0 + a_1 g + \cdots + a_n g^n}{1 + b_1 g + \cdots + b_{n-1} g^{n-1}}.$$

Several trials provide $n = 4$ as the best choice. Therefore the fit function reads:

$$f_4 = \frac{g}{\mu^2} = \frac{a_0 + a_1 g + a_2 g^2 + a_3 g^3 + a_4 g^4}{1 + b_1 g + b_2 g^2 + b_3 g^3}. \tag{148}$$

where we practically assume a linear behaviour of f as $g \to 0$. Taking into account the Ising limit constraint, we fix the parameter b_3 as a constant times a_4. We have in total 7 d.o.f. and we obtain

$$f_0 = 11.179(62) \qquad \text{with} \qquad \chi^2 = 0.73 \tag{149}$$

As can be seen in Fig. 10 the two points at $g = 4$ and $g = 6$, represented by squares, lie perfectly on the curve defined by our fit function. We remark that these point have been computed using the same strategy adopted in [88], as explained in 5.1.6. This represents a further confirmation that our strategy for computing g/μ^2, passing through the limiting procedure described above, works as expected.

Now we introduce a new parameter, η, defined as

$$\eta = \frac{g}{g+1}, \tag{150}$$

in order to better understand the behavior of $f(g)$ for all possible values of g.

The (150) is a map from $g \in [0, \infty)$ to $\eta \in [0, 1]$. With this redefinition, the fit function now reads:

$$f(\eta) = \frac{a'_0 + a'_1\eta + a'_2\eta^2 + a'_3\eta^3}{1 + b'_1\eta + b'_2\eta^2 + b'_3\eta^3}, \tag{151}$$

where one of the parameters is determined by the Ising constraint (147) for $\eta = 1$. As shown in Fig. 12, this choice leads us to a smoother function with respect to (148). With the η parametrization we obtain:

$$f_0 = 11.119(24) \quad \text{with} \quad \chi^2 = 0.95 \quad \text{and} \quad 8 \text{ d.o.f.}. \tag{152}$$

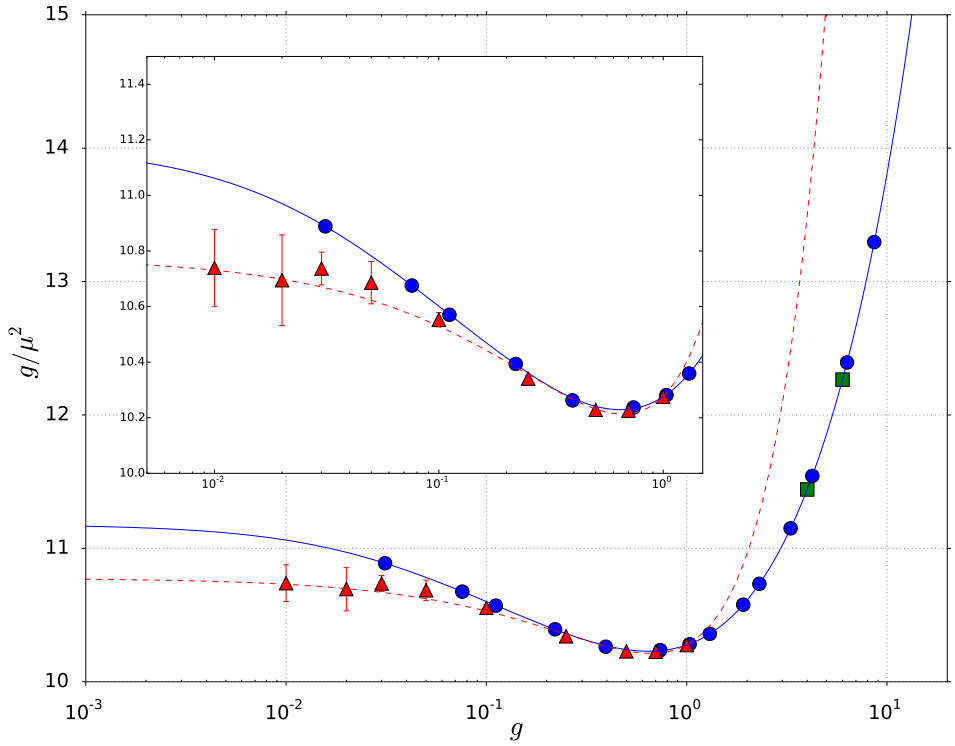

Figure 10: Final results for $f(g)$ against g in logarithmic scale. Error-bars, where not visible, are smaller than symbols size.

Now we are ready to comment Fig. 10. First of all we note that in the intermediate region, *i.e.* in the minimum of the curve, our results are in almost perfect

agreement with those of [88]. Note that the infinite volume limit results of [88] are obtained with a completely different strategy. For lowest simulated values of g we see, in the insert shown in Fig. 10, that our points seem to be a little bit higher. The blue curve is our final fitting function while the red dashed curve is the fit function used in [88].

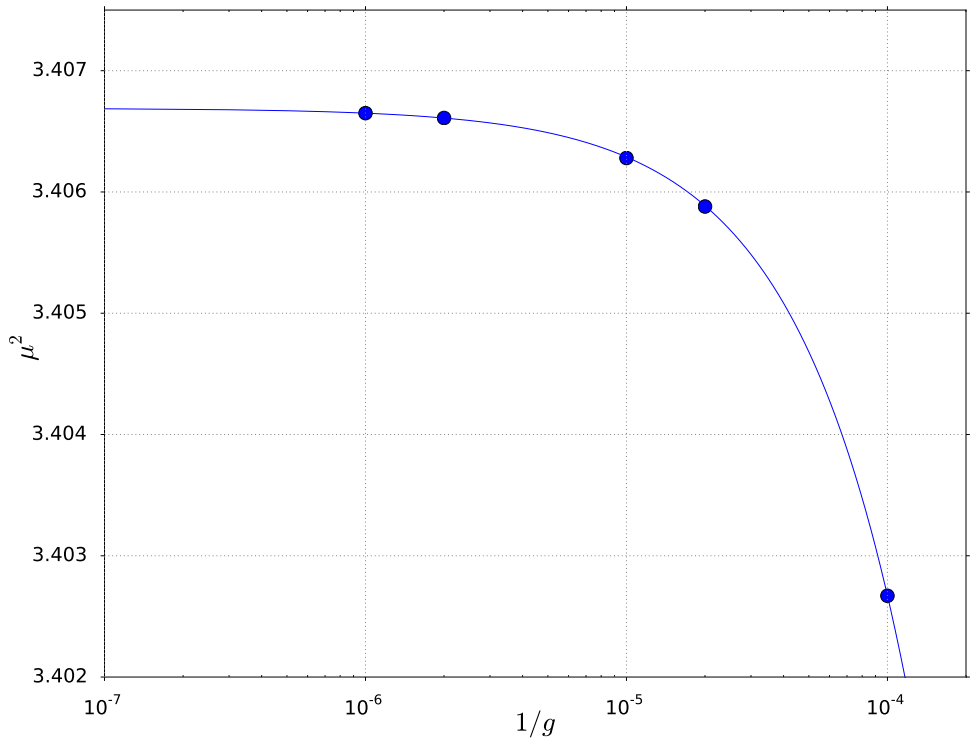

Figure 11: Extrapolation of μ^2 at $g \to \infty$, as described in text.

We decide to quote our final result as:

$$f_0 = 11.15(6)(3). \tag{153}$$

We take as central value the mean of (149) and (152). The first error is purely statistical, and it is conservatively taken as the biggest one between the two fits. The second error is an estimate of the systematic error associated with the particular functional form used to fit data.

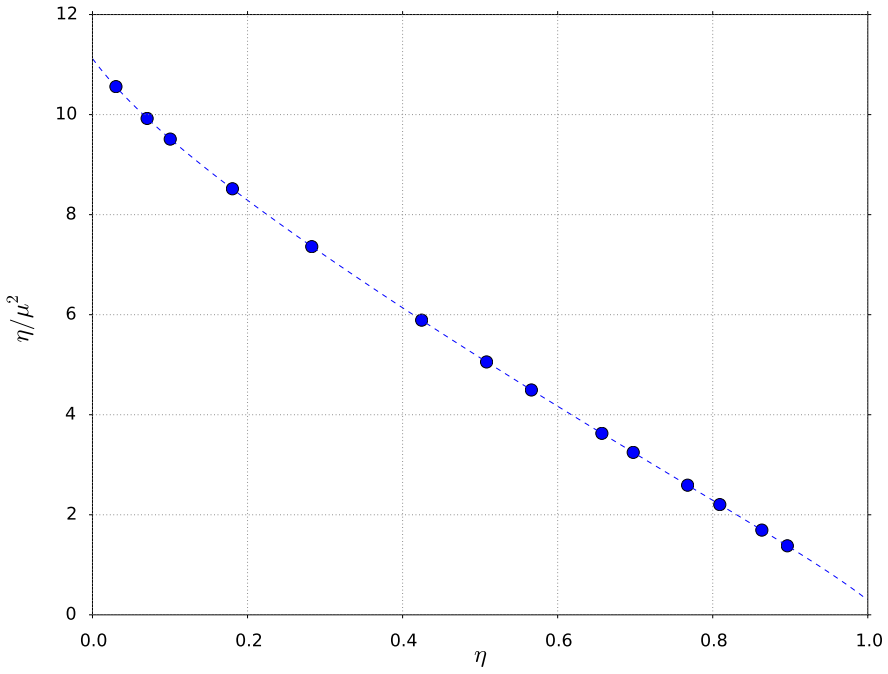

Figure 12: Final plot of $f(\eta)$ with our results.

In Table 4 we summarize some of the latest results for f_0 derived with different approaches.

We note that our result is compatible with the last five determinations (excluding the last one), which come from different methods. We only observe a discrepancy at a 3σ–level with the Monte Carlo results in [88], where a region of very small g–values is reached. Even if we could not reach this region, the worm algorithm allows us to obtain much smaller statistical errors. We also note that the result of our second fit (η–parametrization, see Fig. 12) has a statistical error comparable with that of [71], and the two results are compatible at 2σ–level.

So far we discuss our first attempt to calculate the critical ratio f_0, describing the numerical strategy and commenting the results. Despite our result is quite satisfactory, we want to reach a region of lower values of g. In the following chapter we will explain a new approach to the problem, introducing the Wilson gradient flow technique and presenting new preliminary results.

6

DETERMINATION OF THE CRITICAL COUPLING: PART II

Although our original results for the non–perturbative determination of the critical coupling $f = g/\mu^2$ in ϕ^4 ($d = 2$) look pretty nice, especially compared with the other results in literature, we have several reasons not to be completely satisfied with them.

The main reason for this dissatisfaction is that we were stopped in going to lower values of λ, in order to be nearer to the continuum limit, by a strange kind of "critical slowing down ". The worm algorithm is in fact a very effective one, especially for what concerns the computation of $z = mL$ with a relatively small statistical error, but the efficiency is lost when we go to very small values of λ.

On the other hand, our choice for the condition $z = 4$ seems *a posteriori* a bit unfortunate. We already observed that at a fixed value of λ, the choice $z = 1$ led to much smaller finite-volume effects respect to the case $z = 4$; what we mean is that the value of $\beta_c(z = 1, a/L)$ at a certain finite value of L/a is much closer to the value $\beta_c(z = 4, 0)$ (which is the value we are finally interested in) respect to the case $z = 4$. But this closeness to the infinite volume limit has, as a drawback, a much larger statistical error for the individual simulation. All in all the $z = 4$ choice seemed a good compromise at large or moderately small values of λ; we only had to pay a steeper extrapolation to the infinite volume limit for the smallness of the statistical error.

At very small λ values this is no more a winning strategy; in fact the statistical error we could attain for the largest lattices, at fixed computational time, were too big in order to obtain a reliable extrapolation to the infinite volume limit at fixed λ.

As we'll explain soon, in order to improve our final result by going to smaller values of λ we had to slightly change our strategy. Let us show the new strategy by introducing the so called *Wilson flow*.

6.1 WILSON FLOW

The Wilson flow is a promising tool to study strongly coupled theories on the lattice. Recent studies of the renormalisation of the coupling and composite operators on the lattice involving the Wilson flow prove the success of the method, see e.g. Refs. [24, 65, 67, 72, 98] and references therein.

Here we introduce the Wilson flow only in the contest of a scalar field theory in $d = 3$. Given the euclidean action (141), we introduce a new field $\rho(x, \tau)$ which depends on a space–time index x and on a flow–time τ. The evolution equation of the field $\rho(x, \tau)$ in flow–time is

$$\frac{\partial}{\partial \tau}\rho(x, \tau) = \partial^2 \rho(x, \tau) \tag{154}$$

where ∂^2 is the Laplace operator acting in x space. Note that the flow time has units $[\tau] = [x]^2$. Imposing Dirichlet boundary condition, *i.e.* $\rho(x, 0) = \phi(x)$ it's easy, passing to momentum space, to write the exact solution for the propagator of the ρ field at flow–time τ:

$$G_\rho(\tau, p) = \exp(-2\tau p^2) G(p) \tag{155}$$

As is shown in Ref. [72], the net effect of the flow–time evolution is a "smearing" of the original fields: the flow–time exponentially suppresses the ultraviolet modes. We can associate a smearing radius $r_{\text{sm}} = \sqrt{2d\tau}$ (where d is the dimensionality of the space–time) to a total flow–time τ.

As we explained before, for a fixed value of λ and several lattice size L/a, we search for critical values of β, let's call them $\beta_c(\lambda, a/L)$, such that the quantity

$z = mL$ is held fixed to a reference values z_{ref}, whereas L/a is grown towards the infinite volume limit. In the end we extrapolate $\beta_c(\lambda, a/L) \to \beta_c(\lambda, 0)$. The value of m is computed from the ratio of two propagators: one at zero total momentum and the other one at the smallest lattice momentum p_*. If we now use $G_\rho(\tau, p)$ instead of $G(p)$ for computing m, it's seems reasonable to assume that, for a certain value of τ, the ultraviolet suppression effect of the flow–time should help us to obtain values which are closer to the continuum limit. In this way, at fixed λ, we expect to safely extrapolate $\beta_c(\lambda, a/L) \to \beta_c(\lambda, 0)$ using smaller values for L/a and reducing consequently both the computational time and the statistical errors.

In order to reach this purpose, we must choose a value of τ, the total flow–time, which is fixed in physical units. We'll elaborate on this after a discussing a possible ambiguity: it may seems, in fact, that in the previous line of reasoning we are inconsistently mixing the *infinite volume limit* with the *continuum limit*.

6.1.1 *On the continuum limit of f*

In this subsection, for the sake of clarity we'll reintroduce physical quantities and lattice ones; so, for example, for ϕ^4 theory in $d = 2$ we have

$$\hat{g} \equiv a^2 g \qquad \hat{\mu}^2 \equiv a^2 \mu^2 \tag{156}$$

We imagine to work with a renormalized theory, so that g, μ^2 are already physical quantities. Since we have two dimensionful parameters in the action, the only relevant adimensional constant, in the continuum limit, is their ratio $f_0 = g/\mu_c^2$. This means that if we vary g and μ_c^2 in such a way that f_0 stays constant, we obtain the same physics.

Now we put the theory on a two dimensional lattice, with lattice spacing a, hoping that with numerical simulations we can gain non–perturbative informations about f_0. In a real lattice simulation we are introducing two other dimensional parameters: a, the lattice spacing, and L, the physical (linear) extent of our system. In the end we are interested in the *thermodynamic limit*, *i.e.* $L \to \infty$, and in the *continuum limit*, *i.e.* $a \to 0$.

Now, if we send $a \to 0$ in a naive way, keeping μ^2 constant, we obtain, in $d < 4$, the critical Gaussian model (see [77]). In order to obtain information about f_0 in the full interacting theory we must proceed more carefully. First of all it is important

to understand that we can recover a quantum field theory in the continuum, from its discretized version, only when the lattice system has a second order phase transition. In this case the correlation length ξ, measured in lattice spacing units, goes to infinity. In other words, what is really going to infinity is the adimensional ratio ξ/a. This means that we can see at the problems from two complemetary points of view:

1. if a is held fixed to some physical values, as it may happen in a real solid state physics system, then $\xi/a \to \infty$ means that ξ is physically growing without limits;

2. on the contrary, if we send $a \to 0$, then $\xi/a \to \infty$ means that ξ may reach a finite physical value, which corresponds to the inverse of the physical mass gap of the corresponding quantum field theory in the continuum.

In the end, the final result is the same, but things can change drastically if we measure physical quantities in units of a or in units of ξ.

Considering these points of view, let's give another look at our procedure to obtain f_0 with numerical simulations. We start by fixing a value for $\hat{g}$, we simulate the system for several values of a/L and in each case we compute $\mu_c^2(g, a/L)$. We then extrapolate our results to $a/L \to 0$, and in this way we obtain $f(\hat{g}) \equiv g/\mu_c^2(g)$. This is not yet our final result, because at this point f still depends on $\hat{g}$. Such a dependence can be interpreted from the same complementary points of view we have described before:

1. keeping $\hat{g}$ fixed can be interpreted as keeping a fixed, and this means that also g is fixed to some (unknown) value; at this point sending $a/L \to 0$ means sending $L \to \infty$, and in this way we reach the thermodynamic limit. The value we obtain for $f(\hat{g})$ will, in general, differ from f_0 by $O(a)$ effects, because in this game we kept a fixed. In order to obtain our final result, we must perform several other simulations at different values of $\hat{g}$ and then extrapolate our partial results to $\hat{g} \to 0$. This second extrapolation procedure corresponds to the continuum limit;

2. on the other hand, we can think to measure g (the physical one) in units of ξ, and ξ itself can be identified with L; this means that varying a/L with $\hat{g}$ fixed means that we are varing the value of a and g in such a way that ξ, *i.e.* L, is fixed. The $a/L \to 0$ limit corresponds in this case to the continuum limit at

finite (unknown) physical value of L, and the resulting $f(\hat{g})$ will differ from the expected result because of *finite volume effects*. At this point, in order to recover the infinite volume limit and, at the same time, a finite value for f_0, simple dimensional analysis arguments show that we have to send $\hat{g} \to 0$ once again.

This dual viewpoint is typical to all super–renormalizable theories in which the coupling constant g has a positive mass dimension: only the adimensional ratio g^α/μ_c^2, with some proper exponent α, has physical sense.

6.2 SIMULATIONS

We will follow the same general strategy presented in 5.1, with this only difference: in order to find $\beta_c(\lambda, a/L)$, we assume the condition $z_\rho = 1$, where $z_\rho = m_\rho L$ and m_ρ is the mass we obtain from the ratio

$$R_\rho \equiv G_\rho(\tau, p_*)/G_\rho(\tau, 0) = \frac{m_\rho^2}{\hat{p}_*^2 + m_\rho^2} \tag{157}$$

As we clarify before, the flow–time τ at which we compute m_ρ has to be held fixed in physical units: we choose to fix τ such that at different a/L values, the smearing radius is fixed to $L/4$. Few numerical experiments convinced us that this is a good compromise: smaller values tend to have smaller effects, bigger ones could provoke finite volume effects.

We used the same analysis program of the previous case, since the calculation were performed using the exact solution (155) and, therefore, we have modified only the analysis program.

6.2.1 *First tests*

As a test, we tried to reproduce some old results: we chose a moderately large λ value, $\lambda = 0.25$, and our previous smallest ones, namely $\lambda = 0.002$ and $\lambda = 0.005$.

For $\lambda = 0.25$, we simulate our system for the following values of lattice sizes L/a: 32, 40, 48, 56, 72, 80, 96, 112, 128, 144, 160, 192, 256. We do not repeat here the procedure we used to find $\beta_c(\lambda, a/L)$ since it is the same we used in 8.2.1. In Fig. 13 it is shown an example of the determination of $\beta_c(0.25, a/72)$.

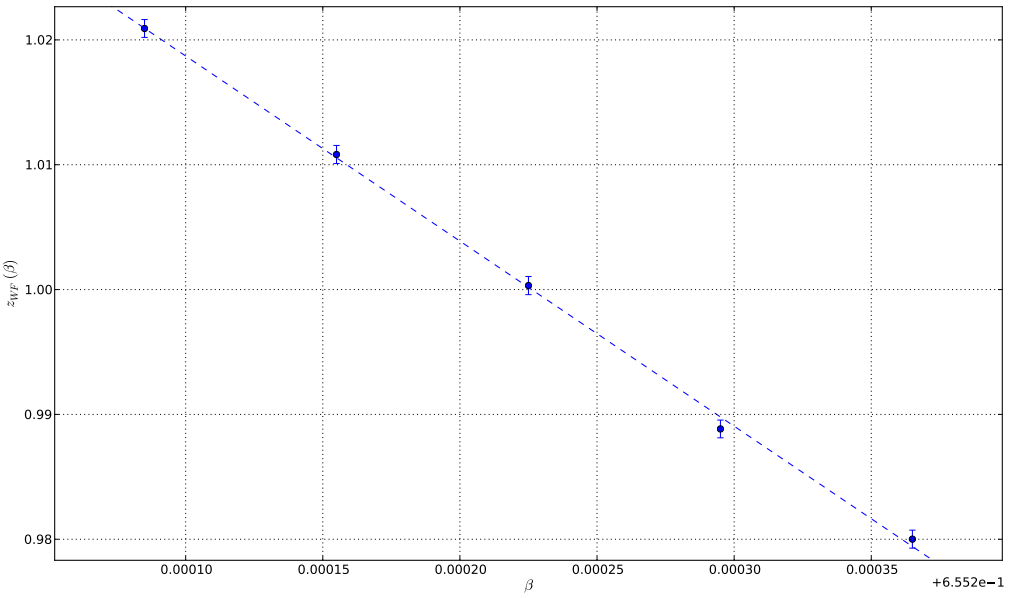

Figure 13: Interpolation of β for $z_{WF} = 1$ at $\lambda = 0.25$ and $L/a = 72$.

Results for $\beta_c(\lambda, a/L)$ (upper set points) are shown in Fig. 14 and are compared to our old results. It is clear that our new results are much nearer to the infinite volume limit, and that the extrapolation can safely start from bigger values of a/L.

In Fig. 15 we show an extrapolation made with a second order polynomial in a/L, with $L_{\min} = 32$, *i.e.* using all data at our disposal, obtaining $\chi^2/\text{d.o.f} = 0.66$. In Fig. 16 we show a plot of the residuals: calling $f(x)$ the fitting function and $y_i \pm e_i$ our results for $\beta_c(\lambda, a/L)$, data are defined as $d_i = [f(x_i) - y_i] \pm e_i$. This plot shows that there is no visible bias and the fitting function can be reasonably considered a suitable one.

Comparing with our previous result $\beta_c^{old}(\lambda = 0.25) = 0.6586276(98)$, the final estimation $\beta_c(\lambda = 0.25) = 0.6586264(20)$ is perfectly compatible within errors and much better than that.

Things are a bit more tricky with the smaller values of λ we used as a check. We had to simulate larger lattices; for $\lambda = 0.002$ we have also $L/a = 192, 256, 384$, and in Fig. 17 we show the result of our best linear fit ($\chi^2/\text{d.o.f} = 0.81$) with $(L/a)_{\min} = 96$. The result is $\beta_c(\lambda = 0.002) = 0.5064161(10)$ to be compared to our

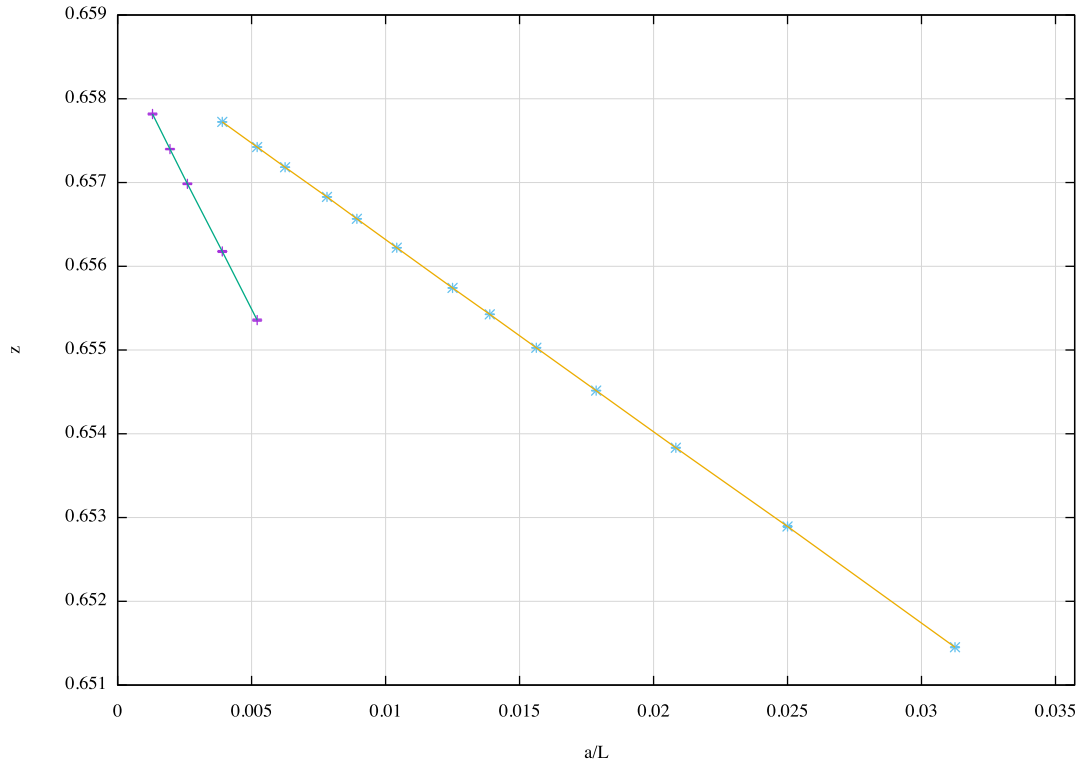

Figure 14: Comparison between our previous results (lower set of points) and the new ones, $\lambda = 0.25$.

old result $\beta_c(\lambda = 0.002) = 0.5064230(16)$. Considering the sum of the two errors, we are more or less at three-sigma distance. The situation is completely analogous for $\lambda = 0.005$.

6.3 RESULTS

The results we are going to present here have to be considered as preliminary. All the details will be given in a forthcoming publication (ref). In Tab. 17 we report the infinite volume results at $\lambda = 0.005, 0.004, 0.003, 0.002, 0.001, 0.00075, 0.0005$. Our new preliminary result is:

$$f_0 = 11.143(11) \qquad \text{with} \qquad \chi^2 = 0.9,$$

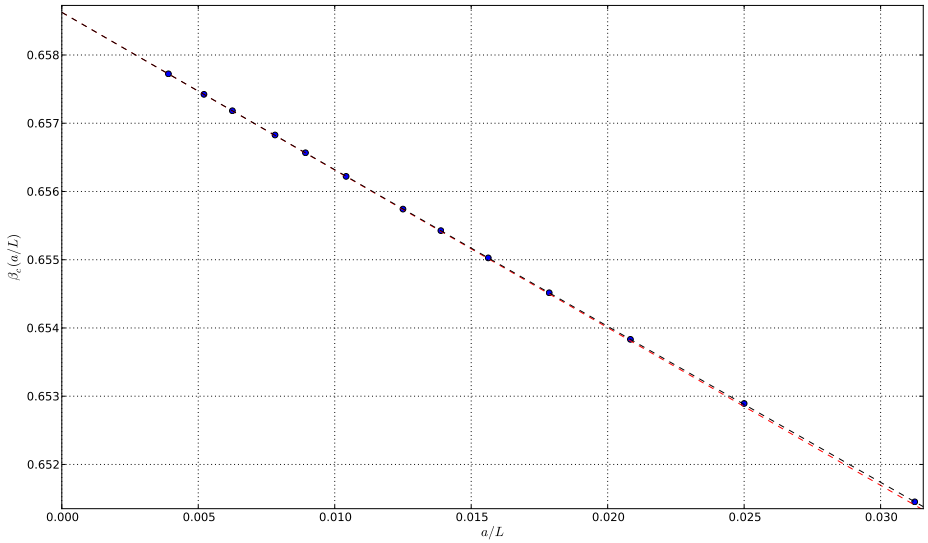

Figure 15: Quadratic fit of $\beta_c(\lambda, a/L)$ to $a/L \to 0$, $\lambda = 0.25$. The red curve is a straight line with angular coefficient which is equal to the linear term in the quadratic fit.

Table 17: Infinite volume results of β_c and $f(\lambda)$ at smaller values of λ and with different linear lattice sizes.

λ	β_c	fit type	$(L/a)_{\min}$	$(L/a)_{\max}$	$f(\lambda)$
0.0005	0.5019534(6)	linear	192	384	10.998(19)
0.00075	0.5027786(6)	linear	160	256	10.944(12)
0.001	0.5035611(10)	linear	160	384	10.922(14)
0.002	0.5064161(10)	linear	96	384	10.8347(77)
0.003	0.5089868(23)	linear	160	256	10.749(12)
0.004	0.5113718(10)	linear	160	384	10.6909(40)
0.005	0.5136162(8)	linear	128	512	10.6457(24)

which is perfectly compatible with our previous result but with a sensibly reduced statistical error.

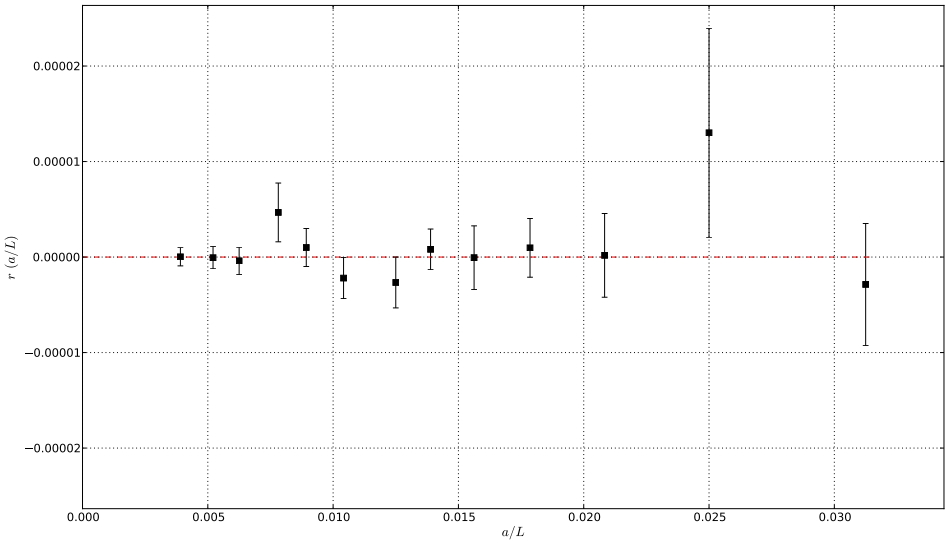

Figure 16: Residuals for the previous fit, $\lambda = 0.25$.

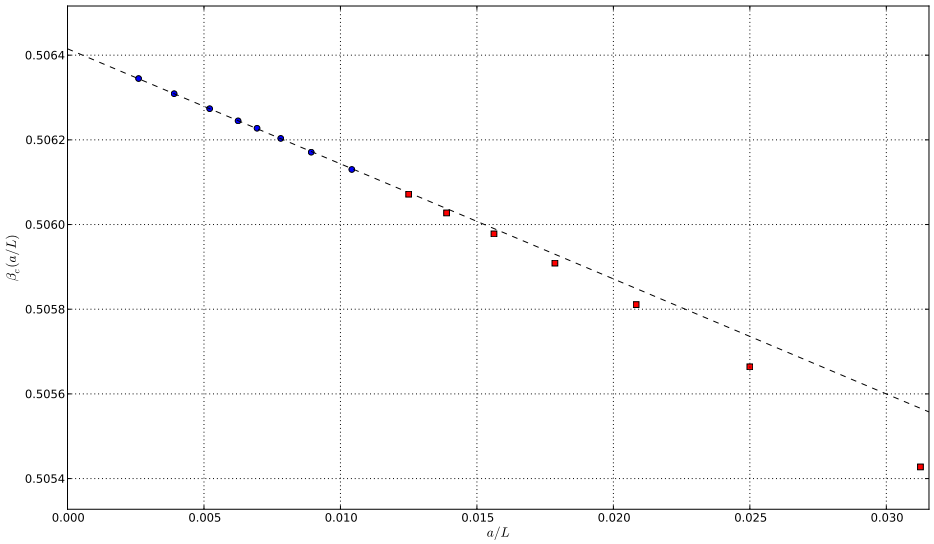

Figure 17: Linear fit of $\beta_c(\lambda, a/L)$ to $a/L \to 0$, $\lambda = 0.002$, $(L/a)_{\text{min}} = 96$.

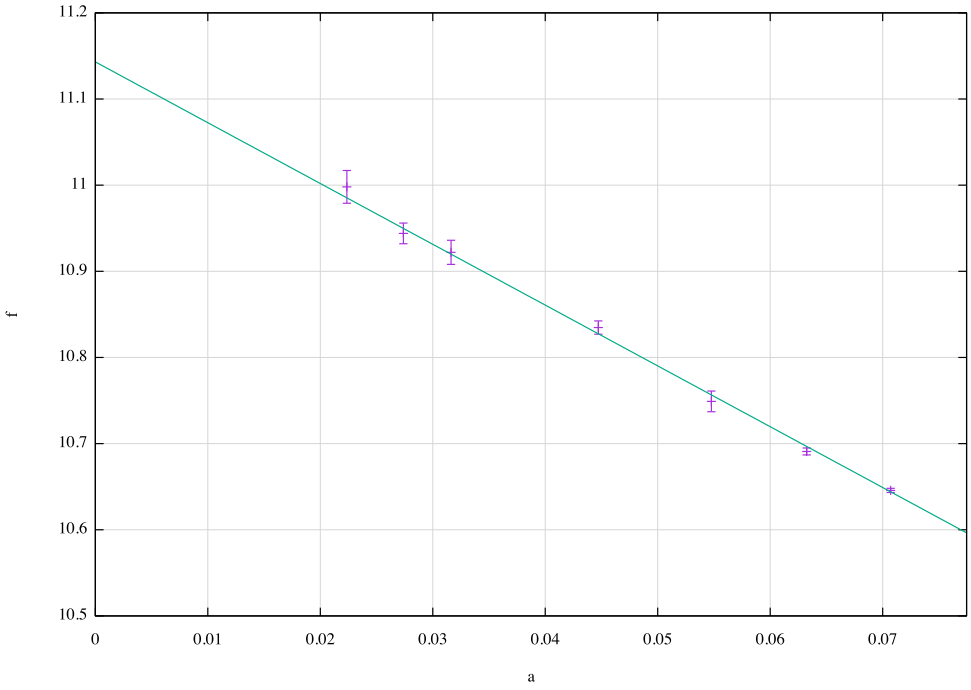

Figure 18: Linear fit of $f(\lambda)$ to the continuum limit.

6.4 CONCLUSIONS

In Table 18 we report, the recent results of f_0, adding our final results. Since we are in perfect agreement with our previous results ([19]), the considerations made in Sec. 5.2 are still valid:

This preliminary result is compatible with the determinations presented in [71, 79, 87, 119], which come from different methods.

Table 18: Sample of the results for the continuum critical parameter f_0 from the literature. DLCQ stands for *Discretized Light Cone Quantization*, QSE diagonalization for *Quasi–Sparse Eigenvector* diagonalization, DMRG for *Density Matrix Renormalization Group* and for DLCH-FS *Diagonalized light-front Hamiltonian in Fock-Space representation*.

Method	f_0	year, Ref.
DLCQ	5.52	1988, [44]
QSE diagonalization	10	2000, [62]
DMRG	9.9816(16)	2004, [97]
Monte Carlo cluster	$10.8^{0.1}_{0.05}$	2009, [88]
Monte Carlo SLAC derivative	10.92(13)	2012, [119]
Uniform Matrix product states	11.064(20)	2013, [71]
Renormalised Hamiltonian	11.88(56)	2015, [87]
Monte Carlo worm	11.15(6)(3)	**2015**, [19]
Borel summability	11.00(4)	2015, [79]
DLCH-FS	4.40(12)	2016, [22]
Our preliminary result	11.143(11)	**2017**

Part IV

SIMULATIONS ON $O(2)$ ϕ^4 THEORY IN THREE DIMENSION ON THE LATTICE

7

$O(2)$ ϕ^4 AND BOSE–EINSTEIN CONDENSATION

The determination of the critical temperature of a uniform, fixed density, dilute Bose gas has always been an intriguing topics in the framework of condensed matter. In particular, finding out the first correction due to the weak repulsive interaction between particles is still a challenging purpose. In the last century there was considerable confusion about how the critical temperature depends parametrically on the scattering length. The main problem of the early works about this phenomena was the perturbative approach to the Bose condensation, which is, instead, inherently non-perturbative since involves long-distance physics. In the last decades a lot of intriguing results came from the effort both of theoretical and numerical approach [6, 7, 9, 12, 15, 42, 45–48, 63, 95, 96, 101]. It can be shown that the first correction to the phase-transition temperature T_c behaves like

$$\frac{\Delta T_c}{T_0} = \frac{T_c - T_0}{T_0} \sim c a_{sc} n^{1/3}, \tag{158}$$

where a_{sc} is the scattering length and the results is obtained in the limit $a_{sc} n^{1/3} \ll 1$, meaning that a_{sc} is small compared to the distance between particles. The value of the constant c is still not well established, since its calculation involves *non-perturbative* physics. In Ref. [7], it is shown that this problem can be related to the

$O(2)\,\phi^4$ theory in three dimensions, characterized by a *continuous* phase transition and described by the continuum action

$$S = \int d^3x \left[\frac{1}{2}|\nabla\phi|^2 + \frac{1}{2}\mu_0^2\phi^2 + \frac{g}{4!}(\phi^2)^2\right], \tag{159}$$

where $\phi = (\phi_1, \phi_2)$ is a two-component real field and $\phi^2 = \phi_1^2 + \phi_2^2$. The evaluation of the constant c is given by the relation

$$c = -\frac{128\pi^2}{\left[\zeta\left(\frac{3}{2}\right)\right]^{4/3}}\frac{\Delta\langle\phi^2\rangle_c}{g} \tag{160}$$

where

$$\Delta\langle\phi^2\rangle_c \equiv [\langle\phi^2\rangle_c]_g - [\langle\phi^2\rangle_c]_0. \tag{161}$$

$[\langle\phi^2\rangle_c]_g$ is the critical-point value for the case with weak interactions ($g \neq 0$) and $[\langle\phi^2\rangle_c]_0$ is the critical value for an ideal gas with no interactions ($g = 0$). Even if $\langle\phi^2\rangle_c$ is an ultraviolet quantity, the difference (161) is and infrared physical quantity and it does not depend on how $\langle\phi^2\rangle_c$ is regularized. Moreover $\Delta\langle\phi^2\rangle_c$ in $O(2)\,\phi^4$ theory depend only on g and, from dimensional analysis, it must be proportional to g. Therefore, Monte Carlo simulations represent an effective tool for computing the numerical constant ratio $\Delta\langle\phi\rangle_c/g$.

In this work we compute a new estimation of the ratio $f_g \equiv \dfrac{\Delta\langle\phi^2\rangle_c}{g}$, exploiting the efficiency of the worm algorithm [83] in simulating Ising–like systems in the non–perturbative regime, using [9] as reference work.

To this aim we extend the method so far developed for Ising [59, 102, 114], Potts and σ model [118], to $O(N)\,\phi^4$ systems [30]. In section 4.3 we presented the method, describing the exact reformulation by means of the hight temperature expansion and the definition of the partition function of a system with ϕ^4 interaction and $O(N)$ symmetry.

8

DETERMINATION OF THE CRITICAL TEMPERATURE IN BOSE-EINSTEIN SYSTEMS

The Lagrangian of ϕ^4 theory with $O(2)$ symmetry is

$$\mathcal{L} = \frac{1}{2}\left(\partial_\mu \phi\right)^2 + \frac{\mu_0^2}{2}\left(\phi \cdot \phi\right) + \frac{g_0}{4!}\left(\phi \cdot \phi\right)^2 \tag{162}$$

where ϕ is a 2-components field, μ_0 is the bare mass and g_0 is the bare coupling, and the corresponding action is given by

$$\mathcal{S} = \int d^3x\, \mathcal{L}.$$

A dimensionless discretized action is obtained by putting the system on a 3–dimensional lattice with spacing a and by using the following parametrization:

$$\hat{\phi}^2 = a\phi_0^2, \qquad \hat{\mu}_0^2 = a^2\mu_0^2, \qquad \hat{g_0} = a g_0.$$

In this way the lattice action is:

$$\mathcal{S} = \sum_x \left\{ -\sum_\nu \hat{\phi}_x \hat{\phi}_{x+\hat{\nu}} + \frac{1}{2}(\hat{\mu}_0^2 + 6)\hat{\phi}_x^2 + \frac{\hat{g}_0}{4}\hat{\phi}_x^4 \right\}. \tag{163}$$

In the following we will omit the "hat" on the top of lattice parameters and the quantity will intend to be expressed in lattice units.

Three–dimensional ϕ^4 theory is super–renormalizable and the only 1PI divergent diagrams of the continuum are those shown in Fig. 19. The first has a linear divergence, while the second has a logarithmic one. For the purpose of computing $\Delta\langle\phi\rangle_c$ a precise definition of μ_0^2 and its relationship to the bare value is not necessary: the difference in (161) cancels the UV divergences when the continuum limit is approached.

However defining the renormalization scheme could be useful for connecting results deriving from simulations performed at different lattices. Following [9], we adopt $\bar{\text{MS}}$ renormalization at a renormalization scale $\bar{\eta}$. The continuum Lagrangian is then, the $\varepsilon \to 0$ limit of the $(3-\varepsilon)$ dimensional action

$$S \int d^{3-\varepsilon}x \left\{ \frac{1}{2} Z_\phi (\partial_\mu \phi)^2 + \frac{1}{2}\mu_0^2 + \mu^\varepsilon \frac{g_{eff}}{4!} (\phi^2)^2 \right\}$$

where

$$\begin{aligned} \mu_0^2 &= \mu^2 + \frac{1}{(4\pi)^2 \varepsilon} \left(\frac{g}{3}\right)^2 \\ \eta &\equiv \frac{e^{\gamma_E/2}}{\sqrt{4\pi}} \bar{\eta}. \end{aligned} \tag{164}$$

Figure 19: 1PI divergent diagrams of ϕ_3^4 theory in the continuum.

8.1 RELATION BETWEEN LATTICE AND CONTINUUM

Let us write the lattice Lagrangian making explicit the relation between lattice and continuum parameters

$$\mathcal{L} = \sum_x a^3 \left[\frac{Z_\phi}{2} |\nabla_{lat}\phi|^2 + \frac{Z_\mu(\mu^2 + \delta\mu^2)}{2}\phi^2(x) + \frac{g + \delta g}{4!}\phi^4(x) \right] \tag{165}$$

where

$$|\nabla_{lat}\phi|^2 = \frac{1}{2}\sum_\nu [\phi(x + a\nu) - \phi(x) + \phi(x - a\nu)]. \tag{166}$$

is the simplest definition of the lattice Laplacian. The relations of the bare mass and the bare coupling to the renormalized quantities are

$$g_0 = (g + \delta g)a, \tag{167}$$
$$\mu_0^2 = Z_\mu(\mu^2 + \delta\mu^2)a^2, \tag{168}$$

and the critical difference of the squared fields is defined as

$$\Delta\langle\phi^2\rangle = Z_\mu\langle\phi^2\rangle_{lat} - \delta\phi^2. \tag{169}$$

In the renormalization scheme we adopt (164), the renormalization counterterms Z_ϕ, Z_μ, $\delta\mu^2$, δg in (167), (168) and (169) are given by

$$\delta g = a^{-1}\left[A_0(ga)^2 + \mathcal{O}((ga)^3)\right], \tag{170}$$
$$\delta\mu = a^{-2}\left[B_0(ga) + B_1(ga)^2 + B_2 \ln\left(\frac{ga}{18}\right)(ga)^2 + \mathcal{O}((ga)^3)\right], \tag{171}$$
$$\delta\phi^2 = a^{-1}\left[\langle\phi^2\rangle_0 + C_0(ga) + C_1\mu^2a^2 + \mathcal{O}((ga)^2)\right], \tag{172}$$
$$Z_\mu = 1 + D_0(ga) + \mathcal{O}((ga)^2), \tag{173}$$
$$Z_\phi = 1 + \mathcal{O}((ga)^2), \tag{174}$$

and depend only on ga at the order of interest. The various coefficients are reported in Table 19. The values b, Σ_u and ξ_u are numerical constants obtained from various integrals in lattice perturbation theory and calculated in [8, 9]: the sub-

script u indicates that the numerical computation is made using the *unimproved* Laplacian (166). $\langle\phi^2\rangle_0$ is the free field ($g = 0$) result for $\langle\phi^2\rangle$ and in the lattice

$\mathcal{O}(ga)$	$\mathcal{O}((ga)^2)$	$\mathcal{O}((ga)^3)$
$A_0 = \frac{5}{12\pi}\xi_u$		
$B_0 = -\frac{\Sigma_u}{6\pi}$	$B_1 = \frac{b}{72\pi^2} - \frac{\Sigma_u\xi_u}{24\pi^2}$	$B_2 = \frac{1}{72\pi^2}$
$C_0 = \frac{\xi_u\Sigma_u}{12\pi^2}$	$C_1 = -\frac{\xi_u}{2\pi}$	
$D_0 = \frac{\xi_u}{6\pi}$		

Table 19: Coefficients of the perturbative expansion of the renormalization factors. The constant b in B_1 comes from the computation of the sun-set diagram and it is equal to 0.08848010 (see Refs. [8, 9] for the details).

theory (165) is given by

$$\langle\phi^2\rangle_{g=0} = 2\int_{\mathbf{k}\in\mathcal{B}} \frac{1}{\tilde{k}^2}, \tag{175}$$

where the integral is over the Brillouin zone $\mathcal{B}$ and $\tilde{k}^2$ is the Fourier transform of the operator (166) and it reads

$$\tilde{k}^2 \equiv a^{-2}\sum_i (2 - 2\cos(ak_i)). \tag{176}$$

The integral over the Brillouin zone of $\tilde{k}^2$ is defined as

$$\frac{\Sigma}{4\pi a} \equiv \int_{\mathbf{k}\in\mathcal{B}} \frac{1}{\tilde{k}^2}, \tag{177}$$

and the numerical integration of (177) for the unimproved Laplacian gives the result $\Sigma_u \simeq 3.17591153562522$. Then, the most straightforward implementation of the ratio $\Delta\langle\phi^2\rangle/g$ is

$$f_{g_0} \equiv \frac{\Delta\langle\phi^2\rangle}{g_0} \equiv \frac{1}{g_0}\left[\langle\phi^2\rangle - \frac{2\Sigma}{4\pi a}\right]. \tag{178}$$

In the limit of $ag \to 0$, (178) gives the awaited continuum value, but with lattice spacing errors of order $O(ga)$ at small ga. In order to improve the result by decreasing the lattice spacing errors, it is necessary not only define an improved Laplacian, but even find an appropriate calculation of the relation between lattice and continuum parameters, as previously given by (167), (168) and (169).

In the following we show the numerical strategy adopted for the computation of (178).

8.2 NUMERICAL STRATEGY

In our simulations we use the following Euclidean lattice action:

$$\begin{aligned} \mathcal{S} &= -\beta \sum_x \sum_\nu \varphi_x \varphi_{x+\hat{\nu}} + \sum_x \left[\varphi_x^2 + \lambda(\varphi_x^2 - 1)^2 \right] \\ &= \mathcal{S}_I + \mathcal{S}_{Site}. \end{aligned}$$

The old action (163) is obtained through the following relations:

$$\phi_x = \sqrt{\beta}\varphi, \qquad \mu_0^2 = 2\frac{1-2\lambda}{\beta} - 6, \qquad g_0 = \frac{4\lambda}{\beta^2}. \tag{179}$$

The strategy is quite similar to that used in (5.1): we fix a value of λ and search for a value of β that realizes the physical condition (142), which we recall for simplicity:

$$mL = L/\xi = \text{const.} = z.$$

The mass m is defined, again, by (143). We remind that the relation (142) guarantees that, since ξ grows linearly with L, we arrive at the critical point when $L/a \to \infty$. We then simulate several lattices with different values of $N \equiv L/a$ and measure some quantities. For each couple of (λ, N) we obtain a value of $\beta(\lambda, N)$, and, through (179), of $g_0(\lambda, N)$. After this step we extrapolate our results to $a/L \to 0$ in order to obtain $\beta(\lambda)$, $g_0(\lambda)$.

We repeat this procedure for several values of λ and finally we extrapolate our results to $\lambda \to 0$ and compute the ratio f_g.

The value we choose for the condition (142) is $z = 2$. A smaller value of z let us to better approach the continuum limit. At fixed value of λ we simulate the system for ten values of L/a, namely: $L/a = 20, 22, 24, 28, 32, 36, 40, 48, 64, 80$. We simulate $\lambda = 0.1, 0.07, 0.05, 0.046, 0.042, 0.0375, 0.03, 0.025, 0.018$.

8.2.1 *Infinite volume limit*

In this step we fix a value of λ and search a value of β such that $z = mL = 2$. At each λ this procedure is repeated for several lattice sizes, in particular for $L/a =$ 20, 22, 24, 28, 32, 36, 40, 48, 64, 80. In Table 20 we report an example at $\lambda = 0.05$ of the main quantities we computed, together with the number of thermalization steps N_{th} and measurements N_m: each measured value is obtain by averaging over 1000 measurements grouped together. The ratio f_g is computed through (178), using relations (170), (171), (172), (173) and (174) at zero order in (ga).

Table 20: Results for $\lambda = 0.05$.

L	z	β	g	$\langle\phi^2\rangle$	f_g	N_{th}	N_m
20	2.0006(4)	0.3759783(7)	8.4889813(314)	1.320768(14)	−0.0010463(6)	1000	3×10^5
22	2.0003(4)	0.3761015(6)	8.4834213(270)	1.320756(13)	−0.0010283(6)	1000	3×10^5
24	2.0002(4)	0.3761973(5)	8.4791030(241)	1.320773(12)	−0.0010132(5)	1000	3×10^5
28	1.9992(4)	0.3763352(4)	8.4728902(191)	1.320849(11)	−0.0009890(5)	1000	3×10^5
32	2.0007(4)	0.3764286(3)	8.4686878(156)	1.320929(10)	−0.0009714(4)	300	3×10^5
36	1.9997(4)	0.3764948(3)	8.4657082(129)	1.321040(9)	−0.0009565(4)	200	3×10^5
40	2.0006(4)	0.3765438(3)	8.4635055(125)	1.321118(10)	−0.0009456(4)	100	2.3×10^5
48	1.9995(6)	0.3766105(3)	8.4605087(121)	1.321322(11)	−0.0009265(5)	100	1.5×10^5
64	1.9992(6)	0.3766811(2)	8.4573383(78)	1.321553(9)	−0.0009055(4)	100	1.5×10^5
80	1.9997(19)	0.3767166(2)	8.4557411(99)	1.321734(14)	−0.0008920(6)	100	0.5×10^5

The computation of $f_g(\lambda, N)$ is obtained through (178), where we multiply $\langle\phi^2\rangle(\lambda, N)$ by the correspondent $\beta(\lambda, N)$, due to the renormalization condition (179). Then we extrapolate the several quantities in the limit of $L/a \to \infty$.

In Fig. 20 we show the infinite volume extrapolation of g against $1/L$ at λ using a cub fit function:

$$\gamma(x) = \gamma_0 + \gamma_1 x + \gamma_2 x^2 + \gamma_3 x^3. \tag{180}$$

The final result with the relative $\chi^2 = 0.31$ can be found in Table 21.

For what concerns the infinite volume extrapolation of $\langle\phi^2\rangle(\lambda, N)$, $\beta(\lambda, N)$ and $g_0(\lambda, N)$ we need to refer to scaling arguments. The $O(2)$ model is in the same universality class as the classical $O(2)$ XY model and, therefore, the large L scaling behaviour depends on universal critical exponent of this model (see 2.1.3.)

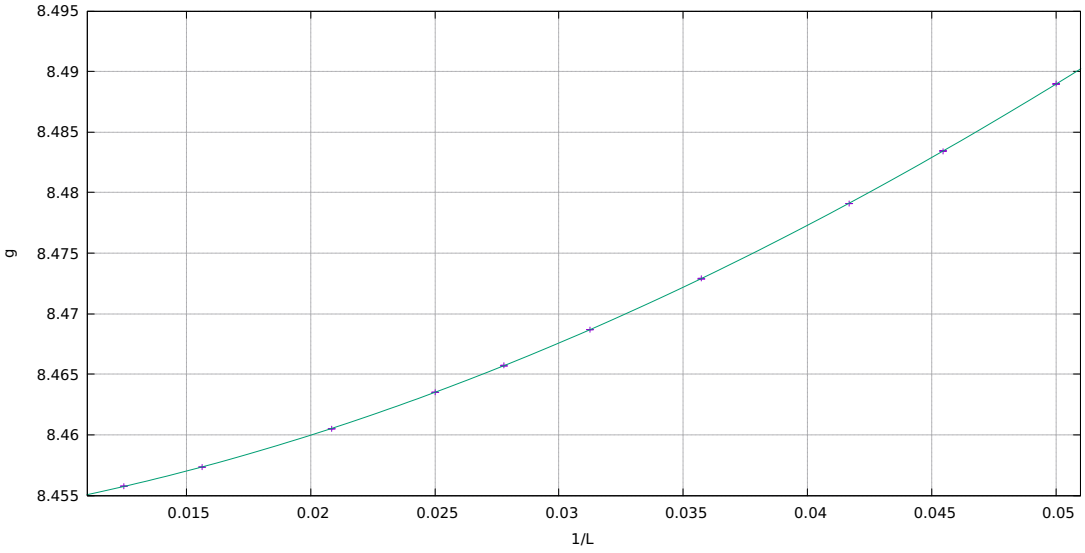

Figure 20: Extrapolation of g at $L \to \infty$, as described in text.

The renormalization group methods provide the following finite–site scaling ansatz about the free energy density $f_{en} = -V^{-1} \ln Z$ for periodic boundary conditions (see 2.1.2):

$$f_{en}(t, \{h_j\}, L^{-1}) = f_{en}^{(reg)}(t, \{h_j\}) + b^{-d} f_{en}^{(sing)}(b^{y_t} t, \{h_j b^{y_j}\}, b/L), \tag{181}$$

where $f_{en}^{(reg)}$ and $f_{en}^{(sing)}$ generate the regular and the singular parts of the free energy in the infinite volume limit. The length b is the *block size*, an arbitrary renormalization scale, and $\{h_j\}$ represents the set of infrared–irrelevant operators with the corresponding $y_j < 0$. Referring to the standard notation of the critical exponents $\nu = 1/y_t$ and we denote with ω the smallest $|y_j|$ associated with $\{h_j\}$. The parameter $t \equiv \beta - \beta_c$ in (181) is the so–called reduced temperature in the Heinsenberg magnet context, even if it is not related to the actual temperature near the critical point (see [38] for more details).

If we choose $b = L$ the (181) becomes

$$f_{en}(t, h_j, L^{-1}) = f_{en}^{(reg)}(t, h_j) + L^{-d} f_{en}^{(sing)}(L^{y_t} t, h_j L^{y_j}, 1). \tag{182}$$

For fixed L (182) is analytic in t since no phase transition occurs in a finite volume system. Then we can make a Taylor expansion of (182) in t, for $L^{y_t}t \to 0$ and as we take $L \to \infty$:

$$\begin{aligned} f_{en} = &(a_0 + b_0 L^{-d} + c_0 L^{-d-\omega} + \dots) + t(a_1 + b_1 L^{-d+y_t} + c_1 L^{-d+y_t-\omega} + \dots) \\ &+ t^2(a_2 + b_2 L^{-d+2y_t} + \dots) + \dots, \end{aligned} \tag{183}$$

where we have only expressed the leading corrections due to irrelevant operators. The large volume scaling behaviour of $\langle \phi^2 \rangle$ is obtained by differentiating (183) with respect to t

$$\langle \phi^2 \rangle = (a_1 + b_1 L^{-d+y_t} + c_1 L^{-d+y_t-\omega} + \dots) + 2t(a_2 + b_2 L^{-d+2y_t} + \dots) + \dots. \tag{184}$$

The condition $z = mL = 2$ used to find β_c implies that

$$t \sim L^{-y_t-\omega}$$

and this satisfies the condition $L^{y_t}t \to 0$ as $L \to \infty$. Then the large volume behaviour of $\langle \phi^2 \rangle$ can be approximate with

$$\begin{aligned} \langle \phi^2 \rangle &= a_1 + b_1 L^{-d+y_t} + a_2' L^{-y_t-\omega} + c_1' L^{-d+y_t-\omega} + \dots \\ &= a_1 + b_1 L^{-(1-\alpha)y_t} + a_2' L^{-y_t-\omega} + c_1' L^{-(1-\alpha)y_t-\omega} + \dots \end{aligned} \tag{185}$$

where in the last term we used the standard scaling relation $\alpha = (2 - \nu d)$ for the specific heat scaling exponent α. In the $O(2)$ model the value of α is very small, namely $\alpha \simeq -0.013$ and since we do not consider such large volumes we can assume $\alpha = 0$ for all practical purpose. This assumption typically generates logarithms in RG analysis (see [9, 82]) and therefore the expected large–scaling behaviour in the limit of $\alpha \to 0$ is, finally, given by:

$$\langle \phi^2 \rangle = a_1 + b_1 L^{-d/2} + L^{-d/2-\omega}(c \ln L + d) + \dots \tag{186}$$

where we substitute $y_t = d/2$.

Since the renormalization Z_μ and $\delta\phi^2$ that convert $\langle \phi \rangle_{lat}$ into $\Delta\langle \phi^2 \rangle$ do not introduce any new powers of L, the large scaling behaviour of $\Delta\langle \phi^2 \rangle$ follows the

same large–L expansion of $\langle \phi^2 \rangle$ (186), but with different coefficients. In Fig. 21 we show an example of $L \to \infty$ extrapolation of f_g at $\lambda = 0.018$, using the fit function suggested by (186) and with $\omega = -2.29$. The final result with the relative χ^2 can be found in Tab. 21.

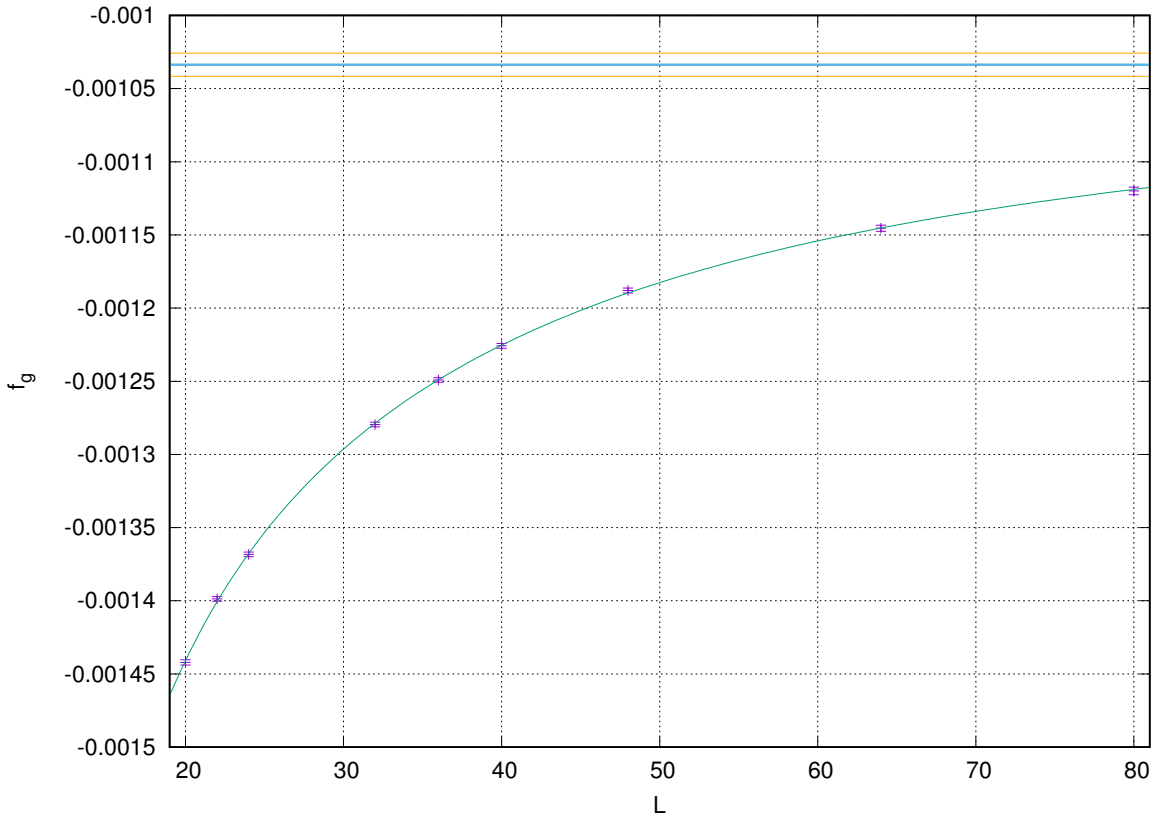

Figure 21: Extrapolation of f_g at $L \to \infty$, as described in text: the blue straight line is our determination of f_g and the orange straight lines represent the error bands.

8.3 RESULTS

In Table (21) we report the infinite volume results of g and f_g with the respective χ^2.

The extrapolation of f_g as $L/a \to \infty$ is performed using (186), the we rewrite as

$$s(x) = s_0 + s_1 x^{-3/2} + x^{-3/2-\omega}(s_2 \ln(x) + s_3) \tag{187}$$

Table 21: Infinite volume limit results of g and f_g at several values of λ, with the relative χ^2 values.

λ	g	χ^2_g	f_g	χ_f
0.018	3.469922(59)	1.52	−0.0010337(79)	0.73
0.025	4.657854(51)	1.33	−0.0009764(47)	0.77
0.03	5.466962(63)	1.04	−0.0009407(58)	1.66
0.0375	6.629048(39)	0.36	−0.0009012(34)	1.08
0.042	7.300162(32)	0.18	−0.0008821(20)	0.54
0.046	7.882140(120)	1.27	−0.0008680(36)	1.28
0.05	8.451722(48)	0.31	−0.0008496(26)	1.15
0.07	11.13980(160)	0.92	−0.0007871(32)	0.85
0.1	14.801082(187)	1.56	−0.0007164(12)	0.74

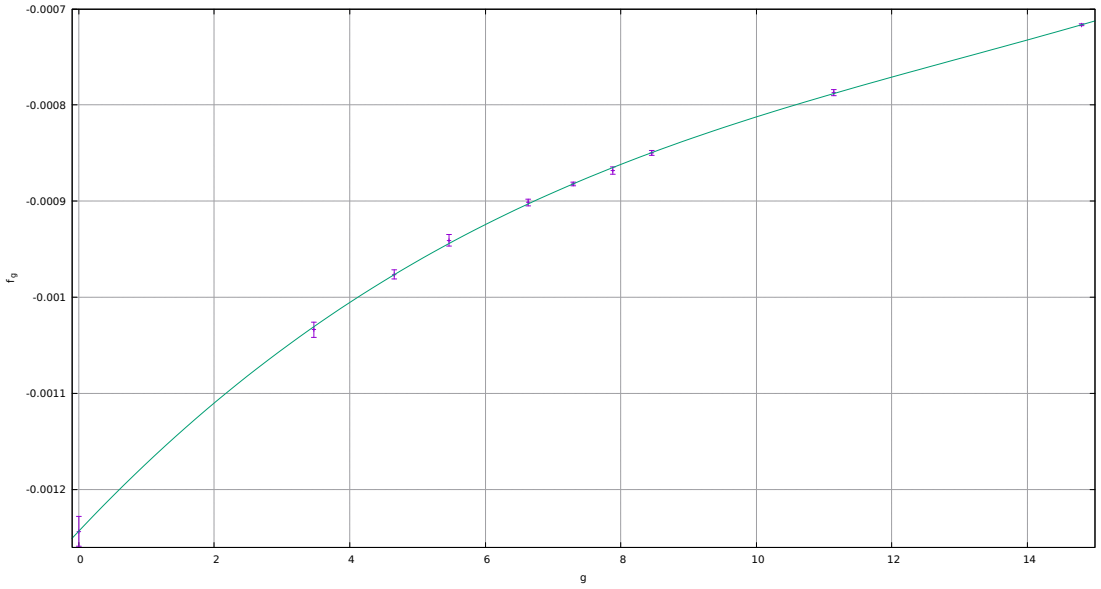

Figure 22: Extrapolation of f_g at $g \to 0$, as described in text.

where $\omega = -2.29$. Notice that the good values of χ^2_f in Table (21), confirm the assumption of (187) derived in 8.2.1.

For what concern the final extrapolation of f_g to the continuum limit, $g \to 0$, we use a cubic fit function (180)

Our final extrapolation lead to

$$f_g = -0.001243(15) \qquad \text{with} \quad \chi^2 = 0.91 \quad 5 \text{ d. o. f.},$$

and if we substitute this value in (160) we obtain our result:

$$c = 1.37(2).$$

8.4 CONCLUSIONS

In Table 22 we report the various computation of c obtained by various analytic and numerical methods of the last decades: in Refs. [61, 95, 122] renormalization–group techniques have been applied to the homogeneous Bose gas at finite temperature; Refs. [4, 10–12] used a nonperturbative method widely used in condensed matter and high energy physics, named $1/N$ expansion ([21, 68]); variational method have also been used in [28, 29, 53], as the *optimized linear δ expansion* (LDE) method (see [93, 94] and references therein), or as the variational perturbation theory ([54–57]). Refs. [7, 9, 42, 46, 50, 120] concerns Monte Carlo results: as reviewed in [5] the discrepancy obtained in [42] lies in the non linear corrections to T_c as a function of a_{sc} at the densities where the simulations were performed; the perturbative treatment of the interaction adopted in [46] is, instead, incorrect, since the physics close to the critical point is nonperturbative. In this work we follow the problem setting of [9], adopting in particular the *unimproved* prescription: we choose the most straightforward definition of the lattice Laplacian and of the self energy. However our numerical strategy is completely different: Arnold and Moore used the Binder cumulant method for finding the transition and the numerical extrapolations of the finite-volume corrections are performed in term of the product Lg, referring to the critical exponents associated with this universality class. We used, instead, the physical condition $z = mL = L/\xi = const.$ for reaching the critical point and we have extrapolated the infinite-volume results in term of L, following the finite-volume behaviour associated to this universality class. We used the *worm* algorithm as in [50], but we implemented the $O(N)$ invariant part in order to simulate the effective theory $O(2)\,\phi^4$.

Even if this is only a preliminary results, since we are waiting for enlarging the statistics, we can see that our estimation of c is in a good agreement within

2σ–level with the most reliable Monte Carlo results [7, 9, 50, 120], even if we use the simplest definition of the Laplacian operator and of the self energy. These fact motivate us to improve our estimation by adopting the gradient Wilson flow technique presented in 6, implementing, if it feasible, the improved Laplacian as in [9] in order to obtain errors of order the $O(a^2)$.

Table 22: Sample of the results for the continuum critical parameter f_g from the literature. PI-MC stands for *path integral* Monte Carlo, PIWP for *path integral without paths*, LDE for *optimized linear δ expansion*.

Method	c	year, Ref.
RG methods	4.66	1992, [15, 95]
MC-PI	0.34(6)	1997, [42]
MC path integral without path	2.3(0.25)	1999, [46]
Ursell operators	0.7	1999, [45]
Large-N approx.	2.9	1999, [12]
PT canonical	-0.93	2000, [105]
NLO Large-N approx.	1.71	2000, [10]
Large-N approx.	2.2(2)	2000, [11]
Lattice MC	1.32(2)	2001, [9]
MC Worm Grand Canonical	1.29(5)	2001, [50]
LDE	1.48	2002, [29]
Variational PT	1.14(11)	2003, [53]
RG methods	1.23	2003, [61]
Classical Field Theory	1.3(4)	2003, [27]
7-loop VPT	1.27(11)	2004, [51]
Large-N approx.	2.33	2006, [4]
RG methods	0.9826(1)	2006, [122]
Self-similar factor approx.	1.29(7)	2017, [120]
This work	1.37(2)	**to be published**

CONCLUSIONS AND OUTLOOK

In this thesis we focused on the super–renormalizable field theory ϕ^4 in two and three dimensions: the coupling constant has a positive mass dimension and the only dimensionless physical parameter which is worthwhile to consider is the ratio

$$f = \frac{g}{\mu^{(4-d)}},$$

in the limit in which both g and μ goes to zero. This limit corresponds to find the critical point of the equivalent statistical system at which the correlation length diverges. The underlying physics of such phenomena is non–perturbative and its investigation needs appropriate tools.

The numerical evaluation of any parameter has to be accompanied by an accurate error analysis. In the case of lattice simulations one is interested in obtaining a statistical error as small as possible, taking into account the unavoidable $O(a, a^2, \dots)$ errors, where a is the lattice spacing.

The main purpose of this thesis is to develop an effective numerical technique for simulating the system near the criticality, associated to a compelling numerical strategy in order to find some non–perturbative quantities, like f, with the best feasible accuracy.

The choices we made to achieve this goal have been presented as follows:

- In Part i we present the theoretical background: in Chapter 1 we review the main features of Euclidean quantum field theory, introducing its path integral formulation and the Euclidean generating functional. After that we describe the lattice regularization, as the procedure for dealing with divergent integrals, and then we provide the main ideas of renormalization and of

renormalization group. In Chapter 2 we highlight the equivalence between Euclidean quantum field theory (in the path integral picture) and statistical mechanics. We focus, in particular, on the second order phase transition and derive the critical exponents with renormalization group scaling laws.

- In Part ii we introduce the numerical tool we chose for our simulations and describe the error analysis adopted. In Chapter 3, after revisiting the main aspect of Monte Carlo simulations, we describe our error analysis method, based on the Γ–method, and introduce the error analysis program we have used. In Chapter 4 we define the algorithm we use for simulating ϕ^4 in two and three dimensions, the *worm algorithm*. After describing its formulation and their update steps in the cases of ϕ^4 with one–component fields and of σ–model, we explain how we extend the algorithm to simulate ϕ^4 with $O(N)$ symmetry.

- In Part iii we present our first application, the determination of the critical coupling f in ϕ_2^4 theory. In Chapter 5 we firstly summarize the state of art, reporting the last evaluation of f for $D = 2$. Then we describe the several steps we performed in order to reach the critical point, providing the simulation details. Finally we present our first result and the theoretical arguments that bring us to it. Since we were not completely satisfied of the evaluation, for reasons explained in Chapter 6, we improve our numerical strategy for achieving the continuum limit, introducing the Wilson gradient flow. This tool, in fact, allowed us to reach smaller values of g. After describing the main changes with respect to the previous case, we present our new preliminary result. In the first and in the improved case we use the worm algorithm as presented in 4.1.

- In Part iv the $O(2)$ ϕ_3^4 theory is introduced as the effective model of a weakly interacting Bose gas. We focus, in particular, on the determination of the first shift of the critical temperature of the Bose–Einstein condensation, computing, in particular, the proportional constant c (see (160)). After explaining the theoretical setting, we give the details of the simulations in the critical region. These are performed by means of the extended version of the worm algorithm, described in 4.3. Finally we present our preliminary result, comparing it with the latest determination, and we outline our future planes for an improved estimation.

The main results of this thesis are the following:

- *Algorithm and numerical strategy.* Starting from the strong coupling expansion of Ising–like systems and of the σ model, we derive the transition probabilities of the worm algorithm for simulating a ϕ^4 system in the loop representation with $O(N)$ symmetry. We applied the so extended algorithm to the $O(2)\phi_3^4$ effective theory for the computation of the constant c. Despite the first preliminary result is obtained using the simplest definition of the Laplacian and without considering particular prescriptions to correct $O(a)$ error, it is compatible with the latest determination of this constant.

  The worm algorithm is, as we already pointed out, an effective tool for simulating the system considered near the continuous transition. Despite the physical condition $z = mL = 4$ we use for achieve the critical point allow us to be closer to the continuum with respect to grater values of z, it provides a decreasing of the worm algorithm efficiency in the case of small values of g. Therefore, for what concerns the determination of f in ϕ_2^4, we try to compensate this deficiency using the Wilson gradient flow.

  A minor, but useful, product was the develop of an open source analysis program, based on [112, 113] which provides a suitable data–handling and which, thanks to its modular structure, is easily exportable.

- *Determination of the critical coupling in ϕ_2^4 theory.* Our first estimation of f is

$$f = 11.15(6)(3).$$

  As we showed in 5.2 this value is compatible, excluding the last one, with the last five determination.

  With improvement gained with the Wilson flow we obtain the preliminary result

$$f = 11.143(11).$$

  This value is perfectly compatible with our previous one, but with a smaller error.
  Outlines. With the end of simulations we hope to sensible reduce the final error and to attest our fitting function which depicts the behaviour of f as g goes to zero, i.e. the continuum limit.

- *Determination of the constant c.* The determination of c constant with the extended worm algorithm is

$$c = 1.37(2).$$

Stressing that this is only a preliminary result, we can see that it is compatible within two–sigma level with the best determination of [9].

Outlines. With the end of simulations we hope to obtain a final result compatible with the most accredited determinations. This will be the basic value for future simulations in which we will apply the Wilson flow technique and we will try to implement an improved laplacian and to use some prescriptions in order to reduce the $O(a)$ errors.

Part V

APPENDIX

A

APPENDIX A

A.1 FUNCTIONAL DERIVATIVE

Consider a functional $F[J]$,where J is some function of coordinates x. The *functional derivative*

$$\frac{\delta}{\delta J(x)} F[J] \tag{188}$$

is defined through the formula

$$\lim_{\epsilon \to 0} \frac{1}{\epsilon} [F[J + \epsilon h] - F[J] = \int d^D x \, h(x) \frac{\delta}{\delta J(x)} F[J]. \tag{189}$$

For example, if we consider the functional $F_1[J] = \int d^D x \, J(x) f(x)$, then

$$\frac{\delta}{\delta J(x)} F_1[J] = f(x).$$

For $F_2[J] = \int d^D x \, d^D y \, J(x) J(y) f(x, y)$, we have

$$\frac{\delta}{\delta J(x)} F_2[J] = \int d^D y \, J(y) [f(x, y) + f(y, x)].$$

If we consider $F_3[J] = J(z)$, then

$$\frac{\delta}{\delta J(x)} F_3[J] = \delta(x - z)$$

A.2 DIMENSIONAL REGULARIZATION OF ϕ_2^4

ϕ^4 theory in two dimensions is super-renormalizable and the only 1–Particle–Irreducible (1PI) divergent diagram is the one–loop self energy, shown in Fig. 1.

In order to eliminate this divergence, now we indicate the propagator as $G_0(p)$ and the self–energy as $\Sigma(p)$. Then the 1PI diagrams can be written as

$$(G_0(p))^2 \Sigma(p).$$

The exact two point function is, then, given by

$$\begin{aligned} G(p) &= G_0(p) + G_0(p)\Sigma(p)G_0(p) + G_0^3(p)\Sigma^2(p) + \cdots \\ &= G_0(p) \sum_{n=0}^{+\infty} (G_0(p)\Sigma(p))^n = \\ &= \frac{G_0(p)}{1 - G_0(p)\Sigma(p)} \\ &= \frac{1}{G_0^{-1}(p) - \Sigma(p)} \end{aligned}$$

We expand $\Sigma(p)$ in a power series of g:

$$\Sigma(p) = \Sigma_1 + \Sigma_2 + \Sigma_3 \cdots$$

where Σ_n contains coupling of order g^n. In order to correct the divergence, we redefine Σ without the Σ_1 term. Therefore Σ reads:

$$\Sigma(p) = \tilde{\Sigma}_2 + \tilde{\Sigma}_3 + \cdots$$

In order to isolate the divergent part from the finite part of the integral we rewrite

$$\mathcal{L} = \frac{1}{2}(\partial_\mu \phi)^2 + \frac{1}{2}\mu_0^2\phi^2 + \frac{\lambda}{4!}\phi^4.$$

by rescaling the coupling constant λ.

The divergent term Σ_1 can be written using Feynman rules:

$$\Sigma_1 = -3\lambda \int \frac{d^2q}{(2\pi)^2}\frac{1}{q^2+\mu_0^2}.$$

If we introduce a dimensional defect $2-\epsilon$, the coupling constant λ varies its mass dimension. Now we point out the mass dimension of the coupling $M^{2-\epsilon}$ and multiply this with a dimensionless constant $\hat{\lambda}$:

$$-3\lambda \longrightarrow -3\hat{\lambda}M^{2-\epsilon}.$$

The measure of integration becomes

$$\frac{d^2q}{(2\pi)^2} = \frac{qdqd\Omega}{(2\pi)^2} \longrightarrow \frac{q^{1-\epsilon}dqd^{1-\epsilon}\Omega}{(2\pi)^{2-\epsilon}},$$

and the whole integral reads

$$\Sigma_1 = -3\hat{\lambda}\frac{M^{2-\epsilon}}{(2\pi)^{2-\epsilon}}\int_0^\infty \frac{q^{1-\epsilon}dq}{q^2+\mu_0^2}\int d^{1-\epsilon}\Omega.$$

We can use the general expression for the integration on a n–sphere,

$$\int d^{n-\epsilon}\Omega = \frac{2\pi^{n/2}}{\Gamma(\frac{n}{2})}, \tag{190}$$

and the hypergeometric function for solving the integral:

$$\int_0^\infty \frac{x^k dx}{(x^n+a^n)^r} = \frac{(-1)^{r-1}\pi a^{k+1-nr}\Gamma(\frac{k+1}{n})}{n\sin(\frac{k+1}{n}\pi)\Gamma(\frac{k+1}{n}-r+1)(r-1)!}. \tag{191}$$

Plugging our parameters into (190) and (191), we obtain

$$\Sigma_1 = -3\hat{\lambda}\frac{M^{2-\epsilon}}{(2\pi)^{2-\epsilon}}\frac{2\pi^{1-\epsilon/2}}{\Gamma(\frac{1-\epsilon}{2})}\frac{\pi\mu_0^{-\epsilon}}{2\sin(\frac{2-\epsilon}{2}\pi)} \tag{192}$$

where

$$\int d^{1-\epsilon}\Omega = \frac{2\pi^{1-\epsilon/2}}{\Gamma(\frac{1-\epsilon}{2})}$$
$$\int_0^\infty \frac{q^{1-\epsilon}dq}{q^2+\mu_0^2} = \frac{\pi\mu_0^{-\epsilon}}{2\sin(\frac{2-\epsilon}{2}\pi)}.$$

Using the *Euler's reflection formula* [1]

$$\Gamma(k)\Gamma(1-k) = \frac{\pi}{\sin(k\pi)} \qquad \text{with} \quad z \notin \mathbb{Z},$$

and recalling the approximation for $\varepsilon \to 0$ of the Γ function and x^ε

$$\Gamma\left(\frac{2}{\epsilon}\right) = \frac{2}{\epsilon} - \gamma + \mathcal{O}(\epsilon)$$
$$x^\epsilon = 1 + \epsilon\log x + \mathcal{O}(\epsilon^2)$$

We obtain

$$\begin{aligned}\Sigma_1 &= \frac{-3\hat{\lambda}M^2\Gamma(\epsilon/2)}{4\pi}\left(\frac{2\pi^{1/2}}{M\mu_0}\right)^{-\epsilon} \\ &= \frac{-3\hat{\lambda}M^2}{4\pi}\left(\frac{2}{\epsilon} - \gamma + \log\left(\frac{2\pi^{1/2}}{M\mu_0}\right) + \mathcal{O}(\epsilon)\right),\end{aligned} \tag{193}$$

where γ is the Euler costant. The only divergent term in (193) is

$$\frac{-3\hat{\lambda}M^2}{2\pi\epsilon} + \text{finite terms.} \tag{194}$$

BIBLIOGRAPHY

[1] Milton Abramowitz and Irene A Stegun. *Handbook of mathematical functions: with formulas, graphs, and mathematical tables*. Vol. 55. Courier Corporation, 1964.

[2] M. Aizenman. "Geometric analysis of $\phi_d{}^4$ fields and Ising models. Parts I and II". In: *Communications in Mathematical Physics* 86 (Mar. 1982), pp. 1–48. DOI: 10.1007/BF01205659.

[3] Michael Aizenman. "Proof of the Triviality of $\phi_d{}^4$ Field Theory and Some Mean–Field Features of Ising Models for $d > 4$". In: *Phys. Rev. Lett.* 47 (1 1981), pp. 1–4. DOI: 10.1103/PhysRevLett.47.1. URL: http://link.aps.org/doi/10.1103/PhysRevLett.47.1.

[4] Jens O. Andersen. "$1/N$-expansion and the dilute Bose gas beyond mean-field theory". In: (2006). arXiv: cond-mat/0608265 [cond-mat].

[5] Jens O. Andersen. "Theory of the weakly interacting Bose gas". In: *Rev. Mod. Phys.* 76 (2 2004), pp. 599–639. DOI: 10.1103/RevModPhys.76.599. URL: https://link.aps.org/doi/10.1103/RevModPhys.76.599.

[6] Jens O. Andersen and Michael Strickland. "Application of renormalization-group techniques to a homogeneous Bose gas at finite temperature". In: *Phys. Rev. A* 60 (2 1999), pp. 1442–1450. DOI: 10.1103/PhysRevA.60.1442. URL: https://link.aps.org/doi/10.1103/PhysRevA.60.1442.

[7] Peter Arnold and Guy Moore. "BEC Transition Temperature of a Dilute Homogeneous Imperfect Bose Gas". In: *Phys. Rev. Lett.* 87 (12 2001), p. 120401. DOI: 10.1103/PhysRevLett.87.120401. URL: https://link.aps.org/doi/10.1103/PhysRevLett.87.120401.

[8] Peter Arnold and Guy D. Moore. "Erratum: Monte Carlo simulation of O(2) φ^4 field theory in three dimensions [Phys. Rev. E 64, 066113 (2001)]". In: *Phys. Rev. E* 68 (4 2003), p. 049902. DOI: 10.1103/PhysRevE.68.049902. URL: https://link.aps.org/doi/10.1103/PhysRevE.68.049902.

[9] Peter Arnold and Guy D. Moore. "Monte Carlo simulation of O(2) ϕ^4 field theory in three-dimensions". In: *Phys. Rev.* E64 (2001). [Erratum: Phys. Rev.E68,049902(2003)], p. 066113. DOI: 10.1103/PhysRevE.64.066113,10.1103/PhysRevE68.049902. arXiv: cond-mat/0103227 [cond-mat].

[10] Peter Arnold and Boris Tomášik. "T_c for dilute Bose gases: beyond leading order in $1/N$". In: *Phys. Rev. A* 62 (6 2000), p. 063604. DOI: 10.1103/PhysRevA.62.063604. URL: https://link.aps.org/doi/10.1103/PhysRevA.62.063604.

[11] G. Baym, J.-P. Blaizot, and J. Zinn-Justin. "The transition temperature of the dilute interacting Bose gas for N internal states". In: *EPL (Europhysics Letters)* 49.2 (2000), p. 150. URL: http://stacks.iop.org/0295-5075/49/i=2/a=150.

[12] G. Baym et al. "The Transition Temperature of the Dilute Interacting Bose Gas". In: *Physical Review Letters* 83 (1999), pp. 1703–1706. DOI: 10.1103/PhysRevLett.83.1703. eprint: cond-mat/9905430.

[13] J.P. Baym G.and Blaizot et al. "Bose-Einstein transition in a dilute interacting gas". In: *The European Physical Journal B - Condensed Matter and Complex Systems* 24.1 (2001), pp. 107–124. DOI: 10.1007/s100510170028. URL: https://doi.org/10.1007/s100510170028.

[14] C.M. Bender et al. "Strong-coupling expansion in quantum field theory". In: *Phys. Rev. D* 19 (6 1979), pp. 1865–1881. DOI: 10.1103/PhysRevD.19.1865. URL: http://link.aps.org/doi/10.1103/PhysRevD.19.1865.

[15] M. Bijlsma and H. T. C. Stoof. "Renormalization group theory of the three-dimensional dilute Bose gas". In: *Phys. Rev. A* 54 (6 1996), pp. 5085–5103. DOI: 10.1103/PhysRevA.54.5085. URL: https://link.aps.org/doi/10.1103/PhysRevA.54.5085.

[16] Kurt Binder et al. "Monte Carlo simulation in statistical physics". In: *Computers in Physics* 7.2 (1993), pp. 156–157.

[17] N Bogoliubov. "On the theory of superfluidity". In: *J. Phys* 11.1 (1947), p. 23.

[18] SN Bose. "Planck's law and light quantum hypothesis". In: *Z. Phys* 26.1 (1924), p. 178.

[19] P. Bosetti, B. De Palma, and M. Guagnelli. "Monte Carlo determination of the critical coupling in ϕ_2^4 theory". In: *Phys. Rev. D* 92 (3 2015), p. 034509. DOI: 10.1103/PhysRevD.92.034509. URL: https://link.aps.org/doi/10.1103/PhysRevD.92.034509.

[20] E Brézin, JC Le Guillou, and J Zinn-Justin. "Phase transitions and critical phenomena". In: *Phase Transitions and Critical Phenomena.* Vol. 6. Domb C and Green M.S. Eds.(Academic, New York), 1976.

[21] Edouard Brézin and Spenta R Wadia. *The large N expansion in quantum field theory and statistical physics: from spin systems to 2-dimensional gravity*. World scientific, 1993.

[22] Matthias Burkardt, Sophia S. Chabysheva, and John R. Hiller. "Two-dimensional light-front ϕ^4 theory in a symmetric polynomial basis". In: *Phys. Rev. D* 94 (6 2016), p. 065006. DOI: 10.1103/PhysRevD.94.065006. URL: https://link.aps.org/doi/10.1103/PhysRevD.94.065006.

[23] Massimo Campostrini et al. "Critical behavior of the three-dimensional XY universality class". In: *Phys. Rev. B* 63 (21 2001), p. 214503. DOI: 10.1103/PhysRevB.63.214503. URL: https://link.aps.org/doi/10.1103/PhysRevB.63.214503.

[24] F. Capponi et al. "Renormalisation of the scalar energy-momentum tensor with the Wilson flow". In: *PoS* LATTICE2016 (2016), p. 341. arXiv: 1612.07721 [hep-lat].

[25] Shau-Jin Chang. "Erratum: Existence of a second-order phase transition in a two-dimensional φ^4 field theory". In: *Phys. Rev. D* 16 (6 1977), pp. 1979–1979. DOI: 10.1103/PhysRevD.16.1979. URL: https://link.aps.org/doi/10.1103/PhysRevD.16.1979.

[26] Shau-Jin Chang. "Existence of a second-order phase transition in a two-dimensional φ^4 field theory". In: *Phys. Rev. D* 13 (10 1976), pp. 2778–2788. DOI: 10.1103/PhysRevD.13.2778. URL: https://link.aps.org/doi/10.1103/PhysRevD.13.2778.

[27] M. J. Davis and S. A. Morgan. "Microcanonical temperature for a classical field: Application to Bose-Einstein condensation". In: *Phys. Rev. A* 68 (5 2003), p. 053615. DOI: 10.1103/PhysRevA.68.053615. URL: https://link.aps.org/doi/10.1103/PhysRevA.68.053615.

[28] Frederico F. de Souza Cruz, Marcus B. Pinto, and Rudnei O. Ramos. "Transition temperature for weakly interacting homogeneous Bose gases". In: *Phys. Rev. B* 64 (1 2001), p. 014515. DOI: 10.1103/PhysRevB.64.014515. URL: https://link.aps.org/doi/10.1103/PhysRevB.64.014515.

[29] Frederico F. de Souza Cruz et al. "Higher-order evaluation of the critical temperature for interacting homogeneous dilute Bose gases". In: *Phys. Rev. A* 65 (5 2002), p. 053613. DOI: 10.1103/PhysRevA.65.053613. URL: https://link.aps.org/doi/10.1103/PhysRevA.65.053613.

[30] B. De Palma and M. Guagnelli. "Monte Carlo simulation of ϕ_2^4 and $O(N)\phi_3^4$ theories". In: 2016. arXiv: 1612.05029 [hep-lat]. URL: https://inspirehep.net/record/1504063/files/arXiv:1612.05029.pdf.

[31] Barbara De Palma et al. "A Python program for the implementation of the Γ–method for Monte Carlo simulations". In: (2017). arXiv: 1703.02766 [hep-lat].

[32] Youjin Deng, Timothy M. Garoni, and Alan D. Sokal. "Dynamic Critical Behavior of the Worm Algorithm for the Ising Model". In: *Phys. Rev. Lett.* 99 (11 2007), p. 110601. DOI: 10.1103/PhysRevLett.99.110601. URL: https://link.aps.org/doi/10.1103/PhysRevLett.99.110601.

[33] Cyril Domb. *Phase transitions and critical phenomena*. Vol. 19. Academic press, 2000.

[34] F. J. Dyson. "The *S* Matrix in Quantum Electrodynamics". In: *Phys. Rev.* 75 (11 1949), pp. 1736–1755. DOI: 10.1103/PhysRev.75.1736. URL: https://link.aps.org/doi/10.1103/PhysRev.75.1736.

[35] Bradley Efron and Robert J Tibshirani. *An introduction to the bootstrap*. CRC press, 1994.

[36] Albert Einstein. "Sitzungsberichte der preussischen akademie der wissenschaften". In: *Physikalisch mathematische Klasse* 261.3 (1924), p. 1925.

[37] R. P. Feynman. "Space-Time Approach to Non-Relativistic Quantum Mechanics". In: *Rev. Mod. Phys.* 20 (2 1948), pp. 367–387. DOI: 10.1103/RevModPhys.20.367. URL: https://link.aps.org/doi/10.1103/RevModPhys.20.367.

[38] Michael E. Fisher. "Renormalization of Critical Exponents by Hidden Variables". In: *Phys. Rev.* 176 (1 1968), pp. 257–272. DOI: 10.1103/PhysRev.176.257. URL: https://link.aps.org/doi/10.1103/PhysRev.176.257.

[39] Michael E Fisher. "The theory of equilibrium critical phenomena". In: *Reports on progress in physics* 30.2 (1967), p. 615.

[40] J. Frohlich. "On the Triviality of Lambda (phi**4) in D-Dimensions Theories and the Approach to the Critical Point in D >= Four-Dimensions". In: *Nucl.Phys.* B200 (1982), pp. 281–296. DOI: 10.1016/0550-3213(82)90088-8.

[41] I. M. Gel'fand and A. M. Yaglom. "Integration in Functional Spaces and its Applications in Quantum Physics". In: *Journal of Mathematical Physics* 1.1 (1960), pp. 48–69. DOI: 10.1063/1.1703636. eprint: http://dx.doi.org/10.1063/1.1703636. URL: http://dx.doi.org/10.1063/1.1703636.

[42] Peter Grüter, David Ceperley, and Frank Laloë. "Critical Temperature of Bose-Einstein Condensation of Hard-Sphere Gases". In: *Phys. Rev. Lett.* 79 (19 1997), pp. 3549–3552. DOI: 10.1103/PhysRevLett.79.3549. URL: https://link.aps.org/doi/10.1103/PhysRevLett.79.3549.

[43] M. Haque. "Weakly Non-ideal Bose Gas: Comments on Critical Temperature Calculations". In: *eprint arXiv:cond-mat/0302076* (Feb. 2003). eprint: cond-mat/0302076.

[44] A. Harindranath and J. P. Vary. "Stability of the vacuum in scalar field models in 1+1 dimensions". In: *Phys. Rev. D* 37 (4 1988), pp. 1076–1078. DOI: 10.1103/PhysRevD.37.1076. URL: http://link.aps.org/doi/10.1103/PhysRevD.37.1076.

[45] M. Holzmann, P. Gruter, and F. Laloe. "Bose-Einstein condensation of interacting gases". In: *eprint arXiv:cond-mat/9809356* (Sept. 1998). eprint: cond-mat/9809356.

[46] Markus Holzmann and Werner Krauth. "Transition Temperature of the Homogeneous, Weakly Interacting Bose Gas". In: *Phys. Rev. Lett.* 83 (14 1999), pp. 2687–2690. DOI: 10.1103/PhysRevLett.83.2687. URL: https://link.aps.org/doi/10.1103/PhysRevLett.83.2687.

[47] Kerson Huang. "Transition Temperature of a Uniform Imperfect Bose Gas". In: *Phys. Rev. Lett.* 83 (19 1999), pp. 3770–3771. DOI: 10.1103/PhysRevLett.83.3770. URL: https://link.aps.org/doi/10.1103/PhysRevLett.83.3770.

[48] Kerson Huang. "Transition Temperature of a Uniform Imperfect Bose Gas". In: *Phys. Rev. Lett.* 83 (19 1999), pp. 3770–3771. DOI: 10.1103/PhysRevLett.83.3770. URL: https://link.aps.org/doi/10.1103/PhysRevLett.83.3770.

[49] Tomasz K., Ingmar V., and U. Wolff. "Performance of a worm algorithm in theory at finite quartic coupling". In: *Comput. Phys. Commun.* 182.7 (2011), pp. 1477 –1480. ISSN: 0010-4655. URL: http://www.sciencedirect.com/science/article/pii/S001046551100110X.

[50] V. A. Kashurnikov, N. V. Prokof'ev, and B. V. Svistunov. "Critical Temperature Shift in Weakly Interacting Bose Gas". In: *Phys. Rev. Lett.* 87 (12 2001), p. 120402. DOI: 10.1103/PhysRevLett.87.120402. URL: https://link.aps.org/doi/10.1103/PhysRevLett.87.120402.

[51] Boris Kastening. "Bose-Einstein condensation temperature of a homogenous weakly interacting Bose gas in variational perturbation theory through seven loops". In: *Phys. Rev. A* 69 (4 2004), p. 043613. DOI: 10.1103/PhysRevA.69.043613. URL: https://link.aps.org/doi/10.1103/PhysRevA.69.043613.

[52] J. Kaupuzs, R. V. N. Melnik, and J. Rimsans. "Corrections to finite–size scaling in the phiˆ4 model on square lattices". In: *ArXiv e-prints* (June 2014). eprint: 1406.7491.

[53] H. Kleinert. "Five-Loop Critical Temperature Shift in Weakly Interacting Homogeneous Bose-Einstein Condensate". In: *Modern Physics Letters B* 17.19 (2003), pp. 1011–1020. DOI: 10.1142/S0217984903006074. eprint: http://www.worldscientific.com/doi/pdf/10.1142/S0217984903006074. URL: http://www.worldscientific.com/doi/abs/10.1142/S0217984903006074.

[54] Hagen Kleinert. "Addendum to "Strong-coupling behavior of φ^4 theories and critical exponents"". In: *Phys. Rev. D* 58 (10 1998), p. 107702. DOI: 10.1103/PhysRevD.58.107702. URL: https://link.aps.org/doi/10.1103/PhysRevD.58.107702.

[55] Hagen Kleinert. "Critical exponents from seven-loop strong-coupling φ^4 theory in three dimensions". In: *Phys. Rev. D* 60 (8 1999), p. 085001. DOI: 10.1103/PhysRevD.60.085001. URL: https://link.aps.org/doi/10.1103/PhysRevD.60.085001.

[56] Hagen Kleinert. "Strong-coupling ϕ^4-theory in 4-ε dimensions, and critical exponents". In: *Physics Letters B* 434.1 (1998), pp. 74 –79. ISSN: 0370-2693. DOI: https://doi.org/10.1016/S0370-2693(98)00750-3. URL: http://www.sciencedirect.com/science/article/pii/S0370269398007503.

[57] Hagen Kleinert. "Strong-coupling behavior of φ^4 theories and critical exponents". In: *Phys. Rev. D* 57 (4 1998), pp. 2264–2278. DOI: 10.1103/PhysRevD.57.2264. URL: https://link.aps.org/doi/10.1103/PhysRevD.57.2264.

[58] John B. Kogut. "An introduction to lattice gauge theory and spin systems". In: *Rev. Mod. Phys.* 51 (4 1979), pp. 659–713. DOI: 10.1103/RevModPhys.51.659. URL: https://link.aps.org/doi/10.1103/RevModPhys.51.659.

[59] Tomasz Korzec, Ingmar Vierhaus, and Ulli Wolff. "Performance of a worm algorithm in ϕ^4 theory at finite quartic coupling". In: *Computer Physics Communications* 182.7 (2011), pp. 1477 –1480. ISSN: 0010-4655. DOI: https://doi.org/10.1016/j.cpc.2011.03.018. URL: http://www.sciencedirect.com/science/article/pii/S001046551100110X.

[60] David P Landau and Kurt Binder. *A guide to Monte Carlo simulations in statistical physics*. Cambridge university press, 2014.

[61] Sascha Ledowski, Nils Hasselmann, and Peter Kopietz. "Self-energy and critical temperature of weakly interacting bosons". In: *Phys. Rev. A* 69 (6 2004), p. 061601. DOI: 10.1103/PhysRevA.69.061601. URL: https://link.aps.org/doi/10.1103/PhysRevA.69.061601.

[62] Dean Lee, Nathan Salwen, and Daniel Lee. "The diagonalization of quantum field Hamiltonians ". In: *Physics Letters B* 503.1-2 (2001), pp. 223–235. ISSN: 0370-2693. DOI: http://dx.doi.org/10.1016/S0370-2693(01)00197-6. URL: http://www.sciencedirect.com/science/article/pii/S0370269301001976.

[63] T. D. Lee and C. N. Yang. "Low-Temperature Behavior of a Dilute Bose System of Hard Spheres. I. Equilibrium Properties". In: *Phys. Rev.* 112 (5 1958), pp. 1419–1429. DOI: 10.1103/PhysRev.112.1419. URL: https://link.aps.org/doi/10.1103/PhysRev.112.1419.

[64] Will Loinaz and R. S. Willey. "Monte Carlo simulation calculation of the critical coupling constant for two-dimensional continuum φ^4 theory". In: *Phys. Rev. D* 58 (7 1998), p. 076003. DOI: 10.1103/PhysRevD.58.076003.

[65] M. Lüscher. "Properties and uses of the Wilson flow in lattice QCD". In: *Journal of High Energy Physics* 2010.8 (2010). DOI: 10.1007/JHEP08(2010)071. URL: https://doi.org/10.1007/JHEP08(2010)071.

[66] M. Lüscher and P. Weisz. "Scaling laws and triviality bounds in the lattice φ^4 theory: (I). One-component model in the symmetric phase ". In: *Nuclear Physics B* 290 (1987), p. 25. DOI: 10.1016/0550-3213(87)90177-5.

[67] Martin Lüscher. "Step scaling and the Yang-Mills gradient flow". In: *Journal of High Energy Physics* 2014.6 (2014). ISSN: 1029-8479. DOI: 10.1007/JHEP06(2014)105. URL: https://doi.org/10.1007/JHEP06(2014)105.

[68] Moshe M. and Zinn-Justin J. "Quantum field theory in the large N limit: a review". In: *Physics Reports* 385.3 (2003), pp. 69 –228. ISSN: 0370-1573. DOI: https://doi.org/10.1016/S0370-1573(03)00263-1. URL: http://www.sciencedirect.com/science/article/pii/S0370157303002631.

[69] N. Madras and A.D. Sokal. "The pivot algorithm: A highly efficient Monte Carlo method for the self-avoiding walk". In: *J. Stat. Phys.* 50.1 (1988), pp. 109–186. ISSN: 1572-9613. DOI: 10.1007/BF01022990. URL: http://dx.doi.org/10.1007/BF01022990.

[70] Bernhard Mehlig and BruceM. Forrest. "Universality in the critical two–dimensional φ^4–model". In: *Zeitschrift für Physik B Condensed Matter* 89.1 (1992), pp. 89–96. URL: http://dx.doi.org/10.1007/BF01320833.

[71] Ashley Milsted, Jutho Haegeman, and Tobias J. Osborne. "Matrix product states and variational methods applied to critical quantum field theory". In: *Phys. Rev. D* 88 (8 2013), p. 085030. DOI: 10.1103/PhysRevD.88.085030. URL: http://link.aps.org/doi/10.1103/PhysRevD.88.085030.

[72] Christopher Monahan and Kostas Orginos. "Locally smeared operator product expansions in scalar field theory". In: *Phys. Rev. D* 91 (7 2015), p. 074513. DOI: 10.1103/PhysRevD.91.074513. URL: https://link.aps.org/doi/10.1103/PhysRevD.91.074513.

[73] István Montvay and Gernot Münster. *Quantum fields on a lattice*. Cambridge University Press, 1997.

[74] MEJ Newman and GT Barkema. *Monte Carlo Methods in Statistical Physics*. Oxford University Press: New York, USA, 1999.

[75] "On the distribution of certain Wiener functionals". In: *Trans. Amer. Math. Soc.* 65 (1949). DOI: http://doi.org/10.1090/S0002-9947-1949-0027960-X.

[76] G. Parisi. *Statistical Field Theory*. Frontiers in Physics. Addison-Wesley, 1988. ISBN: 9780201059854.

[77] Giorgio Parisi. *Statistical field theory*. Addison-Wesley, 1988.

[78] R.K. Pathria and Paul D. Beale, eds. *Statistical Mechanics*. Third Edition. Boston: Academic Press, 2011. ISBN: 978-0-12-382188-1. DOI: https://doi.org/10.1016/B978-0-12-382188-1.00020-7.

[79] Andrea Pelissetto and Ettore Vicari. "Critical mass renormalization in renormalized ϕ^4 theories in two and three dimensions". In: *Physics Letters B* 751.Supplement C (2015), pp. 532 –534. ISSN: 0370-2693. DOI: https://doi.org/10.1016/j.physletb.2015.11.015. URL: http://www.sciencedirect.com/science/article/pii/S037026931500862X.

[80] Michael E Peskin and Daniel V Schroeder. *An introduction to quantum field theory*. Includes exercises. Boulder, CO: Westview, 1995. URL: https://cds.cern.ch/record/257493.

[81] M. B. Priestley. *Spectral analysis and time series / M.B. Priestley*. English. Academic Press London ; New York, 1981, 2 v. (xvii, [45], 890 p.) : ISBN: 0125649010 0125649029.

[82] V Privman and J Rudnick. "Systems with logarithmic specific heat: finite-size scaling". In: *Journal of Physics A: Mathematical and General* 19.18 (1986), p. L1215. URL: http://stacks.iop.org/0305-4470/19/i=18/a=018.

[83] Nikolay Prokof'ev and Boris Svistunov. "Worm Algorithms for Classical Statistical Models". In: *Phys. Rev. Lett.* 87 (16 2001), p. 160601. DOI: 10.1103/PhysRevLett.87.160601. URL: https://link.aps.org/doi/10.1103/PhysRevLett.87.160601.

[84] N.V. Prokof'ev, B.V. Svistunov, and I.S. Tupitsyn. "Worm algorithm in quantum Monte Carlo simulations". In: *Physics Letters A* 238.4-5 (1998), pp. 253–257. ISSN: 0375-9601. DOI: http://dx.doi.org/10.1016/S0375-9601(97)00957-2. URL: http://www.sciencedirect.com/science/article/pii/S0375960197009572.

[85] Micheal Reed and Barry Simon. *Functional Analysis (Methods of modern mathematical physics)*. New York: Academic Press, 1975.

[86] A Rotondi, P Pedroni, and A Pievatolo. *Probabilità Statistica e Simulazione: Programmi applicativi scritti con Scilab*. Springer Science & Business Media, 2011.

[87] Slava Rychkov and Lorenzo G. Vitale. "Hamiltonian truncation study of the φ^4 theory in two dimensions". In: *Phys. Rev. D* 91 (8 2015), p. 085011. DOI: 10.1103/PhysRevD.91.085011. URL: http://link.aps.org/doi/10.1103/PhysRevD.91.085011.

[88] David Schaich and Will Loinaz. "An Improved lattice measurement of the critical coupling in ϕ^4 theory". In: *Phys.Rev.* D79 (2009), p. 056008. DOI: 10.1103/PhysRevD.79.056008. arXiv: 0902.0045 [hep-lat].

[89] Silvan S Schweber. "Some chapters for a history of quantum field theory: 1938-1952". In: *Relativity, groups and topology. 2*. 1984.

[90] Julian Schwinger. "On the Euclidean structure of relativistic field theory". In: *Proceedings of the National Academy of Sciences* 44.9 (1958), pp. 956–965.

[91] S. H. Shenker. "FIELD THEORIES AND PHASE TRANSITIONS". In: *Les Houches Summer School in Theoretical Physics: Recent Advances in Field Theory and Statistical Mechanics Les Houches, France, August 2-September 10, 1982*. 1982, pp. 1–38.

[92] HE Stanley. *Introduction to Phase Transitions and Critical Phenomena Oxford Univ*. 1971.

[93] P. M. Stevenson. "Gaussian effective potential. II. $\lambda\varphi^4$ field theory". In: *Phys. Rev. D* 32 (6 1985), pp. 1389–1408. DOI: 10.1103/PhysRevD.32.1389. URL: https://link.aps.org/doi/10.1103/PhysRevD.32.1389.

[94] P. M. Stevenson. "Optimized perturbation theory". In: *Phys. Rev. D* 23 (12 1981), pp. 2916–2944. DOI: 10.1103/PhysRevD.23.2916. URL: https://link.aps.org/doi/10.1103/PhysRevD.23.2916.

[95] H. T. C. Stoof. "Nucleation of Bose-Einstein condensation". In: *Phys. Rev. A* 45 (12 1992), pp. 8398–8406. DOI: 10.1103/PhysRevA.45.8398. URL: https://link.aps.org/doi/10.1103/PhysRevA.45.8398.

[96] H. T. C. Stoof. "Nucleation of Bose-Einstein condensation". In: *Phys. Rev. A* 45 (12 1992), pp. 8398–8406. DOI: 10.1103/PhysRevA.45.8398. URL: https://link.aps.org/doi/10.1103/PhysRevA.45.8398.

[97] Takanori Sugihara. "Density matrix renormalization group in a two-dimensional lambda phi4 Hamiltonian lattice model". In: *JHEP* 0405 (2004), p. 007. DOI: 10.1088/1126-6708/2004/05/007. arXiv: hep-lat/0403008 [hep-lat]. URL: http://arxiv.org/abs/hep-lat/0403008.

[98] Hiroshi Suzuki. "Energy-momentum tensor from the Yang-Mills gradient flow". In: *PTEP* 2013 (2013). [Erratum: PTEP2015,079201(2015)], 083B03. DOI: 10.1093/ptep/ptt059, 10.1093/ptep/ptv094. arXiv: 1304.0533 [hep-lat].

[99] K. Symanzik. "Euclidean Quantum Field Theory. I. Equations for a Scalar Model". In: *Journal of Mathematical Physics* 7.3 (1966), pp. 510–525. DOI: 10.1063/1.1704960. eprint: http://dx.doi.org/10.1063/1.1704960. URL: http://dx.doi.org/10.1063/1.1704960.

[100] K Symanzik. "Regularized quantum field theory". In: *New Developments in Quantum Field Theory and Statistical Mechanics Cargèse 1976*. Springer, 1977, pp. 265–279.

[101] Tadashi Toyoda. "A microscopic theory of the lambda transition". In: *Annals of Physics* 141.1 (1982), pp. 154 –178. ISSN: 0003-4916. DOI: https://doi.org/10.1016/0003-4916(82)90277-9. URL: http://www.sciencedirect.com/science/article/pii/0003491682902779.

[102] I. Vierhaus. "Simulation of ϕ^4 Theory in the Strong Coupling Expansion beyond the Ising Limit". Diploma thesis, Humboldt Universitat zu Belrin. 2010.

[103] G. C. Wick. "Properties of Bethe-Salpeter Wave Functions". In: *Phys. Rev.* 96 (4 1954), pp. 1124–1134. DOI: 10.1103/PhysRev.96.1124. URL: https://link.aps.org/doi/10.1103/PhysRev.96.1124.

[104] A.S. Wightman and L. Garding. "fields as operator-values distributions in relativistic quantum theory". In: *Arkiv Fys.* Vol: 28 (1965).

[105] Martin Wilkens, Fabrizio Illuminati, and Meret Krämer. "Transition temperature of the weakly interacting Bose gas: perturbative solution of the crossover equations in the canonical ensemble". In: *Journal of Physics B: Atomic, Molecular and Optical Physics* 33.20 (2000), p. L779. URL: http://stacks.iop.org/0953-4075/33/i=20/a=10j.

[106] Kenneth G. Wilson. "Renormalization Group and Critical Phenomena. I. Renormalization Group and the Kadanoff Scaling Picture". In: *Phys. Rev. B* 4 (9 1971), pp. 3174–3183. DOI: 10.1103/PhysRevB.4.3174. URL: https://link.aps.org/doi/10.1103/PhysRevB.4.3174.

[107] Kenneth G. Wilson. "The renormalization group and critical phenomena". In: *Rev. Mod. Phys.* 55 (3 1983), pp. 583–600. DOI: 10.1103/RevModPhys.55.583. URL: https://link.aps.org/doi/10.1103/RevModPhys.55.583.

[108] Kenneth G Wilson and John Kogut. "The renormalization group and the ε expansion". In: *Physics Reports* 12.2 (1974), pp. 75–199.

[109] U. Wolff. "Collective Monte Carlo Updating for Spin Systems". In: *Phys. Rev. Lett.* 62 (4 1989), pp. 361–364. DOI: 10.1103/PhysRevLett.62.361. URL: https://link.aps.org/doi/10.1103/PhysRevLett.62.361.

[110] U. Wolff. "Comparison between cluster Monte Carlo algorithms in the Ising model". In: *Phys. Lett. B* 228 (Sept. 1989), pp. 379–382. DOI: 10.1016/0370-2693(89)91563-3.

[111] U. Wolff. "Erratum to "Monte Carlo errors with less errors" Comput. Phys. Comm. 156 (2004) 143–153". In: *Comput. Phys. Commun.* 176.5 (2007), p. 383. ISSN: 0010-4655. DOI: http://dx.doi.org/10.1016/j.cpc.2006.12.001. URL: http://www.sciencedirect.com/science/article/pii/S0010465506004322.

[112] U. Wolff. "Monte Carlo errors with less errors". In: *Comput. Phys. Commun.* 156 (2004), pp. 143–153. DOI: 10.1016/S0010-4655(03)00467-3,10.1016/j.cpc.2006.12.001. arXiv: hep-lat/0306017 [hep-lat].

[113] U. Wolff. *MATLAB code for "Monte Carlo errors with less errors"*. 2004. URL: http://www.physik.hu-berlin.de/de/com/ALPHAsoft.

[114] U. Wolff. "Simulating the All-Order Strong Coupling Expansion I: Ising Model Demo". In: *Nucl. Phys.* B810 (2009), pp. 491–502. DOI: 10.1016/j.nuclphysb.2008.09.033. arXiv: 0808.3934 [hep-lat].

[115] Ulli Wolff. "Critical slowing down". In: *Nuclear Physics B-Proceedings Supplements* 17 (1990), pp. 93–102.

[116] Ulli Wolff. "Collective Monte Carlo Updating for Spin Systems". In: *Phys. Rev. Lett.* 62 (4 1989), pp. 361–364. DOI: 10.1103/PhysRevLett.62.361. URL: http://link.aps.org/doi/10.1103/PhysRevLett.62.361.

[117] Ulli Wolff. "Precision check on triviality of ϕ^4 theory by a new simulation method". In: *Phys.Rev.* D79 (2009), p. 105002. DOI: 10.1103/PhysRevD.79.105002. arXiv: 0902.3100 [hep-lat].

[118] Ulli Wolff. "Simulating the all-order strong coupling expansion III: O(N) sigma/loop models". In: *Nuclear Physics B* 824.1 (2010), pp. 254 –272. ISSN: 0550-3213. DOI: https://doi.org/10.1016/j.nuclphysb.2009.09.006. URL: http://www.sciencedirect.com/science/article/pii/S0550321309004726.

[119] Christian Wozar and Andreas Wipf. "Supersymmetry Breaking in Low Dimensional Models". In: *Annals Phys.* 327 (2012), pp. 774–807. DOI: 10.1016/j.aop.2011.11.015. arXiv: 1107.3324 [hep-lat].

[120] V I Yukalov and E P Yukalova. "Bose-Einstein condensation temperature of weakly interacting atoms". In: *Laser Physics Letters* 14.7 (2017), p. 073001. URL: http://stacks.iop.org/1612-202X/14/i=7/a=073001.

[121] Jean Zinn-Justin. *Quantum Field Theory and Critical Phenomena; 4th ed.* Internat. Ser. Mono. Phys. Oxford: Clarendon Press, 2002. URL: https://cds.cern.ch/record/572813.

[122] O. Zobay. "Condensation temperature of interacting Bose gases with and without disorder". In: *Phys. Rev. A* 73 (2 2006), p. 023616. DOI: 10.1103/PhysRevA.73.023616. URL: https://link.aps.org/doi/10.1103/PhysRevA.73.023616.

LIST OF PUBLICATIONS

[1] Paolo Bosetti, Barbara De Palma and Marco Guagnelli. "Monte Carlo determination of the critical coupling in ϕ_2^4 theory". In: *Physical Review D* 92 (3 2015), p. 034509. URL: https://link.aps.org/doi/10.1103/PhysRevD.92.034509.

[2] Michele Brambilla, Francesco Di Renzo, Marco Guagnelli and Barbara De Palma. "Clover fermions in Numerical Stochastic Perturbation Theory" In: *Proceedings, 33rd International Symposium on Lattice Field Theory (Lattice 2015)* (2016), p. 270. URL: https://pos.sissa.it/251/270/pdf

[3] Barbara De Palma and Marco Guagnelli. "Monte Carlo simulation of ϕ_2^4 and $O(N)\phi_3^4$ theories". In: *Proceedings, 34rd International Symposium on Lattice Field Theory (Lattice 2016)* (2016), p. 277. arXiv:1612.05029

[4] Barbara De Palma, Marco Erba, Luca Mantovani, and Nicola Mosco. "A Python program for the implementation of the Γ–method for Monte Carlo simulations" (Beto collaboration 2017). arXiv preprint arXiv:1703.02766 (2017) — To be published in *Computer Physics Communications*.

[5] Simone Bronzin, Barbara De Palma and Marco Guagnelli. Work in progress on Wilson flow application to ϕ_2^4 theory.

[6] Barbara De Palma and Marco Guagnelli. Work in progress on the determination of the shift of criticial temperature in Bose–Einstein condensation.

ACKNOWLEDGMENT

Even if it means oblivion, friends, I'll welcome it, because it won't be nothing. We'll be alive again in a thousand blades of grass, and a million leaves; we'll be falling in the raindrops and blowing in the fresh breeze; we'll be glittering in the dew under the stars and the moon out there in the physical world, which is our true home and always was.

Philip Pullman
[Philip Pullman, The Amber Spyglass]

An important moment is to say thanks to all the people that supported me for all these three years and more, I know that I am not able to express my whole gratitude that they deserve.

I want to firstly thanks my supervisor Marco, for always supporting me in the high and in the low moments. You showed me what humanity is and this quality is not always owned by people with a vivid curiosity and brightness that you have.

Thanks to the PhD examiners, Ulrich and Enzo, for their careful reading of my thesis. I want to thank, in particular, Ulrich for the precious and accurate suggestions.

I thank the 3D–spin group, a big family that keeps increasings. Thanks to Simone and Stefano for the laughs and coffees we had together. A special thanks goes to my tutor Barbara for the mutual support, the chats and the *swimming pool*: for this latter, it's the thought that counts.

Thanks to the Beto Collaboration, for the constructive and funny launches and afternoons.

A heartfelt thanks goes to our doctoral coordinator LCA, for his meticulous work and his support. Thanks to the whole Physics Department and to INFN, a home for nine long years.

Finally thanks to my family, all the family. I simply love you.

COLOPHON

This document was typeset using the typographical look-and-feel `classicthesis` developed by André Miede. The style was inspired by Robert Bringhurst's seminal book on typography "*The Elements of Typographic Style*". `classicthesis` is available for both LaTeX and LyX:

`https://bitbucket.org/amiede/classicthesis/`

Happy users of `classicthesis` usually send a real postcard to the author, a collection of postcards received so far is featured here:

`http://postcards.miede.de/`